DEPARTMENT OF CIVIL ENGINEERING
YOKOHAMA NATIONAL UNIVERSITY

STRUCTURAL AND FINANCIAL RISK ASSESSMENT OF CAISSON BREAKWATERS AGAINST WIND WAVES AND TSUNAMI ATTACK

(ケーソン防波堤の風波、津波に対するリスク評価の研究)

By

Miguel Esteban

A dissertation submitted in partial fulfillment of the requirements for the Doctoral Degree of Engineering

Academic Advisor: Professor TOMOYA SHIBAYAMA, *D. Eng.*

September, 2007

ABSTRACT

Coastal areas are potentially at risk from waves caused by a variety of natural disasters such as storms, typhoons or tsunamis. In order to protect people and property against the effects of these waves caisson breakwaters are often built at key risk locations. These massive structures are costly, and can often be displaced during their lifetime due to sporadic episodes of high wave energy. Due to the fact that they are located out in the sea it is often possible for them to continue to provide effective protection despite these deformations, though it is necessary to understand the possible extent of the movement in order to formulate an adequate risk assessment for a given structure.

The first part of this thesis deals with a method to investigate the long-term deformations of the rubble mound of a breakwater during its working life, which is essential for the movement of the structure to be able to be measured effectively. In order to do so laboratory experiments were carried out, from which the probability distribution functions of sliding and tilting were obtained for a series of three storms of similar intensity. The laboratory results were then reproduced using a computer model, which decomposed the movement of the caisson into its vertical and horizontal components. The horizontal movement uses the equations developed in the Deformation Based Reliability Design (DBRD) method by Shimosako and Takahashi (1998), as modified by Kim and Takayama (2004). For the vertical movement a new method was developed based on simple soil mechanics theory, which uses a similar principle to that of Shimosako and Takahashi (1998) to compute the vertical displacement. The results obtained overestimate the deformation slightly during the first storm but can predict well the deformation that will occur over subsequent storms, and thus allow for greater degree of accuracy to be achieved than in the original DBRD method.

This new methodology to estimate the deformation in the rubble mound was then applied to the case when the breakwater is attacked by a solitary wave, to attempt to

reproduce a tsunami attack. Laboratory experiments were also carried out to measure the movements that could be expected from such a type of attack, which could be reproduced by the deformation model introduced in this thesis.

To further verify that the deformation model proposed was accurate, the displacement recorded after the failure of a real-life caisson (that of Susami Breakwater in Japan in 2004, as reported by Kim et al., 2005) was reproduced using the new model. The results showed how the deformations could be successfully predicted, although the effect of the failed wave-dissipating concrete blocks was not well understood and their influence was ignored. The results obtained were thus superior to those of Kim et al. (2005) in that the present model could reproduce not only the sliding but also the tilting of the breakwater.

Finally, a management tool for the risk assessment of a breakwater during its construction phase was introduced by using the new deformation model proposed. A computer model of the construction process that a contractor would follow to build a caisson breakwater was developed, with the wave climate for each month of the duration of works modelled using data obtained from the NOWPHAS Reports. Possible damage to the caisson was determined using the DBRD method proposed in the present dissertation, and damage to the rubble mound and toe armour was determined using the methods of Merkle (1989) and Madrigal and Valdes (1995). By using the Monte Carlo technique the expected cost and time to finish the breakwater could be obtained, allowing for the determination of the risk associated with the breakwater construction. Thus it is possible to determine when would be the most appropriate time to begin construction and the likelihood of encountering problems during the construction phase. A case study of breakwater construction for Honshu Island in Japan was shown, with the results comparing well with the experience of Japanese contractors.

ABSTRACT (SPANISH)

Las costas son regiones que corren el riesgo de poder ser atacadas por desastres naturales como tormentas, tifones o tsunamis. Para proteger a la población y las diversas infraestructuras contra los oleajes producidos por estos desastres a menudo se construyen diques en lugares de especial peligro. Estas estructuras son por su naturaleza costosas desde un punto de vista financiero, y pueden ser desplazadas durante su vida útil a causa de olas de extraordinario tamaño. Debido a que estas construcciones se encuentran situadas en el mar es posible que puedan continuar desenvolviendo su función a pesar de las deformaciones sufridas, con lo cual es necesario analizar la magnitud de tales movimientos con el fin de analizar correctamente el riesgo asociado con cada estructura.

La primera parte de esta tesis propone un método para investigar las deformaciones a largo plazo de las fundaciones de un dique vertical durante su vida útil, esencial para analizar el movimiento de la estructura de forma eficaz. Para ello se llevaron a cabo experimentos de laboratorio de los cuales se obtuvieron las funciones de distribución de probabilidad de los movimientos horizontal y vertical del dique a lo largo de tres tormentas de similar intensidad. Estos experimentos fueron después reproducidos utilizando una simulación, que descompone el movimiento del dique en sus componentes horizontal y vertical. El movimiento horizontal utiliza las ecuaciones desarrolladas por Shimosako y Takahashi (1998) en su "Deformation Based Reliability Design (DBRD)" siguiendo la modificación propuesta por Kim y Takayama (2005). Para analizar el movimiento vertical se propone una nueva metodología, basada en mecánica de suelos tradicional, que usa un principio similar al de Shimosako y Takahashi (1998). Los resultados obtenidos sobreestiman ligeramente las deformaciones obtenidas durante la primera tormenta pero son capaces de predecir adecuadamente las deformaciones de las tormentas subsiguientes, y por lo tanto permiten una mejor aproximación que las ecuaciones desarrolladas en el DBRD original.

La metodología desarrollada para estimar la deformación de las fundaciones del dique vertical puede ser aplicada también al caso de un tsunami. Para ello se realizaron también experimentos de laboratorio para investigar los movimientos que se pudieran esperar durante un ataque de este tipo, que luego fueron reproducidos con éxito por la simulación por ordenador.

Como verificación adicional el modelo propuesto se utilizo para analizar las deformaciones sufridas por el dique de Susami en Japón en el 2004 (Kim et al. 2005). El modelo es capaz de reproducir las deformaciones siempre y cuando el efecto de los bloques de protección (que fueron removidos durante la tormenta) sea ignorado. Los resultados así obtenidos permiten un análisis mas exacto que el de Kim et al (2005) debido a que el modelo de estos autores no puede reproducir el movimiento vertical del dique.

Finalmente, se desarrollo un procedimiento para ayudar en la planificación de los riesgos asociados con la construcción de un dique vertical. Una simulación por ordenador del proceso de construcción de un rompeolas fue desarrollado, en el cual la modelizacion del oleaje se llevo a cabo utilizando los parámetros obtenidos en los informes NOWPHAS. El movimiento de los diques verticales fue determinado utilizando el método DBRD propuesto en la presente tesis, y el daño de las fundaciones y del recubrimiento de las fundaciones fue obtenido utilizando los métodos de Merkle (1989) y Madrigal y Valdes (1995). El tiempo y coste medio para la construcción del rompeolas puede ser obtenido por el Método de Monte Carlo, con lo cual el riesgo asociado a la construcción del rompeolas puede ser analizado. Es posible por lo tanto determinar cual es el mes más adecuado para comenzar la construcción y la probabilidad de encontrar problemas durante la ejecución de las obras. Un ejemplo de utilización de este método para la Isla de Honshu en Japón fue también calculado, que demuestra como el modelo se aproxima a la forma de construir rompeolas en Japón.

ACKNOWLEDGMENTS

First of all, I would like to thank Prof. Tomoya Shibayama for his inspiring and enthusiastic support. When I first arrived at Yokohama University it was not my intention to study for a Ph.D. and without his belief in me the present work would have never been possible. Especially I would like to thank him for the long time dedicated each week to discussing research, which provided invaluable guidance in my otherwise erratic thought processes.

Next, I would like to also thank Prof. Jun Sasaki for his suggestions during the multiple progress reports that we had during my three and a half years at Yokohama University. I was always surprised by his ability to understand better than myself certain aspects of my research, which encouraged me to always try to understand more deeply each element of my research. Special mention is the help I received from Prof. Kazuo Tani in developing the tilting model for the movement of the breakwater, as my understanding of soil mechanics was not adequate enough to come up with the proposed methodology on my own. As this was to eventually become the main part of my research, I am profoundly grateful to the time he gave me to discuss my model. My sincere gratitude goes also to Research Associate Hiroshi Takagi for his help in conducting many of the laboratory experiments and for his input into the modeling of the construction process of a breakwater. His practical experience in these maters ensured that the final model reflected the reality of breakwater construction, and hence without him its development would have not been possible.

I would like to recognize the help received from the other students at the Coastal Engineering Laboratory, Thao Nguyen Danh for the execution and analysis of the joint experiment on solitary waves, Thamnoon Rasmeemasmuang for his words of wisdom regarding engineering in particular and life in general, and all the other members for the positive environment of the laboratory.

The current research would not have been possible without the scholarship provided by the Japanese Ministry of Education (Mombukagakusho), a fact that I will remember throughout my life.

I would like to extend my gratitude to all the people that have supported me during my time in Japan. I would have never been able to do this work without them.

Before arriving to Japan several people played a crucial part in mentoring me throughout my life, Prof. John Davis at Bristol University and Anthony Pooley at JacobsGIBB. I probably would probably not be an engineer if it were not for people like them.

The greatest thanks however goes to my mother, she did not always have such an easy job in bringing me up but has never ceased to believe in me. This work is dedicated to her.

INDEX

INDEX OF FIGURES

INDEX OF TABLES

Index of Notation and Abbreviations

α_1, α_3	factors in Goda formula
α_{IH}, α_{IB}	factors in Goda formula to calculate α^*
α^*	impulse pressure factor introduced to Goda formula by Takahashi et al.
β	angle between the direction of wave approach and a line normal to the breakwater
β_0, β_1, β_{max},	parameters to determine wave deformation due to random breaking
β_0^*, β_1^*, β_{max}^*	parameters to determine wave deformation due to random breaking
γ_P	modification factor that indicates the reduction in the standing wave force due to the occurrence of the impulsive wave force
δ_1, δ_2, δ_{11}, δ_{12}	parameters used to calculate α_{IH} and α_{IB}
ε	strain
ε_e	elastic strain
ε_p	plastic strain
η^*	elevation to which the wave pressure is exerted in the Goda formula
θ	slope of the coastline
θ_r	residual tilting angle
θ_v	variable tilting angle
κ	safety index of a level 2 Reliability based design
μ	coefficient of friction between the caisson and the rubble mound
ν_D	dynamic response factor
ρ	density of water
ρ_a	density of gravel as a whole (water and solids)
ρ_c	density of caisson
ρ_s	density of foundation gravel stones
σ	stress
σ_L	standard deviation of mean load
σ_R	standard deviation of mean resistance
$\hat{\vartheta}(c)$	expected cost of construction
$\vartheta(c)$	cost obtained from one simulation
ϕ	angle of friction between gravel particles
$\Theta_{tot.}$	component of the mass matrix

a_H	amplitude of a tsunami wave
a_x , a_z	distance from the centre of gravity to the point where the resistance forces from the foundation in the x and z co-ordinates are applied
$A_{caisson}$	maximum advance of caissons
$A_{foundation}$	maximum advance of foundations
B	caisson width
B_c	berm length of the rubble mound foundation
BoQ	Bill of Quantities
c	Shear strength of gravel
C	Wave celerity
C_y	Cauchy number
CoV	coefficient of variation of a Gaussian distribution
d	depth of water above the armour layer of the rubble foundation
d_z	active depth of foundations
D_{50}	diameter of gravel particles
DBRD	Deformation-Based Reliability Design Method
e	void ratio of gravel
E	Young's Modulus
E_C	compaction energy
E_p	plastic Young's Modulus
ESD	Estimated Sliding Distance
ESD_{limit}	Limit of Tolerable Sliding Distance
EOF	Expected Occurrence in Frequency Index
$f(x)$	failure probability density function.
F_r	Froude Number
F_D	force related sliding velocity including wave-making resistance force
F_R	frictional resistance force
F_w	additional restraining force on caisson due to tilting
$F_{dyn,max}$	peak of the hydraulic load to the wall.
$F.S.$	Factor of Safety
$F_{stat,eq}$	equivalent static pressure
g	acceleration of gravity.
G	shear modulus
h	depth of water in front of the breakwater

h_{30}, h_{50}	water depth parameters for determination of shoaling
h'	distance from the design water level to the bottom of the caisson
h_b	water depth at a location at a distance $5H_{1/3}$ seaward of the breakwater
h_c	the crest elevation of the breakwater above the design water level.
h_c*	minimum of η* and h_c
h_d	depth of deep water for tsunami height computation
h_h	height of the caisson
h_r	height of the rubble mound
h_r*	relative berm height (h_r/h)
h_s	depth of shallow water for tsunami height computation
H	incident wave height
H_0'	deepwater wave height.
$H_{1/3}$	significant incident wave height
H_{max}	highest wave in the design sea state
H*	relative wave height
H_s	tsunami waveheights in shallow water
H_d	tsunami waveheights in deep water
H_{ram}	height of strike of the Rammer
H2-H1	water step
HWL	High Water Level
k_x , k_φ,	components of the stiffness matrix
K	bulk modulus of elasticity
$K.E.$	Kinetic Energy
K_s	shoaling coefficient
K_{si}	shoaling coefficient for a small amplitude wave
$(K_{si})_{30}$	shoaling coefficient at h=h_{30}
$(K_s)_{50}$	shoaling coefficient at h=h_{50}
l	length or height in Froude No. calculation
L	wavelength at water depth h
L_c	caisson length
L_0	wavelength in deep water
LWL	Low Water Level
m	distance from heel of caisson to point of maximum pressure
m_s	mass of solid

m_{tot}	total mass of system
m_{cai}	mass of the caisson
m_{hyd}	added mass of water
m_{geo}	geodynamic mass
m_L	mean load
m_R	mean resistance
m_{tot}	components of the mass matrix
$m_{last.section}$	mass of the rammer section
M_a	added mass of caisson
M_p	moment around the bottom on an upright section due to P
M_u	momentum around the heel of the caisson due to U
n	distance from front of caisson to point of maximum pressure
N	number of repetitions in a Monte Carlo simulation
N_L	number of layers placed in rammer test
N_s	stability number
N_{od}	number of units displaced
P	total wave pressure at face of the breakwater
P_{acc}	probability of an accident occurring per day
P_{death}	probability of a death occurring per day
$P_1(t)$	time history of slowly varying standing wave component
$P_2(t)$	time history of impulsive "churchroof" shaped wave force
$P(t)$	time history of wave profile
P_{1max}	horizontal wave force estimated from the Goda formula (1974) neglecting impulsive pressure
P_{2max}	horizontal wave force exerted by the Goda formula considering an impulsive pressure coefficient
$P_{foundations}$	total pressure applied to the foundation by one wave
$P_{foundations.max}$	maximum pressure applied to any one point of the foundation
P_r	actual placement rate of materials on a given month
P_{r_max}	maximum rate of placement
p_1, p_2, p_3, p_4	pressure parameters used in the Goda formula
p_e	largest bearing pressure at the heel of caisson
p_m	maximum wave pressure due to tsunami attack
p_u	uplift pressure at toe

q	maximum pressure on a strip area of width n
q_U	bearing capacity of the foundation
Q	the number of workers active during a particular month
R_1, R_2	distance from top of the foundation to certain point in the soil
$R(t)$	reliability of a system
R_{acc}	accident rate per 100,000 workers per year
R_{death}	death rate per 100,000 workers per year
SD	sliding distance of one simulation
SD_b	sliding distance at bottom of caisson
SD_t	sliding distance at top of caisson
$SD_{t(onewave)}$	sliding distance caused by each individual wave
t	horizontal distance between the centre of gravity and heel of caisson
t_d	total impact duration
t_r	time rise
t_1	beginning of impulsive wave force
t_2	end of impulsive wave force
t_{total}	total number of working time periods in a month
$t_{inactive}$	number of periods Contractor is not able to work due to bad weather
t_{health}	number of periods Contractor is not able to work due to H&S issues.
T	wave period
T_N	natural period of mass-spring system
T_{N1}	natural period of single degree of freedom system in horizontal direction
T_{N2}	natural period of the rotation of the structure
U	total uplift pressure on the bottom of the caisson
U_{max}	uplift force calculated from the Goda formula
U_{mou}	mould volume of rammer test
$U(t)$	uplift time history
V_S	volume of gravel particles only –excluding air and water voids-
V	volume of gravel particles including air and water voids
$V_{unconstrained}$	unconstrained maximum velocity
V_W	volume of material resisting the sliding movement
$V_{WA}(t)$	volume of the wedge of accumulated material at the shoreside of the caisson after a certain number of waves

$V_{WA}(t\text{-}1)$	volume of accumulated material by previous waves
W	weight of the caisson per unit extension in air
W'	weight of the caisson per unit extension in still water
W_S	weight of gravel particles only
W_R	Rammer Weight
$\ddot{x}_G$	acceleration at the centre of gravity of the caisson
Y	the number of working days in one year
z	distance from bottom of caisson to a certain point in the soil
z'	height from the still water level to a point along the vertical face
z_a	total vertical displacement caused by each wave

CHAPTER 1

INTRODUCTION

Since early times humans have inhabited coastal regions, which has provided them both with opportunities for the development of civilization (in the form of fishing and commerce) and threats to its existence. From the antiquity coastal defences were built to protect settlements and ports from the onslaughts of the sea, as recorded by Pliny in the 1st Century. In modern times, with the increase in population density in coastal areas and the rapid growth of maritime commerce, these constructions have become more widespread. However coastal engineering is an area where many phenomena are still not well understood, and the design of breakwaters in particular is still carried out using methods that sometimes date back 20 years or longer.

1.1. Statement of the Problem

In order to carry out a Risk Assessment for a caisson breakwater it is necessary to understand the Reliability of the structure i.e. how able is the structure to perform its function under normal and episodic conditions. To do so it is of paramount importance to understand the failure mode of the structure, which lead Shimosako and Takahashi (1998, 1999) to develop the Deformation-Based Reliability Design Method (DBRD). However, this method considers only sliding of the caisson, and from numerous caisson failures it is clear that bearing capacity failure at the heel also

occurs at the same time as sliding. The caisson will thus not only slide, but also tilt, and this tilting will have an effect on the sliding distance. Though Kim and Takayama (2005) introduced a method to calculate the restraining effect due to this tilt, to date there is no methodology available to calculate the tilt of a caisson. The development of this method is of paramount importance for the DBRD to provide adequate results.

The life-cycle management of projects is of great importance to the adequate formulation of a Risk Management Strategy for coastal engineering projects. Due to the uncertain nature of wave climate, the construction of coastal structures is a risky business that is critical to this life-management. A storm can easily damage an unfinished breakwater, increasing the project's cost and causing great difficulties to stakeholders. However this aspect of construction has so far received very little attention, with only simplified statistical models having been developed so far, such as that of Balas and Ergin (2002). It is thus necessary to develop a methodology that can simulate the construction of a breakwater in more detail, by representing each of the stages of construction and how the wave climate can affect them.

1.2. Objectives

The objectives of the research can thus be divided into several groups:

- To understand how the gravel foundation under the caisson behaves, by analysing the transmission of loads throughout the berm and what type of loading the caisson actually applies to the foundation
- To ascertain the failure mode of caisson breakwaters for a variety of waves types, mainly impact waves produced by wind but also solitary ones (such as

tsunamis). Thus the probability distribution functions of failure must be obtained and the failure modes analysed.

- To develop a computational methodology for the estimation of the deformation in the rubble mound due to various types of wave attack.
- To check that the computational methodology thus developed can actually reproduce the deformations observed in real-life failures of caisson breakwaters.
- To develop a computational methodology to obtain the expected cost and time to finish the construction of a breakwater so that an adequate Risk Assessment of the construction process can be made.
- To use the Risk Assessment Model thus developed to give an indication of what type of insurance premium would have to be paid for the construction risk to be transferred from the Client or Contractor onto an Insurer.

1.3. Scope

There are infinite variations in the possible geometries of a caisson breakwater and therefore it is necessary to clearly define the scope of the present research. This thesis will only concern itself with caisson breakwaters that are not protected by wave-dissipating concrete blocks or situations in which the effect of these blocks can be ignored. Also, the research will assume that the rubble mound foundation on which the caisson sits is formed of a homogeneous gravel of fairly small diameter, and that this rubble mound has a depth of several meters. Geometries where the caisson sits on a thin layer of gravel overlaying sand are clearly out of the scope of the present research, due to complex interactions between the gravel and sand layers which could confound the basic methodologies set out in the current dissertation.

As all the laboratory experiments that were carried out were small in scale it was impossible to measure the elastic deformations that took place. Only the final plastic movements could be recorded, which was thought to be adequate for the purposes of the present research.

The effects of only two types of waves (wind waves and solitary waves) will be considered in the calculation of the deformations to the rubble mound, as these are the main types of waves which cause damage to breakwaters and coastal areas in general.

Regarding breakwater failure modes, for the laboratory experiments only sliding and tilting of the upright sections will be considered. Overturning failure will also be considered in the methodology to assess risk during the construction phases, but slip failure will be ignored as this phenomenon sufficiently well understood and rare enough that it can be prevented by adequate design.

The methodology to calculate the cost and time to construct a breakwater is only valid for the Japanese Islands, as all factors not related to climate and construction accidents were omitted as a source of risk. This methodology also assumes that fairly small breakwaters will be constructed, and it would be necessary to modify it for the calculation of long breakwaters by introducing extra construction phases.

1.4. Organization of the dissertation

The present dissertation is organized into eight chapters. The current chapter has given a brief background of the subject of the study, highlighting the need, relevance, objectives and scope of the thesis.

Chapter two will summarise the background of the research and highlight key studies carried out by other authors to date.

Chapter three will provide a justification for the limitation of the active depth of foundations to the top area of the caisson breakwater. This justification is backed by laboratory experiments which were analysed to show that the traditional Bousinesq theory can be applied to calculate the stress in the top of a gravel rubble mound subjected to impact waves.

Chapter four will show the laboratory experiments that were carried out to obtain the probability distribution functions of sliding and tilting of a caisson breakwater subjected to several storms of similar intensity.

Chapter five will introduce a modification to the Deformation-Based Reliability Design Method developed by Shimosako and Takahashi (1998, 1999) to include tilting and the effect that this will have on the computation of the sliding distance.

Chapter six deals with the deformations that can be expected in the rubble mound of a caisson breakwater subjected to solitary wave attack. The laboratory experiments that were carried out will be shown, and the model introduced in chapter five will be used to reproduce the deformations recorded.

Chapter seven highlights real-life failures of caisson breakwaters and attempts to reproduce the deformations recorded in one case study by applying the methodology introduced in chapter five.

Chapter eight will develop a new methodology for the risk assessment of a breakwater during its construction, which allows for the determination of the expected cost, time to complete and insurance premium that would have to be paid to insure the breakwater against the damage due to adverse weather.

Chapter nine summarizes the findings of the study and gives recommendations for future research.

1.4. Rationale

Hopefully, the results of the present dissertation will allow designers to be able to make an adequate risk assessment of the construction process of a caisson breakwater, thus allowing the life-cycle costs to be more accurately estimated. This should result in leaner breakwater sections, with the risk and reliability of the structure being more clearly defined.

CHAPTER 2

LITERATURE REVIEW

2.1. Definition of Caisson Breakwater

Different authors use the term caisson breakwater to define structures that are not necessarily identical. The European Research Project PROVERBS (regarding the PRObabilistic methods to design VERtical BreakwaterS) states that it concerns itself

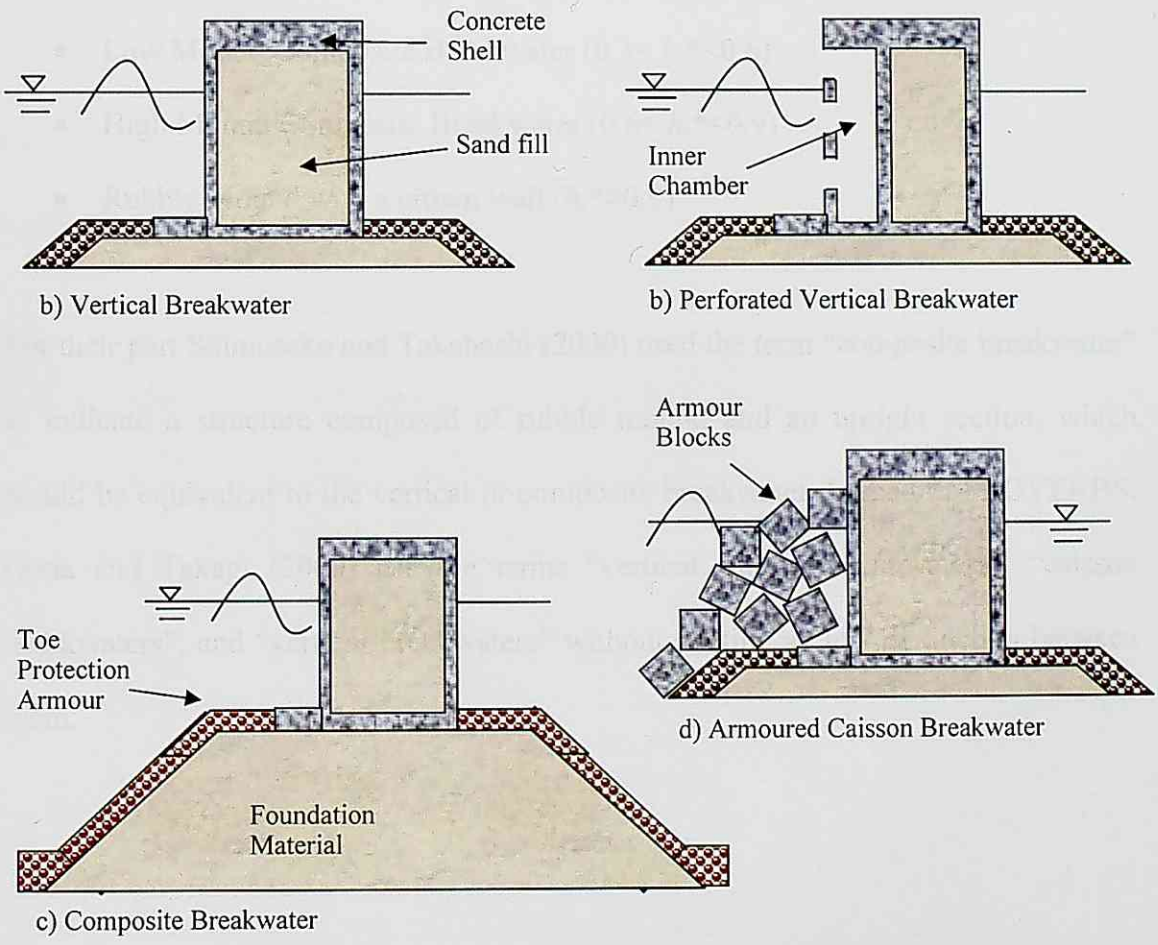

Fig. 2.1: Breakwater Types according to PROVERBS

with a number of breakwater that are not identical. Each of these breakwaters has a caisson structure in it, but the way the breakwater as a whole is defined depends on other components as shown on Fig. 2.1:

According to this report the breakwaters can be classified according to their relative berm height (h_r*),

$$h_r^* = h_r/h \qquad (2.1)$$

where h_r is the height of the rubble mound and h is the depth of water in front of the breakwater as shown in Fig. 2.2.

Thus the structure can be classified as:

- Vertical Breakwater (h_r*<0.3)
- Low Mound Composite Breakwater (0.3< h_r*<0.6)
- High Mound Composite Breakwater (0.6< h_r*<0.9)
- Rubble Mound with a crown wall (h_r*>0.9)

For their part Shimosako and Takahashi (2000) used the term "composite breakwater" to indicate a structure composed of rubble mound and an upright section, which would be equivalent to the vertical or composite breakwater defined in PROVERBS. Goda and Takagi (2000) use the terms "vertical caisson breakwaters", "caisson breakwaters", and "vertical breakwaters" without making a clear distinction between them.

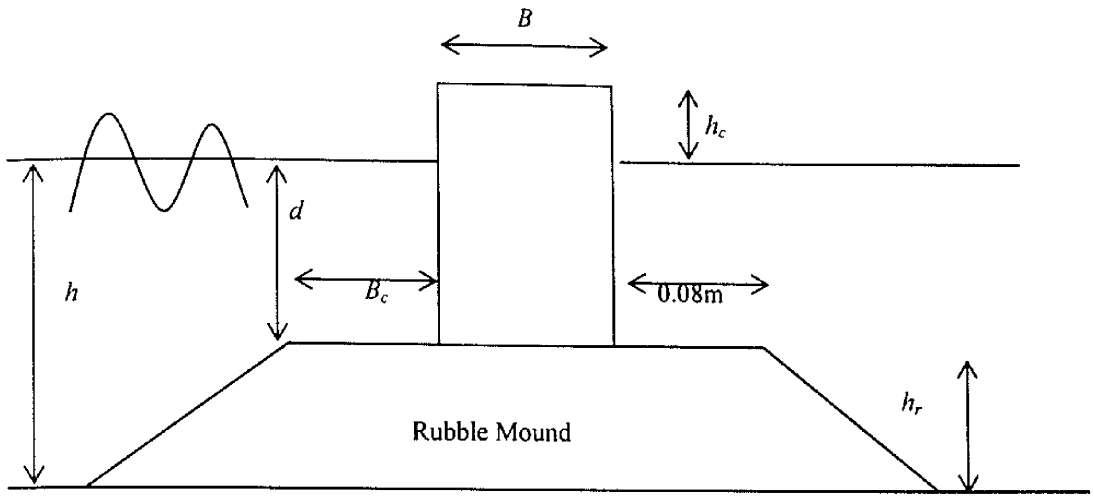

Fig.2.2. Basic geometric parameters

In the present work the term caisson breakwater will be used for any type of vertical structure made of a caisson that does not have any form of armour units protecting it that are located above sea level. This corresponds to the classification of vertical and composite breakwater of PROVERBS and composite breakwater of Shimosako and Takahashi. The majority of the work in the present thesis will concern itself with the design of this type of structures, though in Chapter 7 the failure of an "armoured caisson breakwater" will also be analysed.

2.2. Failure modes of caisson breakwaters

When designing a caisson breakwater a number of failure modes must be considered during design. Burcharth and Sorensen (1998) give a list of the most important failure modes:

- Shoreward sliding
- Overturning around the heel
- Slip failure in the subsoil and settlement
- Slip failures in the rubble foundation and subsoil

- Erosion of rubble foundation, forward tilt and settlement
- Scour in the seabed, forward tilt and settlement
- Breakage and displacement of armour units (in the case of rubble mound with a crown wall type breakwaters).

The bearing capacity failure in the rubble foundation may take place in several ways. With a shallow rupture surface underneath the harbour side edge of the wall, the wall will strongly rotate, and so it can be called a "rotational failure". This is similar to what is called the "overturning" mode of failure, which normally involves some bearing capacity failure. PROVERBS stresses how the rotation axis will never be at the very edge of the caisson, and it recommends to consider rotation failure instead of overturning in design.

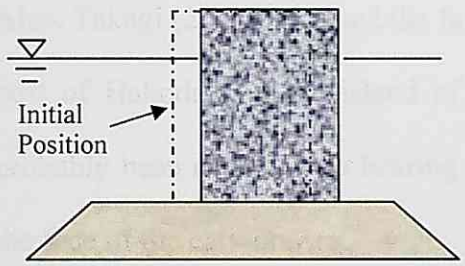

a) Sliding Failure

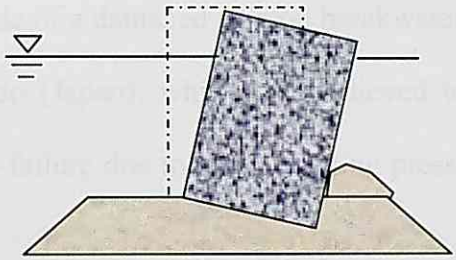

b) Bearing Capacity Failure in Rubble

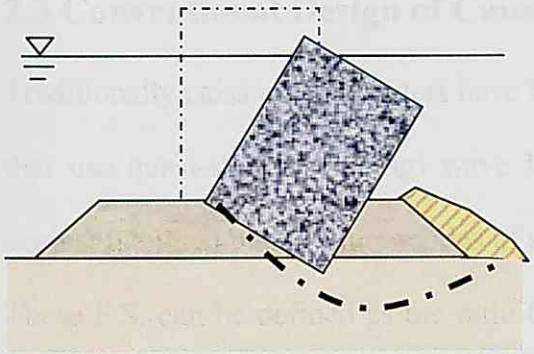

c) Bearing Capacity Failure in subsoil

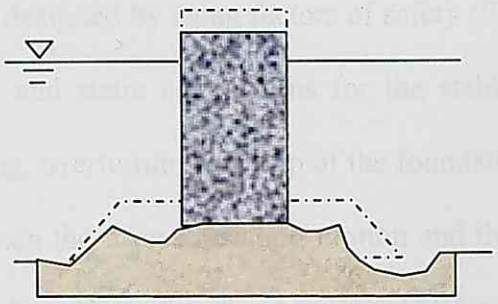

d) Settlement by consolidation, creep or loss of fine grains

Fig. 2.3. Illustration of Some Failure Modes of Caisson Breakwaters

Goda (1999) provides some case studies of the well-documented failures of the breakwater at Sines Harbour (Portugal) and the Mustapha breakwater at Algiers Harbour in Algeria. The Mustapha breakwater failed during its construction in 1930-31, and interestingly most of the failed sections fell towards the seaside. At the time it was assumed that the heavy scouring of the seabed in front of the breakwater was the cause of collapse, yet recently it is thought that maybe a slip failure through the seabed could have caused the failure.

A more recent example of breakwater failure is that of Susami West Breakwater as described by Kim et al, 2005. This armoured caisson breakwater was severely damaged by Typhoon Tokage in 2004, with the wave-dissipating concrete units collapsing and the caissons being displaced by a distance of between 6 to 10 metres. Also, Takagi (2007) analysed the failure mode of a damaged caisson breakwater at the port of Hakodate in the island of Hokkaido (Japan), which was believed to have probably been caused by a bearing capacity failure due to large standing pressures at the face of the caisson.

2.3 Conventional Design of Caisson Breakwaters

Traditionally caisson breakwaters have been designed by using factors of safety (F.S.) that use quasi-static (standing) wave loads and static calculations for the stability against the three main failure modes of sliding, overturning and slip of the foundation. These F.S. can be defined as the ratio between the forces resisting motion and those causing it and, for example, Goda (1974) defines the safety factors against sliding as the ratio of the frictional resistance to the horizontal wave force.

The traditional design method is also referred to as "deterministic design" as it does not consider the uncertainty in the determination of the deepwater wave height, wave period, wave transformation, wave forces or friction factor, as these uncertainties are considered to be covered by the F.S. Traditional coastal engineering practice establishes that a structure must have a F.S. of at least 1.2 in order to take into account the aforementioned uncertainties in the design process, though this safety factor does not guarantee the stability of the breakwater.

The offshore design wave height is determined as the wave which has a return period equal to the service lifetime in the extreme distribution function of wave heights (typically Weibull, FT-I or FT-II distributions). This extreme distribution function is obtained from a historical record of the observed extreme waves and/or hindcasting over many years. As these waves approach the coastline they undergo significant changes in their height, period, and shape due to the processes of reflection, refraction and wave breaking as described by Goda (1974). It is therefore possible to obtain the wave parameters in front of the breakwater, and by using the Goda formula as modified by Takahashi (1994) or that of Minikin (1950) the pressure due to the wave on the structure can be calculated.

However, a number of authors have identified problems related to this type of design, as summarised by Kim and Takayama (2002):

1. Possibility of over-design (Shimosako et al., 1998)
2. No consideration of the uncertainties in the various factors involved in the design process (Shimosako and Takahashi, 1998)
3. No information on the possible degree of breakwater damage (Goda, 2001)
4. Inability to explain the integrated failure mechanism (Oumeraci, 1994)

All these limitations have led to the research into different philosophies for breakwater design.

2.4. Reliability Design of Caisson Breakwaters

Reliability engineering is the discipline of ensuring that a structure will be reliable when operated in a specified manner. Reliability can be thus defined as the probability that a system will perform its intended function during a specified period of time under stated conditions. This can be expressed mathematically as:

$$R(t) = \int^{\infty} f(x)dx \qquad (2.2)$$

where $f(x)$ is the failure probability density function.

Under traditional design, deformations in structures are not allowed and any movement is considered as a failure. However, most coastal structures can maintain their functionality providing the deformations incurred are relatively small. This concept of deformation-based design has already been adopted in some other fields, such as the design of harbour facilities against earthquakes, where a limited deformation is allowed for in the design. In this type of design it is accepted that there is always some chance of failure, and hence reliability engineering is concerned with meeting the specified probability of success, at a specified statistical confidence level. To be noted is how this reliability design applies only to a specified period in time (i.e. the system has a specified chance that it will operate without failure before a certain time). Reliability design is key to the concept of life cycle management, and

comprises development, testing, construction, operation and eventual decommissioning of the structure.

2.4.1. Reliability-Based Design Categories

Three types of reliability design methods exist:

Level 1 methods are similar to the traditional design methods described previously, and use partial safety coefficients for the limit state design. Level one methods are the easiest to use and from April 2007 they will be introduced to at least some of the Japanese Codes of Practice for coastal structures.

Level 2 methods are the next higher level, and they use a reliability index which expresses the safety level in consideration of all probabilities. This safety index is given by

$$\kappa = \frac{m_L - m_R}{\sqrt{\sigma_L^2 + \sigma_R^2}} \tag{2.3}$$

where κ is the safety index, m_L and m_R are the mean of the load and resistance respectively, and σ_L and σ_R the standard deviations. Level 2 methods (such as the Hasofer-Lind method) are more complicated to use than Level 1 methods, however they give a more robust idea of the risks associated with the design of the structure.

Level 3 methods are the highest level of reliability design, and they use probability distributions at all design steps. Level 3 methods indicate more directly how safe a structure is as they can be highly effective in simulating complex phenomena. Previously the large amount of computational time required to use these methods

discouraged their use, but the constant improvements in computational power are slowly allowing these methods to become viable. Representative of these methods is the use of stochastic algorithms such as the Monte Carlo simulation technique as described is subsequent sections.

2.4.2. History of Reliability Design of Breakwaters

The probabilistic design of structures has been developed from as early as the 1960's. Ito el al. (1966) conducted a study on the stability of caisson breakwaters including sliding and proposed a design concept of the expected sliding distance against a certain design wave. Other researchers such as Horikawa et at. (1972) also discussed the sliding distance of a composite breakwater, though at the time is was difficult to estimate the wave pressure precisely and hence it was difficult to obtain an accurate sliding distance.

Application of the reliability-based design method to breakwaters only really started in the mid-1980's. Van der Meer (1988) offered a probabilistic approach to the design of rubble mound breakwaters, which gives the necessary armour weight at a certain damage level directly from the wave height and Burcharth (1991 and 1992) introduced the reliability-based design methods for breakwaters. Regarding caisson breakwaters, Toyama (1985) and Suzuki (1987) discussed the sliding stability by using a reliability-based design method. Franco et al (1986) carried out an application of a reliability-design method to estimate the design risk of a breakwater in Italy. Their approach was to consider the estimation error of the occurrence probability of abnormally high waves and in the determination of the friction factor. However the uncertainties in other factors such as the estimation of the wave transformation or

wave forces were not considered, so Takayama and Fujii (1991) proposed a method to evaluate the sliding by taking into account the uncertainties in some parameters (such as wave height, friction factor and wave forces). Later, Takayama and Ikeda (1993) developed a method to estimate the errors of uncertain factors by employing the assumption that the estimation errors can be expressed as a Gaussian distribution (with a defined mean and standard deviation). They also provided values for the parameters of these normal distributions based on existing observed and experimental data. Takayama et al (1994) studied a reliability-based design which considered the reconstruction cost of a breakwater by analyzing the probability of failure.

2.4.3. Deformation-Based Reliability Design Method

In various papers Shimosako and Takahashi (1998, 1999, 2000) developed what they called the "Deformation-Based Reliability Design Method"(DBRD). The main idea of this method is that caisson breakwaters can maintain their functionality even if a limited amount of deformation takes place. These studies concern themselves only with the sliding of the caisson and hence they use the concept of estimated sliding distance (*ESD*). This *ESD* is estimated by carrying out a Monte Carlo (level III) simulation and obtaining the average sliding distance of a few thousand simulations:

$$ESD = \frac{\sum_{1}^{N} SD}{N} \tag{2.4}$$

where *SD* is the sliding distance of one simulation and *N* is the number of simulations.

Recently a significant amount of research into DBRD has been done in Japan, as shown in Table 2.1. Kim and Takayama (2005) introduced a modification to the original model of Shimosako and Takahashi (1999) to take into account the reduction

in the sliding distance due to the tilting of the caisson. Esteban and Shibayama (2006, 2007) separated the movement of the caisson into vertical and horizontal components, with the vertical movement (tilt) influencing the sliding movement. This work is described in more detail in Chapter 5 of the present thesis.

Although the breakwater can slide and maintain its function, as Shimosako and Takahashi (1998, 1999) indicate, after it has slid by a certain distance (ESD_{limit}) it should be considered to have failed and remedial action should take place. Shimosako and Takahashi (2000) limit this distance to 0.3m, though they give no reason for their choice. Goda and Takagi (2000) propose a more restricted limit of 0.1m, though again no reason is given for this choice. Later, Goda (2001) proposed to define the optimal design in a way where the probability of the total sliding distance throughout the caisson's lifetime exceeding 0.3m is equal to or less than 10%.

The issue of which failure mechanism is most likely to occur for a given storm within the framework of the DBRD is often not clear, and to this effect Takagi (2007) introduced the concept of "Expected Occurrence in Frequency (EOF)". This index associates a degree of potential risk for each failure mode according to the wave conditions at a certain storm.

Table 2.1. Recent Studies on Deformation-Based Design Methods

Author(s)	Year	Description
Shimosako and Takahashi	1998, 1999, 2000	Development of DBRD Method
Takayama et al.	2000	Consideration of the effect of directional occurrence distribution of extreme waves in the computation of ESD
Goda and Takagi	2000	Economical optimization of life-cycle of caisson breakwaters by using DBRD, introduction of optimal return period for the selection of design wave heights
Goda	2001, 2004	Proposal of spread parameter of extreme wave height distribution
Takahashi et al.	2003	Application of performance design based on DBRD method to caisson-type breakwaters
Hanzawa et al.	2003	Consideration of damage to wave-dissipating concrete blocks in computation of *ESD*
Kim and Takayama	2003	Introduction of a doubly-druncated normal distribution to improve the estimation of the *ESD*
Kim and Takayama	2005	Consideration of the effect of tilting on the calculation of the *ESD*
Kim and Takayama	2005	Case Study of the deformation of a breakwater damaged by a typhoon
Esteban and Shibayama	2006	Calculation of tilting angle and effect of this angle in computation of the *ESD*
Takagi and Shibayama	2006	Improvement in the estimation of the standing wave for the *ESD* of deepwater caissons
Takagi	2007	Introduction of an Expected Occurrence in Frequency (EOF) Index

2.4.5. Monte Carlo Simulations

Monte Carlo methods are a widely used type of computational algorithms for simulating the behaviour of various physical and mathematical systems. They are distinguished from other simulation methods by their stochastic nature i.e they use random or pseudo-random numbers and therefore these methods are non-deterministic.

The name ``Monte Carlo'' was coined during the Manhattan Project of World War II, because of the similarity of this statistical simulation to games of chance (with the capital of Monaco being a well know centre for gambling).

Central to the Monte Carlo methodology is the concept that each parameter in the model is not defined by a single number but by a probability distribution function. At each stage in the calculation process the computer will pick up a random value from within this probability distribution and use this value in the computation. These probability distribution functions can take many shapes, and the computer programs developed in the present thesis will deal mainly with normal (Gaussian) and Rayleigh distributions.

In order to obtain a random value from each probability distribution the computer needs to simulate sets of random numbers. These random numbers are used to pick up values from within the probability distribution, and are generated using pseudo-random number generators. Pseudo-random number generators use deterministic algorithms and hence the sequences of numbers they produce are purely deterministic and thus can only approximate a true random sequence. To be able to generate different sets of numbers it is necessary to specify a different initial value, or *seed*, as typically initialising the generator with the same seed will give the same sequence of random numbers.

2.4.6. Uncertainty in the Design Factors

In order for a Level III Design Method to be accurate it is important that the range and probability of occurrence of the different design parameters is known. Takayama and

Ikeda (1993) assumed that these parameters would follow a Gaussian distribution and as such would have a characteristic probability distribution function -defined by a mean value and a Coefficient of Variation (CoV). Since then research in the DBRD has assumed that the uncertainty in the factors associated with caisson structures (estimation of deepwater wave, wave transformation, wave force, friction factor, wave period and storm surge) follow this normal distribution. As the effect of changes in these factors has not been completely clarified up to now different researchers have used different factors as shown in Table 2.2. The original values proposed by Takayama and Ikeda (1993) were based on existing experimental and observed data. However Shimosako and Takahashi (1998) thought it was appropriate to modify these values by citing the following reasons:

- Wave transformation. The bias (-0.13) given by Takayama and Iked (1993) a has a negative value and by employing it the sliding distance obtained is smaller than that computed without considering the effect of uncertain factors.
- Friction factor. Shimosako and Takahashi investigated the data used by Takayama and Ikeda (1993) to determine the friction factor. They found that there were a small number of extreme values which were distorting the results. Thus by excluding these values they arrived at smaller values for the bias and the CoV.
- Wave force. The occurrence frequency distribution of the wave force ratio (of the experimental data to the values computed by Goda's wave force formula) that is used by Takayama and Ikeda (1993) is unsymmetrical, though it is assumed to be a symmetrical normal distribution. Hence some wave forces, which are not sustained by the experimental data, have a possibility of occurring in the computation.

Goda and Takagi (2000) and Goda (2001) use the values of previous researchers but Takayama et al. (2000) changed the values for the wave forces because of the effect of the modification of the Goda formula by Takahashi et al. (1994).

Table 2.2. Uncertainties in Design Parameters according to different authors.

		Uncertain Factors											
		Deepwater wave		**Wave transform.**		**Wave Force**		**Friction factor**		**Significant wave period**		**Storm Surge**	
Researcher	**Year**	**Bias**	**CoV**	**Bias**	**CoV**	**Bias**	**CoV**	**Bias**	**CoV**	**Bias**	**CoV**	**Bias**	**CoV**
Takayama and Ikeda	1993	0	0.1	-0.1	0.09	-0.1	0.17	0.06	0.16	-	-	-	-
Shimosako and Takahashi	1998	0	0.1	0	0.1	0	0.1	0	0.1	0	0.1	0	0.1
Takayama et al.	2000	0.06	0.11	.0.03	0.04	-0.1	0.22	0.06	0.16	-	-	-	-
Goda and Takagi	2000	0	0.1	-0.1	0.1	-0.1	0.1	0.06	0.1	-	-	-	-

2.5. Wave Forces on a Vertical Structure

The most commonly used method to determine the wave pressure on a vertical breakwater is that formulated by Goda (1974) and successively modified by Takahashi (1994).

2.5.1. Main Assumptions of the Model

The model assumes the existence of a trapezoidal pressure distribution along a vertical wall, as shown in Fig. 2.4, regardless of whether the waves are breaking or nonbreaking. In the figure, h denotes the water depth in front of the breakwater, d the depth above the armour layer of the rubble foundation, h' the distance from the design

water level to the bottom of the upright section and h_c the crest elevation of the breakwater above the design water level.

The elevation to which the wave pressure is exerted (η^*) is given by the formula:

$$\eta^* = 0.75(1+\cos\beta)H_{\max} \tag{2.5}$$

where β denotes the angle between the direction of wave approach and a line normal to the breakwater and $H_{\max}$ is the highest wave in the design sea state (which Goda (1985) recommends should be taken as $1.8H_{1/3}$)

2.5.2. Wave pressure on the front of a vertical wall

The following pressure parameters have to be calculated

$$p_1 = \frac{1}{2}(1+\cos\beta)(\alpha_1 + \alpha^*\cos^2\beta)\rho g H_{\max} \tag{2.6}$$

$$p_2 = \frac{p_1}{\cosh(2\pi h/L)} \tag{2.7}$$

$$p_3 = \alpha_3 p_1 \tag{2.8}$$

in which

$$\alpha_1 = 0.6 + \frac{1}{2}\left[\frac{4\pi h/L}{\sinh(4\pi h/L)}\right]^2 \tag{2.9}$$

$$\alpha^* = \max(\alpha_2,\ \alpha_1)\begin{cases} \alpha_2 = \min\left[\dfrac{h_b - d}{3h_b}\left(\dfrac{H_{\max}}{d}\right)^2,\ \dfrac{2d}{H_{\max}}\right] \\ \\ \alpha_1 = \alpha_{1H}\alpha_{1B} \end{cases} \tag{2.10}$$

$$\alpha_3 = 1 - \frac{h'}{h}\left[1 - \frac{1}{\cosh(2\pi h / L)}\right] \tag{2.11}$$

where h_b is the water depth at a location at a distance $5H_{1/3}$ seaward of the breakwater, $H_{1/3}$ is the significant incident wave height, L is the wavelength at water depth h, ρ is the density of water and g is the acceleration of gravity.

The factor α^* was originally proposed by Takahashi et al. (1994) to estimate the intensity of the impulsive waves and replaced the factor α_2 in the original Goda formula. The factors α_{IH} and α_{IB} were also proposed by Takahashi et al. (1994) and can be evaluated using the following sets of equations:

$$\alpha_{IH} = \min\left(H/2,\ 2.0\right) \tag{2.12}$$

$$\alpha_{IB} = \begin{cases} \cos\delta_2 / \cos\delta_1 & \delta_2 \le 0 \\ 1/(\cosh\delta_1 \cosh^{1/2}\delta_2 & \delta_2 > 0 \end{cases} \tag{2.13}$$

$$\delta_1 = \begin{cases} 20\delta_{11} & : \delta_{11} \le 0 \\ 15\delta_{11} & : \delta_{11} > 0 \end{cases} \tag{2.14}$$

$$\delta_2 = \begin{cases} 4.9\delta_{22} & : \delta_{22} \le 0 \\ 3.0\delta_{22} & : \delta_{22} > 0 \end{cases} \tag{2.15}$$

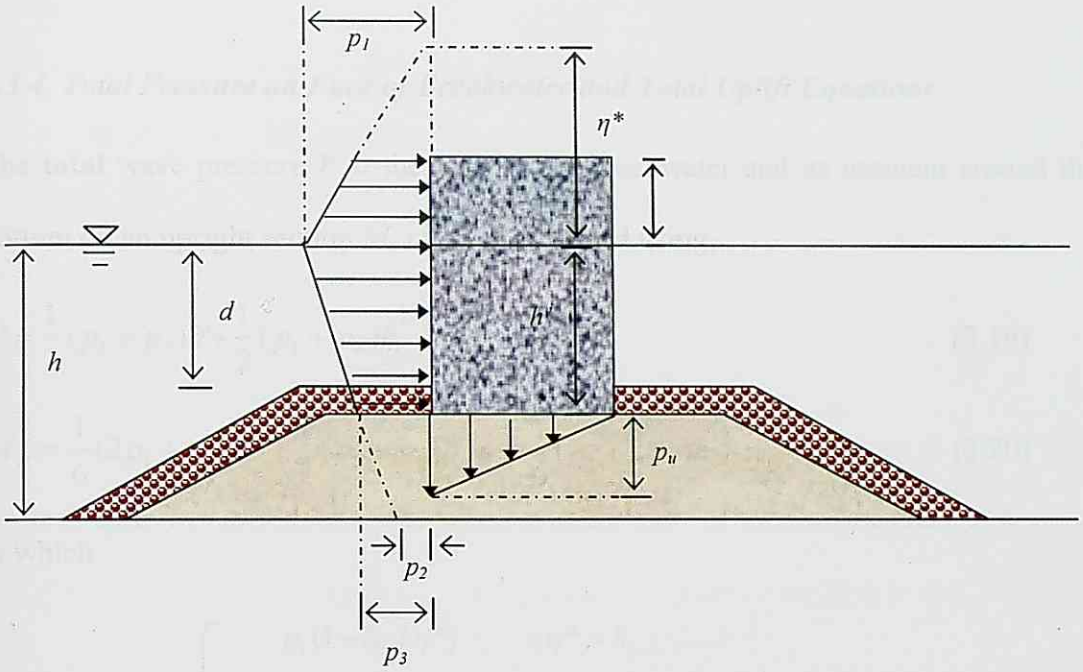

Fig. 2.4 Distribution of wave pressure on an upright section of a vertical

$$\delta_{11} = 0.93\left(\frac{B_C}{L} - 0.12\right) + 0.36\left(0.4 - \frac{d}{h}\right) \tag{2.16}$$

$$\delta_{22} = -0.36\left(\frac{B_C}{L} - 0.12\right) + 0.93\left(0.4 - \frac{d}{h}\right) \tag{2.17}$$

where B_c denotes the berm length of the rubble mound foundation.

2.5.3. Buoyancy and uplift pressure

The buoyancy of the displaced volume of the upright section in still water below the design water level has to be calculated. The uplift pressure acting at the bottom of the caisson is assumed to have a triangular distribution as shown in Fig. 2.4, and the value of the toe pressure p_u is given by the following Eq.:

$$p_u = \frac{1}{2}(1 + \cos\beta)\alpha_1\alpha_3\rho g H_{\max} \tag{2.18}$$

2.5.4. Total Pressure on Face of Breakwater and Total Uplift Equations

The **total** wave pressure P at the face of the breakwater and its moment around the bottom on an upright section M_p can be calculated using,

$$P = \frac{1}{2}(p_1 + p_3)h' + \frac{1}{2}(p_1 + p_4)h_c^* \tag{2.19}$$

$$M_P = \frac{1}{6}(2p_1 + p_3)h'^2 + \frac{1}{2}(p_1 + p_4)h'h_c^* + \frac{1}{6}(p_1 + 2p_4)h_c^{*2} \tag{2.20}$$

in which

$$p_4 = \begin{cases} p_1(1 - h_c/\eta^*) & : \eta^* > h_c \\ 0 & : \eta^* > h_c \end{cases} \tag{2.21}$$

$$h_c^* = \min(\eta^*, h_c) \tag{2.22}$$

The **total** uplift pressure U and its momentum around the heel of the caisson M_u can be calculated by using

$$U = \frac{1}{2}p_u B \tag{2.23}$$

$$M_U = \frac{2}{3}UB \tag{2.24}$$

where B denotes the width of caisson.

2.5.5. Safety factors against sliding and overturning

The safety factor against sliding and overturning of an upright section under wave action can be defined by the following equations:

Sliding $$F.S. = \frac{\mu(W'-U)}{p} \tag{2.25}$$

Overturning $$F.S. = \frac{Wt - M_U}{M_p} \tag{2.26}$$

where μ indicates the coefficient of friction between the upright section and the rubble mound, t the horizontal distance between the centre of gravity and the heel of the upright section and W' is the weight of the caisson per unit extension in still water.

Goda (1985) indicates how in the design of vertical breakwaters in Japan, the safety factors against sliding and overturning must not be less than 1.2 and μ is usually taken to be 0.6.

2.5.6. Analysis of bearing capacity of foundations according to Goda

Goda (1985) indicates how the bearing capacity of the foundation is to be analysed by means of the methodology of foundation engineering for eccentric inclined loads. However, for sites where the seabed consists of a dense sand layer or soil of good bearing capacity a simplified technique of examining the magnitude of the heel pressure can be used. In this case, it is assumed that a trapezoidal or triangular distribution of bearing pressure exists beneath the bottom of the upright section, and the largest bearing pressure at the heel p_e can be calculated by using:

$$p_e = \frac{2W_e}{3t_e} \qquad : t_e \le \frac{1}{3}B$$

$$p_e = \frac{2W_e}{B}(2 - 3\frac{t_e}{B}) \qquad : t_e > \frac{1}{3}B \tag{2.27}$$

in which

$$t_e = \frac{M_e}{W_e}, \qquad M_e = Wt - M_U - M_P, \qquad W_e = W' - U \tag{2.28}$$

Goda (1985) recommends that the bearing pressure at the heel should be kept below a value of about 50 ton/m^2, but also indicates how in recent breakwater designs this limit is gradually being increased to 60 ton/m^2 or greater.

2.6. Wave Deformations

2.6.1. Wave Shoaling

As waves propagate towards the coastlines in gradually decreasing depths the wave height will change due to the effect of the bottom on the wave profile. The change in wave height due to varying depth is called shoaling. The cause of the variation in the wave height is the variation in the speed of energy propagation (i.e. the group velocity).

For the case of random sea waves, the variation of wave height occurring in relatively shallow water can be modelled using the equations proposed by Shuto (1974). In these equations the shoaling effect can be evaluated by:

$$K_s \equiv \frac{H}{H_0'} \tag{2.29}$$

where K_s is the shoaling coefficient, H is the incident wave height and H_0' is the deepwater wave height.

In order to evaluate K_s the following equations are used,

$$\left.\begin{array}{ll} K_s = K_{si} & : h_{30} \le h \\ K_s = (K_{si})_{30}\left(\dfrac{h_{30}}{h}\right)^{2/7} & : h_{50} \le h \le h_{30} \\ K_s\left(\sqrt{K_s} - B\right) - C = 0 & : h \le h_{50} \end{array}\right\} \qquad (2.30)$$

in which K_{si} denotes the shoaling coefficient for a small amplitude wave, h_{30} and $(K_{si})_{30}$ are the water depths satisfying Eq. 2.31 below and the shoaling coefficient for that depth, respectively, h_{50} is the water depth satisfying Eq. 2.32, and B and C are constants given by Eq. (2.33).

$$\left(\frac{h_{30}}{L_0}\right)^2 = \frac{2\pi}{30}\frac{H_0'}{L_0}(K_{si})_{30} \qquad (2.31)$$

$$\left(\frac{h_{50}}{L_0}\right)^2 = \frac{2\pi}{50}\frac{H_0'}{L_0}(K_s)_{50} \qquad (2.32)$$

$$B = \frac{2\sqrt{3}}{\sqrt{2\pi H_0'/L_0}}\frac{h}{L_0} \qquad C = \frac{C_{50}}{\sqrt{2\pi H_0'/L_0}}\left(\frac{L_0}{h}\right)^{3/2} \qquad (2.33)$$

where L_0 is the wavelength in deep water, $(K_s)_{50}$ is the shoaling coefficient at $h=h_{50}$ and C_{50} is given by

$$C_{50} = (K_s)_{50}\left(\frac{h_{50}}{L_0}\right)^{3/2}\left[\sqrt{2\pi\frac{H_0'}{L_0}(K_s)_{50}} - 2\sqrt{3}\frac{h_{50}}{L_0}\right] \qquad (2.34)$$

In the computation of the shoaling coefficient, the water depths h_{30} and h_{50} are first solved by an iterative method, in order to determine at which range the water depth at the design site is located.

2.6.2. Wave Deformation due to Random Breaking

As waves approach the coastline they go through the process of shoaling till they eventually break. This breaking takes place in a relatively wide zone of variable water depth, which is called the breaking zone or surf zone. Goda (1985) provides a mathematical expression for the estimation of the wave height within this surf zone

$$H_{1/3} = \begin{cases} K_s H_0' & : h/L_0 \geq 0.2 \\ \min\left\{(\beta_0 H_0' + \beta_1 h), \beta_{\max} H_0', K_s H_0'\right\} & : h/L_0 < 0.2 \end{cases} \tag{2.35}$$

$$H_{\max} = \begin{cases} 1.8 K_s H_0' & : h/L_0 \geq 0.2 \\ \min\left\{(\beta_0 H_0' + \beta_1 * h), \beta_{\max} * H_0', 1.8 K_s H_0'\right\} & : h/L_0 \geq 0.2 \end{cases} \tag{2.36}$$

in which

$$\beta_0 = 0.028\left(H_0' / L_0\right)^{-0.38} \exp\left[20 \tan^{1.5}\theta\right] \tag{2.37}$$

$$\beta_1 = 0.52 \exp\left[4.2 \tan\theta\right] \tag{2.38}$$

$$\beta_{max} = \max\left[0.092, \quad 0.32\left(H_0^{'} / L_0\right)^{-0.29} x \exp[2.4\tan\theta]\right] \tag{2.39}$$

$$\beta_0 * = 0.052\left(H_0^{'} / L_0\right)^{-0.38} \exp\left[20\tan^{1.5}\theta\right] \tag{2.40}$$

$$\beta_1 * = 0.63\exp[3.8\tan\theta] \tag{2.41}$$

$$\beta_{max} * = \max\left[1.65, \quad 0.53\left(H_0^{'} / L_0\right)^{-0.29} x \exp[2.4\tan\theta]\right] \tag{2.42}$$

where θ is the slope of the coastline,

2.7. Scaling

In using the results of laboratory experiments great care must be taken to ensure that the parameters used in the model can be adequately scaled to prototype parameters, and hence it is necessary to use scaling laws that ensure that these parameters can be equated without incurring in errors. One such scaling law is that of Froude, which keeps the ratio of the fluid inertia forces to the gravitational forces equal in both the model and prototype. In this type of scaling, it is considered that the only force producing motion is that of gravity, and hence other forces (such as fluid friction or surface tension) are neglected. The ratio of the inertia forces to gravitational forces can be expressed by using the Froude Number (F_r):

$$F_r = \frac{C_p}{\sqrt{l_p \cdot g_p}} = \frac{C_m}{\sqrt{l_m \cdot g_m}} \tag{2.43}$$

where l is the length or height, C is the celerity, and g is the acceleration due to gravity. Subscript 'm' is used for the model and 'p' is used for the prototype.

In contrast Cauchy scaling considers the bulk modulus of elasticity of a liquid similar to that of a solid, as it denotes the ratio of an increment in stress to a decrement in

volume caused nearby. A decrement in volume represents an increment in density. In model tests where the compressibility of the fluid is important, the ideal is for the ratio of the inertia force to the elastic force to be the same in the model as in the prototype. This implies an equality of Cauchy numbers (C_y):

$$C_y = \frac{u_p \rho_p^2}{K_p} = \frac{u_m \rho_m^2}{K_m}$$

where K is the bulk modulus of elasticity and ρ is the density of the fluid

As the acceleration due to gravity is equal in both model and prototype the following scaling relations in comparison to Cauchy's law can be derived:

Table 2.3. Scaling parameters for Froude's and Cauchy's scaling laws

Parameter	**Froude**	**Cauchy**
Length	N_L	N_L
Area	$N_A = N_L^2$	$N_A = N_L^2$
Volume	$N_V = N_L^3$	$N_V = N_L^3$
Time	$N_t = \sqrt{N_L}$	$N_t = \sqrt{\frac{N_\rho}{N_K}} \cdot N_L$
Velocity	$N_u = \sqrt{N_L}$	$N_u = \sqrt{\frac{N_K}{N_\rho}}$
Acceleration	$N_a = 1$	$N_a = \frac{N_K}{N_\rho \cdot N_L}$
Mass	$N_m = N_\rho N_L^3$	$N_m = N_\rho N_L^3$
Pressure	$N_p = N_\rho \cdot N_L$	$N_p = N_K$
Force	$N_F = N_\rho \cdot N_L^3$	$N_F = N_K \cdot N_L^2$

N_L is the length scale of the model (length in prototype divided by length in model). PROVERBS indicates how the choice of scaling law to be used for a certain wave type will strongly depend on the level of aeration and the amount of entrapped air, both of which determine the compressibility of the impacting fluid mixture. The report recommends using Froude's law for scaling results from hydraulic model tests as long

as non breaking (quasi-static) waves occur at the structure. In the case of impact waves Cauchy scaling should be used for the impact component (governed by compressibility) and Froude for the quasi-static component of the wave governed by gravity, as shown in Fig. 2.5.

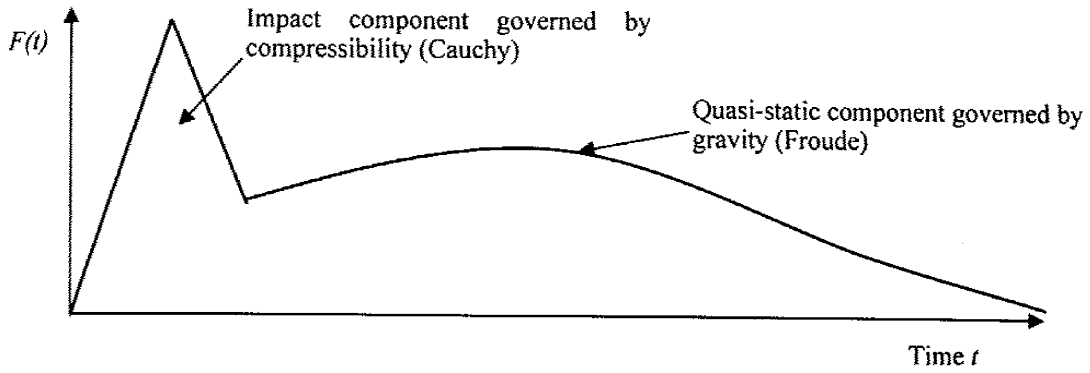

Fig. 2.5. Suggested scaling laws for each part of the wave according to PROVERBS.

2.9. Impact Loads

Waves breaking on a vertical wall sometimes cause shock pressures which are characterised by a high magnitude and short duration compared to non-breaking waves. These waves are called impact waves and are very dangerous to the stability of caisson structures, to the point that in Japan care is taken to avoid their occurrence during the design process.

2.9.1. Prediction of Impact loading

The parameter map used in PROVERBS (see Fig 2.6.) can be used to predict the type of wave loading which would be present at the breakwater. This parameter map uses details of the geometry and incident wave characteristics in order to classify

breakwaters into several types and determine what type of wave loading is likely at a certain structure.

The main parameters used in the parameter map for determination of the wave loading on the structures are:

$$h_r^* = h_r / h \tag{2.44}$$

$$H^* = H / d \tag{2.45}$$

where H^* is the relative wave height, h_r^* the relative berm height, H the incident wave height, d the depth of water at the berm, h the waver depth in front of the berm and h_r the height of the rubble mound.

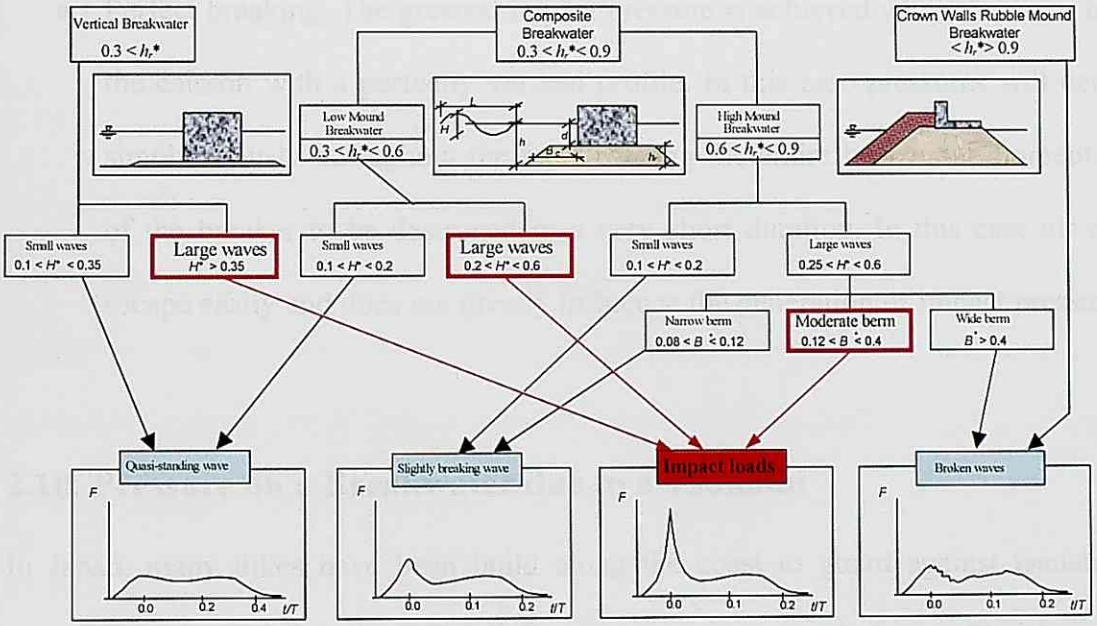

Fig. 2.6. Parameter map used in PROVERBS to determine impact loading

2.9.2. Classification of Impact Waves

Kirkgöz (1978) classified the way in which impact waves break onto a vertical face into three categories, as outlined below,

- Early breaking. If the breaking point of the wave is seaward of the breakwater, the face of the plunging breaker will become vertical before it reaches the wall. This causes the crest to curl over and strike the wall in a jet-like fashion before falling down. A considerable amount of air is entrapped within the wave, which will mix with the air to form bubbles, the exact effect of which is still not clearly understood.
- Late breaking. If the wave profile has not become vertical before it hits the wall, impact pressures will not be produced simultaneously throughout the face of the caisson. In this case very little air is entrapped within the breaker.
- Perfect breaking. The greatest impact pressure is achieved when the wave hits the caisson with a perfectly vertical profile. In this case pressures will occur simultaneously throughout the face, causing the entire horizontal momentum of the breaker to be destroyed in a very short duration. In this case air can escape easily and does not greatly influence the generation of impact pressures.

2.10. Pressure on a Breakwater due to a Tsunami

In Japan, many dikes have been build along the coast to guard against tsunamis, storms surges and high waves. These dikes can prevent tsunamis from infiltrating into the hinterland, although the tsunami heights that can be expected in the future can be larger than the height of the coastal dikes in some areas (Naksuksakul 2006). The possible damage that these tsunamis could cause and how effective the dikes will be should be assessed in order to formulate a comprehensive disaster management policy.

A number of studies on the wave forces due to tsunamis have been made, some of which are summarised below.

2.10.1 Tanimoto et al. (1984)

Tanimoto et al (1984) performed large-scale experiments on an upright breakwater using a sine wave, and proposed the following formulas to estimate the wave pressue:

$$p_m(z')/\rho g a_H = 2.2(1 - z'/3\alpha_H) \qquad \text{for} \quad (0 \le z'/a_H \le 3)$$

$$p_m(z')/\rho g a_H = 2.2 \qquad \text{for} \quad (z'/a_H \le 0) \qquad (2.45)$$

where p_m is the maximum wave pressure, z' is the height from the still water level, a_H is the amplitude of the wave, ρ is the density of water and g is the acceleration of gravity.

2.10.2. Ikeno et al. (2001 and 2003)

This formula was developed by conducting laboratory experiments to simulate a bore-like tsunami colliding on an offshore upright wall, and basically introduced an extra coefficient α to simulate wave breaking into the formula of Tanimoto et al. (1984). Later, Ikeno et al. (2003) revised their original formula so that it would give larger pressures around the still water level, using the following equation:

$$p_m(z')/\rho g a_H = 3 - z'/a_H \qquad \text{for} \quad (0.5 \le z'/a_H \le 3)$$

$$p_m(z')/\rho g a_H = 4 - 3z'/a_H \qquad \text{for} \quad (0 \le z'/a_H \le 0.5)$$

$$p_m(z')/\rho g a_H = 4 + 3.6z'/a_H \qquad \text{for} \quad (-0.5 \le z'/a_H \le 0)$$

$$p_m(z')/\rho g a_H = 2.2 \qquad \text{for} \quad (z'/a_H \le -0.5) \qquad (2.46)$$

2.11. Risk Management

In recent times a number of coastal structures have failed due to various natural disasters such as typhoons, tsunamis or storm surges. To combat potentially more frequent failures of coastal structures, a more active approach to the design and setting of risk levels has been discussed in recent times. Mockett and Simm (2002) estimate how if the coastal engineering community could make a 5% saving in the life costs of coastal and fluvial engineering projects this would lead to a benefit of about US$100 to 200 million annually in the U.K. alone. They also suggest how a better approach to the establishment of risk levels could be a key element in achieving this purpose.

2.11.1. Definition of Risk

Risk is generally expressed as the product of two separate elements, namely,

$$\text{Risk} = \text{Probability} \times \text{Consequence} \tag{2.47}$$

The consequences of a certain risk can be seen as good or desirable (an opportunity) or as bad and undesirable. In decision making it is important to understand both the probability and the consequences involved, and what level of risk is considered acceptable. The English Health and Safety Executive (HSE, 1999) states that a risk concerns the likelihood of an event that an individual does not wish to occur and, therefore, any risk will be unwelcome. However, when making decisions, risk or concerns can be divided into three different levels:

- Unacceptable, when the risk cannot be justified except in exceptional circumstances.

- Tolerable or as low as reasonably practicable, where control measures must be introduced to drive the risk towards the broadly acceptable region
- Broadly acceptable, when the level of risk is regarded as insignificant, and any resources used to further reduce the risk would be disproportionate to the risk reduction achieved.

In the design of coastal and fluvial structures Mockett and Simm (2002) identified a number of risk areas associated with coastal engineering as engineering, financial, economic, insurance, construction, operation, environment, health and safety, political and societal.

2.11.3. Risk Management Procedures

Risk management is a management process which integrates the recognition or risk, its assessment, management and the formulation to mitigate its consequences. It involves a series of sequential steps,

1. Identification of the risk in the selected domain of interest
2. Mapping out the social scope of risk, the identity and objectives of all the stakeholders involved, how the risks will be evaluated and the constraints.
3. Defining a framework for the activity and an agenda for identification
4. Analyzing the risks involved in the process
5. Developing a mitigation strategy

There are a number of approaches to manage the risk, depending on the degree of acceptability of the risk to each of the stakeholders, with the most common approaches outlined below:

- Removal of risk, generally by removing the hazard that might cause this risk to arise.
- Reduction or risk, which can involve reducing either the likelihood or consequence (or both) of the risk.
- Contingency planning, even if a risk is minimized the designer must still need to plan for what will be done if it does actually materialize.
- Acceptance of risk, which can be done in an active way by accepting that a certain event might take place and nothing will be done about it, or passively if it has not been identified.
- Transfer of risk, for example by taking out insurance.
- Sharing of risk, when several stakeholders agree to share the consequences of a risk between them.

2.11.4. Life-cycle Management of Construction using a Risk Framework

Essential to the life-cycle management of a certain construction is to use an adequate risk framework that identifies the potential sources of risks and how these will be dealt with through-out the life of the structure. By doing this it is possible to understand how reliable the structure is (i.e. what is the probability that it will be able to fulfill its purpose through-out its lifetime) and what are the possible consequences of it failing to do so. The main stages in order to do this are summarized below:

1. Identification of Need, which generally involved collecting a lot of information, talking to all the stakeholders to understand what is required and trying to achieve a consensus.

2. Functional Analysis, including a decision of the design life of the structure, acceptable levels of failure, defining the design parameters, financing, economic return, environmental impact and aesthetics, amongst others.
3. Generation of alternative solutions, which can include other projects and the consequences of "doing nothing".
4. Comparison and selection, when the various solutions will be compared to the cost of "doing nothing".
5. Final design and detailing
6. Construction
7. Management
8. Decommission and identification of a new need

2.12. Insurance

Insurance is a form of risk management primarily used to reduce or cancel the losses that could arise from a certain situation arising. Insurance is defined as the equitable transfer of the risk of a potential loss, from one entity to another, in exchange for a premium. Risk management is concerned with the practice of appraising and controlling risk. Avoiding, mitigating and transferring certain risk creates greater predictability for consumers and business, and allows people and organizations to use risk intelligently to maximize their opportunities.

Typically insurers make money in two different ways:

- underwriting, the process by which insurers select the risks to insure and decide how much in premiums to charge for accepting those risks
- investing the premiums they collect from the insured.

The calculation of the underwriting is the most difficult part of the insurance business. Using a wide assortment of data, insurers predict the likelihood that a claim will be made against their policies and price products accordingly. In order to do so, insurers use actuarial science to quantify the risks they are willing to assume and the premium they will charge to assume them.

Though in Europe caisson breakwaters are often insured during the construction stage, in Japan this practise is not usual. In Europe, in order to calculate the insurance premium (i.e. the cost to insure the breakwater) the insurer will typically use a fraction of the total cost of the breakwater, independent of the methodology and timing of the construction. However in many countries such as Japan the start date of the construction will greatly influence the risk associated with the construction of the breakwater.

Regarding breakwaters it is desirable to have a form of insurance to cover weather related risks or other possible sources of delays associated with the construction process. The actuarial profession nowadays used a combination of tables, loss models, stochastic methods and financial theory for a wide range of insurance policies, though to date no methodology to calculate the insurance premium for the construction of a breakwater has been developed.

2.13. Properties of Granular Foundation Materials

According to current Japanese design methods, the bearing capacity of a rubble mound under eccentric and inclined loads is calculated using the simplified Bishop

method. This method uses two shear strength parameters, c and ϕ, which should be determined by triaxial compression tests. Mizukami and Kobayashi (1991) established that the value of ϕ is strongly related to particle breakage at failure, and provided that the strength of the parent rock is greater than 300kgf/cm^2 recommended the use of c=2tf/m^2 and ϕ=35 degrees.

2.14. Health and Safety Characteristics of Construction Industry

The construction industry is particularly hazardous due to the complex and changing environment that workers are subjected to on a daily basis. The large number of casualties reported is disproportionate to that reported in other manufacturing sectors and greatly influences the construction procedure. It is an important factor contributing to cost overruns due to large compensation claims and delays due to accident shutdowns, inspections, etc.

2.14.1. Japanese Worker's Accident Compensation

The workers' accident compensation insurance system in Japan is under the control of the government, based on the Workmen's Accident Compensation Law (1947). It gives workers insurance benefits in order to protect them against injuries, diseases, disabilities or deaths incurred because of their duties or commuting to work. It is also applied to "diseases or disorders to workers engaged in work with hazards that can harm health from sudden or chronic action of such hazards".

The following types of insurance benefits are available for on-the-job injuries and diseases:

- medical benefit
- temporary disability benefit, when unable to work and earn wages because of treatment
- injury and disease compensation pension, when not recovered one-and-a-half years after starting to receive treatment
- physical handicaps compensation benefit: according to the degree of physical handicap the workers are left with
- bereaved family compensation benefit: to relatives who had been supported by the income of the workers concerned
- expenses for funeral rites
- nursing compensation benefit: for full-time or occasional nursing

The income benefits are calculated on the basis of the average daily wage of the workers concerned. The temporary disability benefit amounts to 60% of the average daily wage and is given starting from the fourth day of absence from work, together with the temporary disability special supplement equivalent to 20% of the average daily wage (the employer must pay compensation equivalent to 60% of the average wage for the first three days). The amount of injury and disease compensation pension, given when workers do not recover within one-and-a-half years, ranges from 245 to 313 days of the average daily wage. The physical handicaps benefit ranges from 131 to 313 days of the average daily wage. The amount of the bereaved family compensation lump sum ranges from 153 to 245 days of the average daily wage.

The government collects the insurance premium from employers. The premium is calculated by multiplying the total wages payable to all the workers in the enterprise

in the insurance year by the premium rate. This premium rate is determined for each category of enterprise, taking into account the past accident rates and other factors. A merit system is applied in determining the premium rate for different industries. The premium rates as of April 1992 for different construction sectors are shown below:

- New construction or power plants and tunnels :0.149
- New construction of railroads: 0.068
- New construction of roads: 0.049
- Others: 0.025-0.038

2.14.2. Accident statistics in Japan

The Japanese International Center for Occupational Safety and Health (JICOSH, http://www.jicosh.gr.jp/english/statistics/jcsha/) publishes various statistics regarding Health and Safety in Japanese Construction. Fig. 2.7 shows the number of accidents per 100,000 workers in one year, where an accident is defined as a worker having to stay away from work for 4 or more consecutive days.

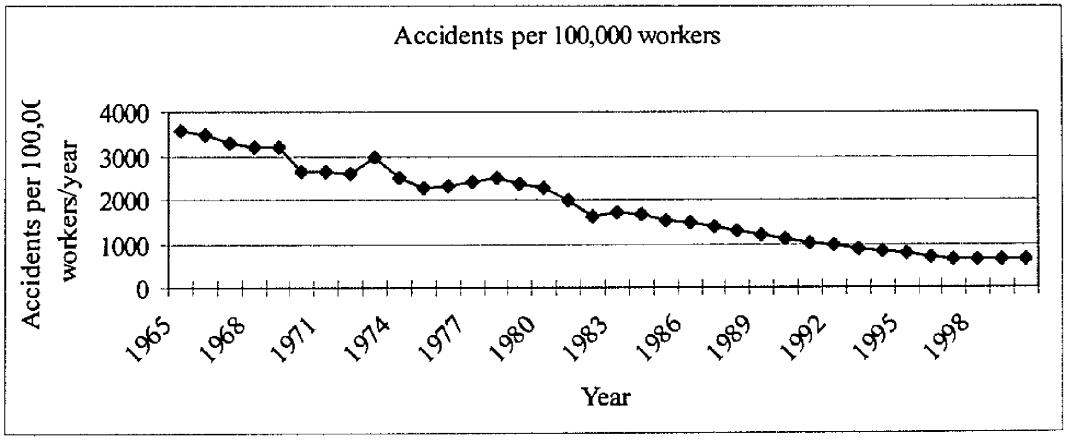

Fig. 2.7. Accident trend rate in Japanese Construction Industry

2.14.3. Accident statistics in a developing country (Thailand)

Chongsuvivatwong et al (1998) carried a survey of construction sites in Thailand by interviewing contractors and workers at a total of 184 construction sites and found the incidence of accidents for each of them. Companies on small construction sites generally provided less protection facilities than at large scale sites. The work-related death rate was 68 per 100,000 worker-years, which they considered to be 2-5 times higher than those reported in western countries. They also point how "safety measures provided by the companies were scant" and as a consequence, "injury rates and death rates were high". The pattern of deaths is similar to previous studies in other countries, with falls and electrocution amongst the most common causes.

The work-related fatality rate from this survey (68 per 100,000 worker-years) is less than half that reported previously by the Thai Department of Labour (152 per 100,000 worker-years). They attribute this to a gross underestimate by the government of the true number of construction workers.

The study concludes that "safety measures for construction workers in Thailand are poor as work-related morbidity and fatality rates are high and there is a clear need to improve this situation."

2.14.4. Comparison of H&S statistics of different countries

There is a great disparity in the Health and Safety (H&S) statistics between different countries, owing to differences in culture, construction methodologies and regulations. Generally the most economically developed countries tend to have the lower number of accidents and deaths, as can be seen from Fig. 2.8. To be noted how in the case of

Thailand there are two sets of data points. One corresponds to the number of deaths recorded by the insurance companies and the other one that observed in the study by Chongsuvivatwong et al (1998). As not all workers in Thailand are insured then this second –and higher- rate can be considered to be closer to the true real one in the case of Thailand. Chongsuvivatwong (1998) notes how there is a big difference in the safety levels observed between big construction sites –run by the bigger contractors- and the smaller sites. The larger sites have a higher concentration of insured workers and health and safety is a higher priority. The death rate of these insured workers is similar to that observed in developed countries, and for example, 19.4 workers per 100,000 worker years were killed in Thailand in 1995 compared to 15 in the United States.

A large drop in the number of deaths can be observed in Japan between 1965 (73.3 deaths per 100,000 worker-years) and 1976 (32.15). The 1950's and 1960's were a period of rapid economic growth in Japan (the real GDP per capita –measured in 1990 dollars- went from $1,921 in 1950 to $11,669 in 1976, an increase of more than 600%) and building new infrastructure was paramount in this development. Thus, considerations toward human life were second to those of schedule and cost. The situation between 1951 and 1960 was particularly bad, and eventually the government introduced new legislation such as the 1971 Construction Equipment Legislation (where Contractors were made to get licenses and were forced to introduce new safety programs). This change in legislation forced a re-thinking of the way construction was carried out and the consequent drop in the number of casualties was quite significant.

This high rates (of about 70 deaths per 100,000 workers) observed in Japan during the 1960's are of the same order as those reported in the study by Chongsuvivatwong

(1998). Also, the GDP per Capita of Thailand in 1995 ($6,573) is similar to that of Japan in 1960's (for example in 1965 it was $5,934), so it appears that countries which are at similar stages of development generally show similar levels of construction related deaths.

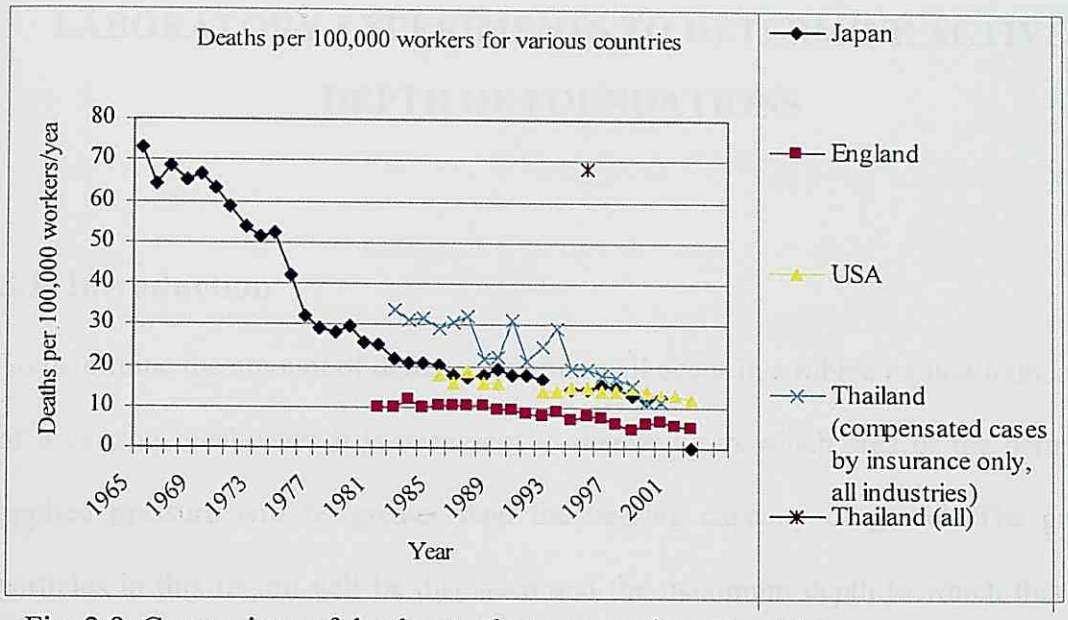

Fig. 2.8. Comparison of death rates between various countries

CHAPTER 3

LABORATORY EXPERIMENTS TO DETERMINE ACTIVE DEPTH OF FOUNDATIONS

3.1. Introduction

To determine the amount of deformation that will occur in a rubble mound foundation of a caisson breakwater it is necessary to determine in which area of the berm the applied pressure will be greater than the bearing capacity of gravel. The gravel particles in this region will be displaced and the maximum depth to which this will happen is defined as the active depth of foundations. To calculate this depth it is necessary to determine what will be the stress at different points within the rubble mound and what the bearing capacity of the gravel is. These bearing capacities can be obtained from British Standard BS 8004: 1986, which tabulates representative values for gravels of various densities.

The stresses within a homogeneous, isotropic, semi-infinite mass, due to a point load on the surface were given by Boussinesq in 1885. This theory deals with soils in which a linear stress-strain relationship is valid, and the stresses due to surface loads distributed over an area can be obtained by integrating each of the point load solutions. The stresses at a point due to more than one load can be obtained by superposition.

3.2. Laboratory Experiments

Laboratory experiments to determine the behaviour of the rubble mound foundations of a caisson breakwater under wave attack were carried out at Yokohama National University.

3.2.1 Experimental Set-Up

The wave flume used (15.3m long x 0.6m wide x 0.55m deep) together with the layout of the experimental apparatus is shown in Fig. 3.1. A scale of 1:100 was used and the water depth in the tank was kept constant throughout the experiments at h=0.30m. A submerged breakwater and a wave absorption beach were set at one end of the tank in order to dissipate the energy of the waves created by the overtopping of the caisson.

Two wave gages were placed to measure the wave conditions, one mid-way through the tank and one close to the breakwater to measure the incident wave height. Both of the wave gages were connected to a digital recorder.

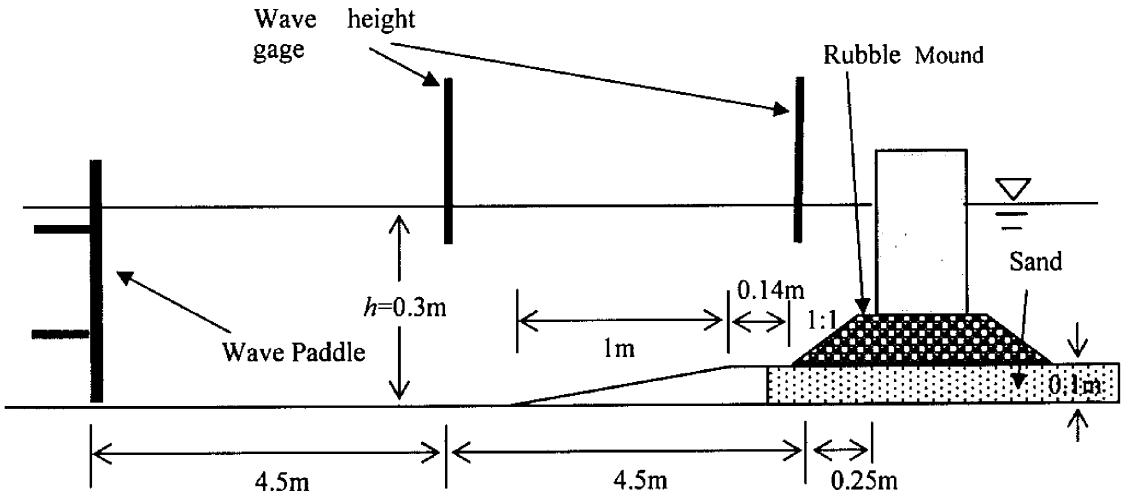

Fig.3.1 Experimental Set-Up

The experiments were repeated for two different configurations of the measuring devices:

- The 1st layout included load cells placed at 3 different locations within the rubble mound (top, middle and bottom, as shown in Fig. 3.2). At the top of the foundations two load cells were placed, one with the centre point of the load cell situated 0.5cm from the heel and the other 1.5cm from the heel. It was not possible to place the load cell directly on the heel as any small movement in its position would cause it to lose contact with the caisson and thus fail to record.
- The 2nd layout (see Fig. 3.3) had all the load cells placed at the top of the rubble mound, each within 1cm of each other, to measure the distribution of the pressure exerted by the caisson onto the rubble foundation.

To ensure that there was contact between the gravel and the load cell head a stone (1 cm^2 in area) was attached to the top of the load cell using adhesive tape, as otherwise there was a high chance that no stone would be touching the head and thus no pressure being recorded. Also, the gravel on the top of the foundation was lightly compacted so that the load cells under the caisson breakwater would rest on a level surface. This procedure served also to attempt to reproduce the compaction that the gravel foundation would undergo under the normal construction process.

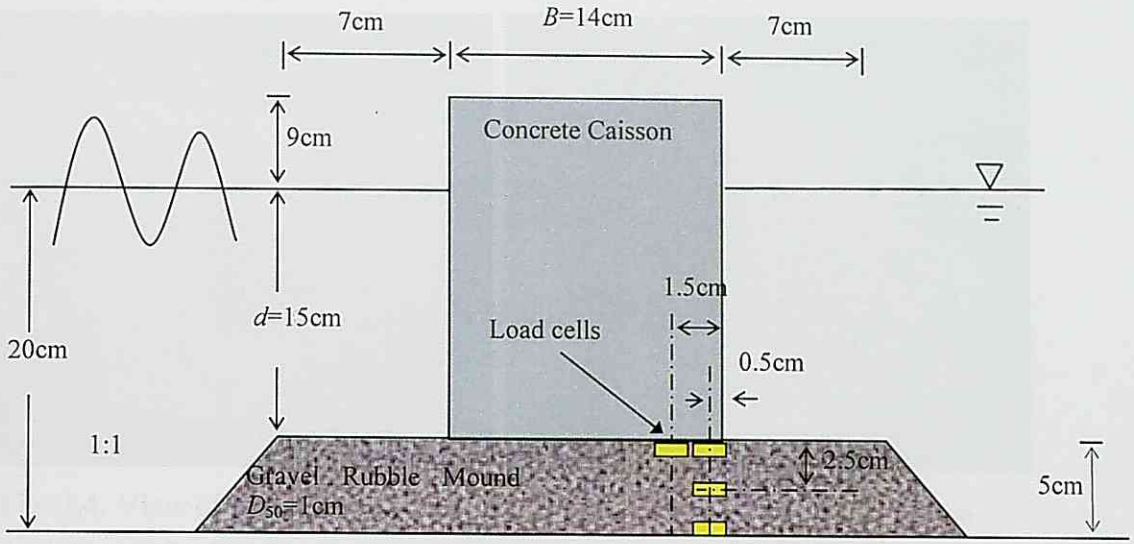

Fig.3.2. 1st Layout of measuring devices.

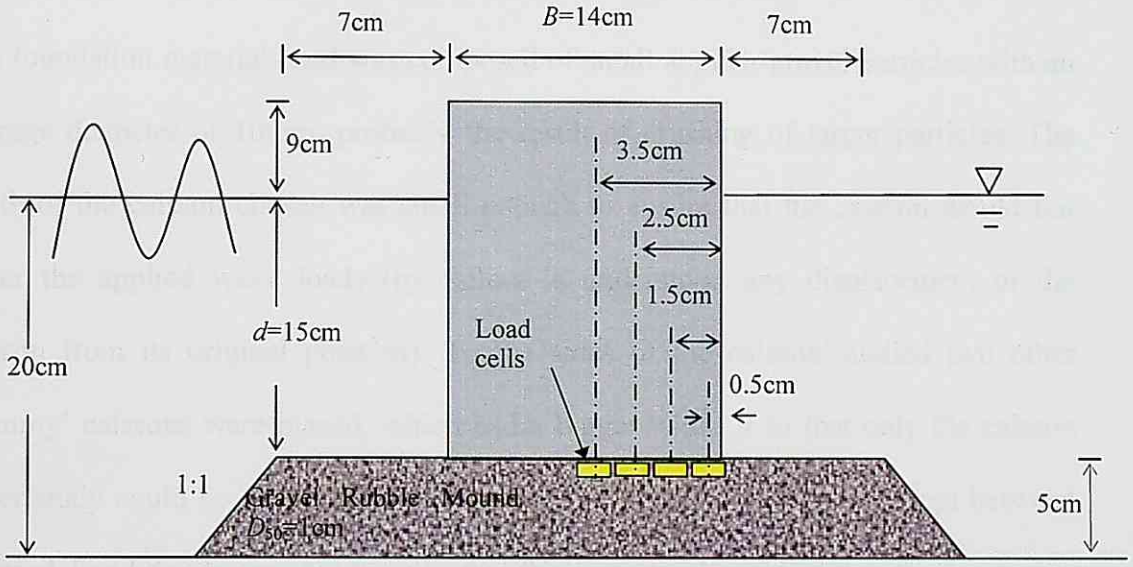

Fig.3.3. 2nd Layout of measuring devices.

The caisson units were made out of glass (24cm tall x 14cm long x 20cm wide) and filled with normal and metallic sands to obtain an overall similar density to that of a real life caisson (ρ=2,000kg/m^3). A thin layer of cement was applied to the bottom of the caisson so that the friction coefficient of the model caisson would be similar to that of a real caisson. A 1cm wide channel was cut through the middle of this cement layer and the load cells were placed along it and held in place using adhesive tape, as shown in Fig. 3.4.

Fig. 3.4: View of instrumentation at the bottom of caisson.

Fig. 3.5: View of the back of the rubble mound foundation.

The foundation material used was composed of small angular gravel particles with an average diameter of 10mm, probably the result of crushing of larger particles. The width of the caisson chosen was small enough to ensure that the caisson would fail under the applied wave loads (by failure is understood any displacement of the caisson from its original position). To the sides of the caisson studied two other 'dummy' caissons were placed, which had a bigger width B so that only the caisson under study could be displaced by the waves. A clearance of 2mm was kept between the model and the dummy caissons so that friction on either side did not occur during the experiments. No toe armour was placed on top of the rubble mound gravel as the gravel was heavy enough so that it could not be displaced by the waves.

The experiments were recorder using a Sony Cyber-shot video camera, which was placed on a tri-pod directly in front of the caissons.

3.2.2. Wave conditions

The caisson units were subjected to a variety of wave conditions, as outlined in Table 3.1. Regular waves were used in the experiment, and in the analysis of the results the data used only comprises the waves recorded before a standing wave developed in the tank. Table 3.1 shows both the input value for the H given to the wavemaker and the recorded incident H. For the non-breaking wave conditions there is a clear relation between the input parameter and the value recorded at the breakwater. However, the depth of the tank limits the wave height and after a certain height is reached the wave will deform and start to break. Hence after Set Number S4 the incident H does not change significantly, though the wave profile becomes increasingly more eccentric until perfect breaking is achieved for Set No. S8. Each Set of experiments was repeated for a variety of T, though due to the limitations of the wave flume some sets could only be carried out for a limited range of T. (for the Set Numbers S7 to S9 the wave broke around the middle section of the wave tank when low T values were employed).

Table 3.1.: Summary of wave conditions

Set No.	Wave Classification	Wave-Maker Input H (cm)	Recorded Incident H (cm)	T (s)	Notes
S1	Non-breaking	4	3.26	0.8 to 1.2	
S2	Non-breaking	6	6.5	0.8 to 1.2	
S3	Non-breaking	8	8.55	0.8 to 1.2	
S4	Non-breaking	10	8.6	0.8 to 1.2	
S5	Slightly breaking	12	8.62	0.8 to 1.2	
S6	Slightly breaking	14	8.65	0.8 to 1.2	
S7	Almost Breaking	16	8.7	1.0 to 1.2	Caisson oscillates
S8	Breaking Wave	18	8.7	1.0 to 1.2	Caisson rocks
S9	Breaking Wave	20	8.82	1.2	Caisson failure

Each Set of experiments was run for both of the layouts of measuring devices shown in Figs. 3.2 and 3.3.

3.2.3 Experimental Results

Figs 3.6 to 3.11 show the loads at the top of the rubble mound foundation for experimental layout No. 2 at various locations close to the heel of the caisson. From these it can be seen how in most of the loading conditions the maximum load does not occur at the edge of the caisson but at a certain distance from this edge. As the wave becomes more eccentric a clear evolution in the loading can be observed, with the sinusoidal profile of standing waves (Fig. 3.6) giving way to a more rapid and short lived initial load followed by the quasi-static load component (Fig. 3.7 and 3.8). The peak of this initial impulsive load increases as the shape of the wave approaches that of "perfect" breaking (Figs 3.7-3.9). The pressure at the heel of the breakwater (the load cell situated 0.5 cm from the edge) increases also as the caisson starts to approach the overturning equilibrium position (i.e. the point at which the overturning forces are equal to the resisting forces) as seen in Fig. 3.9. Eventually the caisson starts to rock on its back part and hence the load at the heel becomes greater than the load at other parts of the foundation (Fig. 3.10). Once perfect breaking is achieved the force on the caisson is much greater than what it can withstand, with most of the base of the foundation losing touch with the ground and the caisson effectively rocking over its heel (Fig. 3.11). Waves of higher energy than those of Set S9 made the caisson overturn and hence the experiments were stopped after this condition.

Fig. 3.12 shows the distribution of pressures at 4 different points close to the heel of the caisson for experimental conditions S4 to S9. From this figure the increase in the pressure at the heel as the caisson approaches the limit of overturning failure can be clearly seen. This figure also shows in a clear way how the pressure distribution under a caisson breakwater only follows a triangular distribution for the case when the caisson is about to fail (cases S8 and S9).

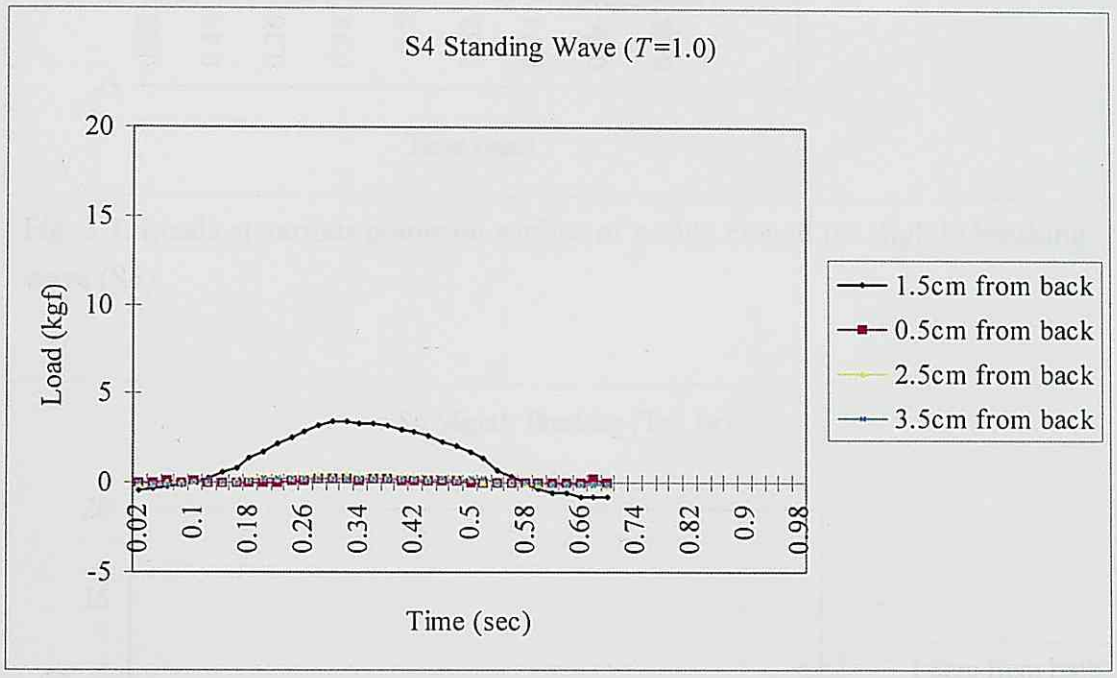

Fig. 3.6. Loads at various points on surface of rubble mound for standing wave

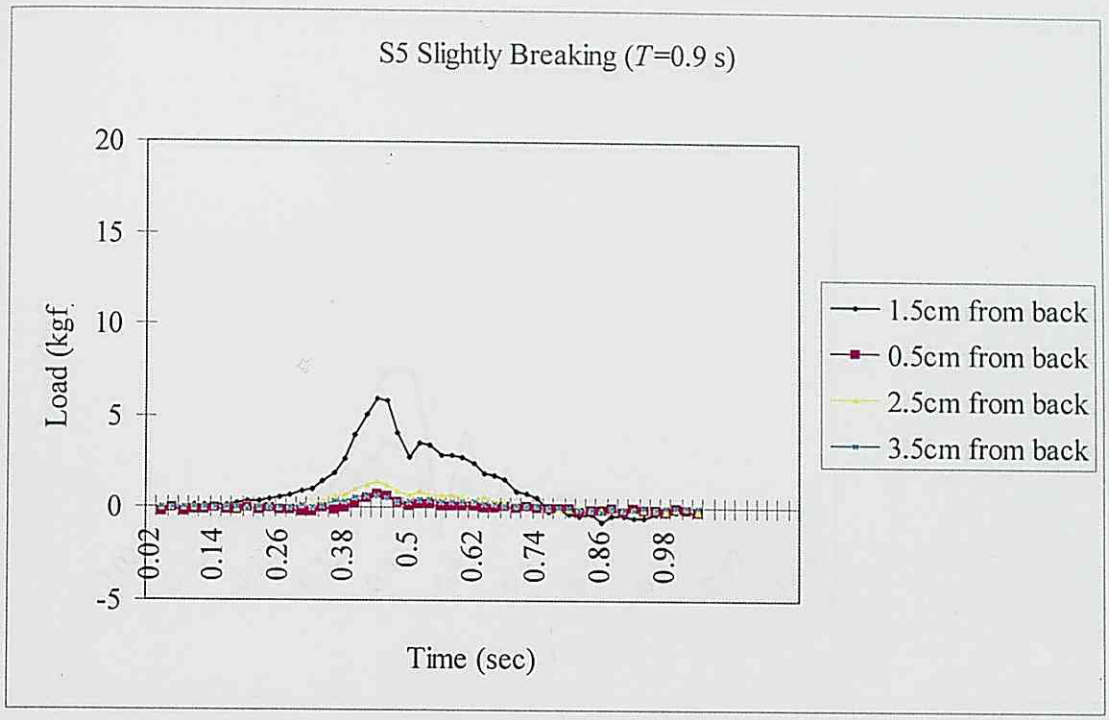

Fig. 3.7. Loads at various points on surface of rubble mound for slightly breaking wave (S5)

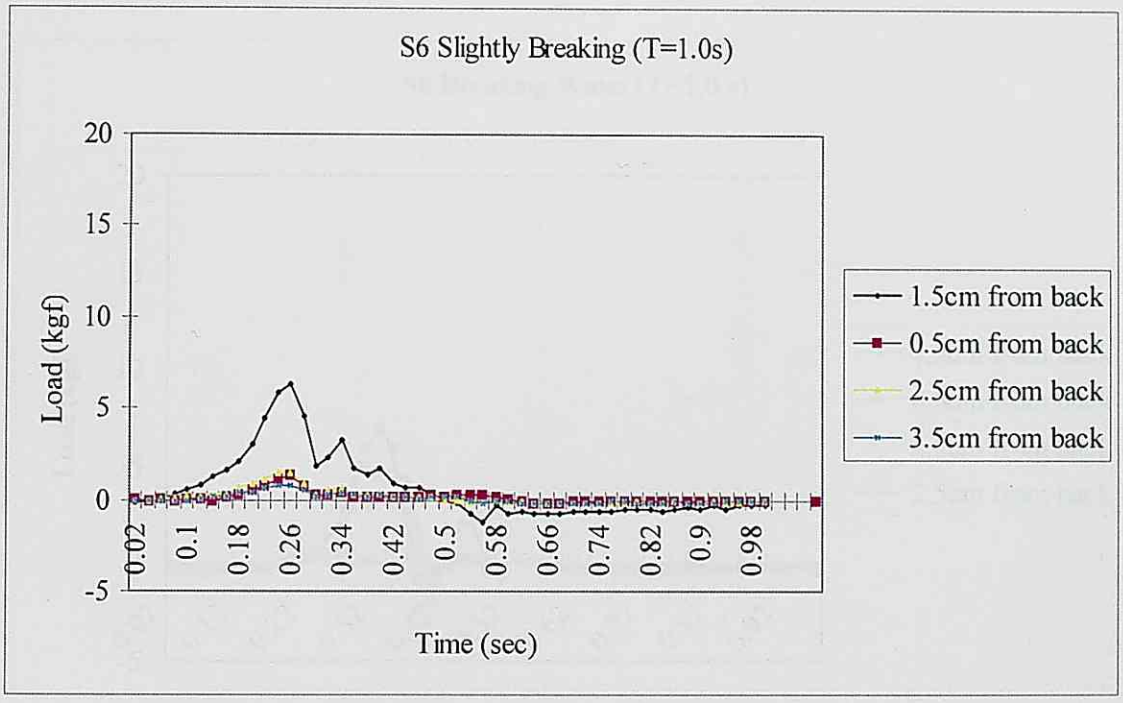

Fig. 3.8. Loads at various points on surface of rubble mound for slightly breaking wave (S6)

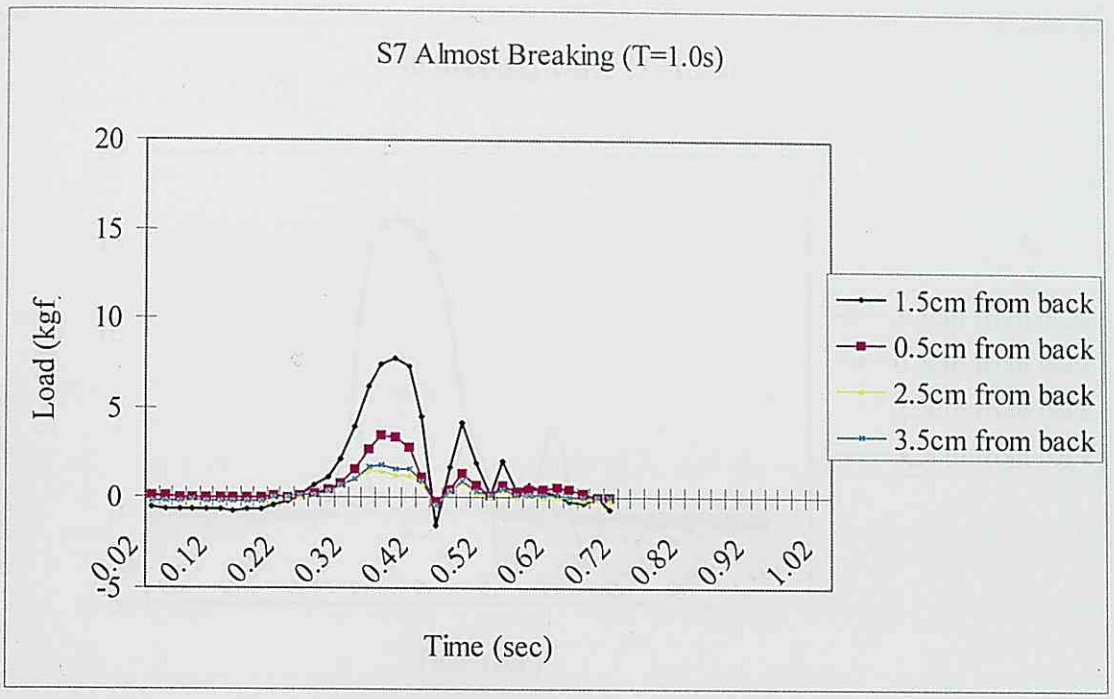

Fig. 3.9. Loads at various points on surface of rubble mound for almost breaking wave (S7)

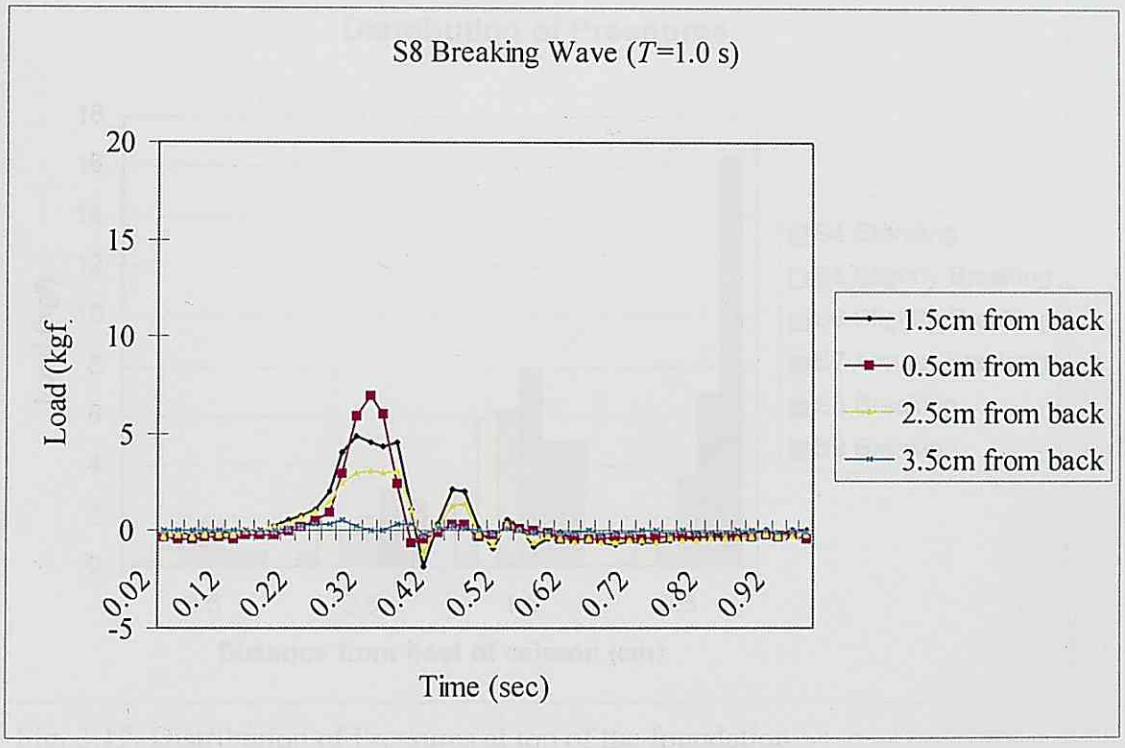

Fig. 3.10. Loads at various points on surface of rubble mound for breaking wave (S8)

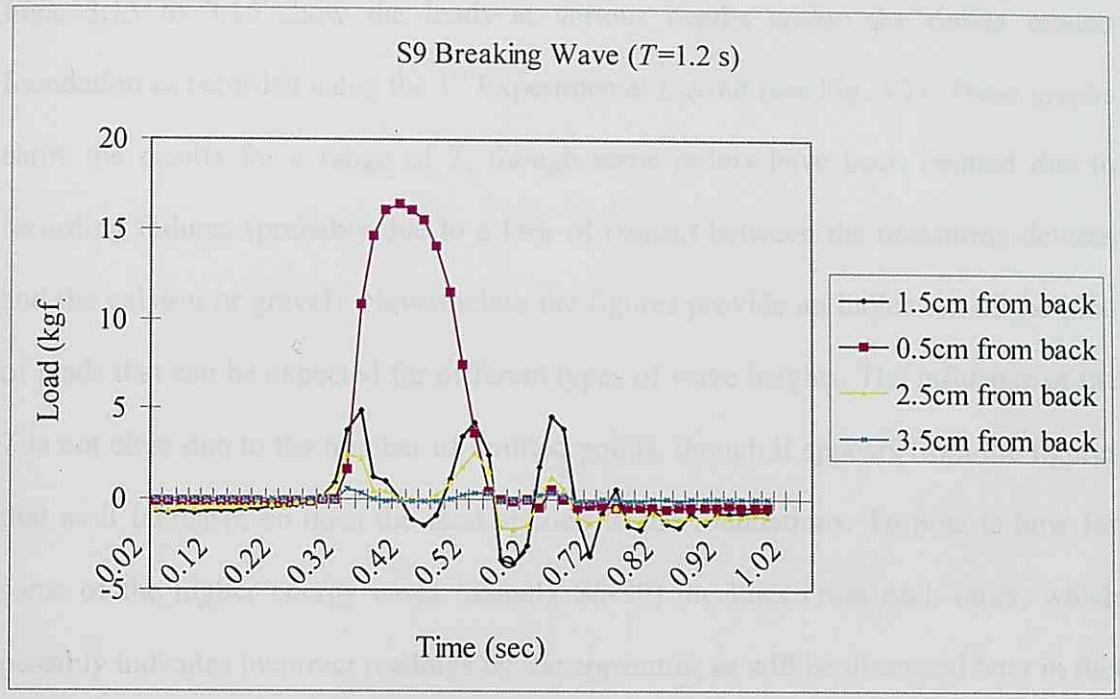

Fig. 3.11. Loads at various points on surface of rubble mound for breaking wave (S9)

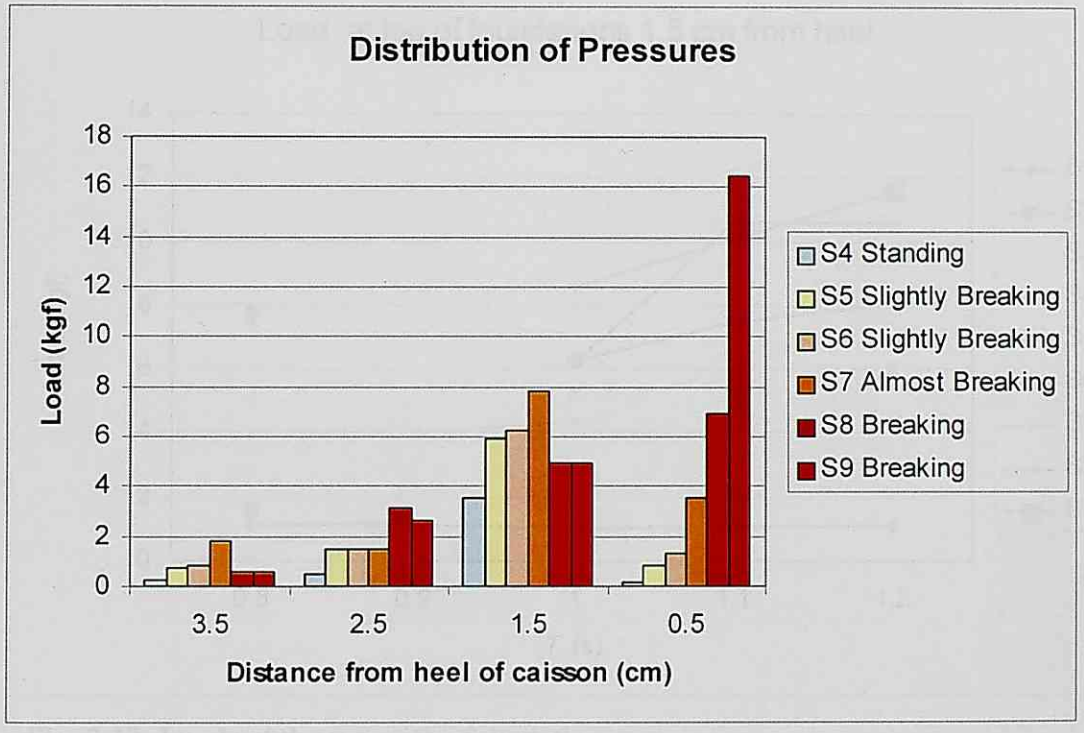

Fig. 3.12. Distribution of Pressures at top of the foundation

Figs. 3.13 to 3.15 show the loads at various depths within the rubble mound foundation as recorded using the 1st Experimental Layout (see Fig. 3.2). These graphs show the results for a range of T, though some points have been omitted due to recording failures (probably due to a lack of contact between the measuring devices and the caisson or gravel). Nevertheless the figures provide an indication of the kind of loads that can be expected for different types of wave heights. The influence of the T is not clear due to the number of omitted points, though it appears from the figures that as it increases so does the load applied to the foundations. To note is how for some of the higher energy cases (namely S6-S9) the lines cross each other, which possibly indicates incorrect readings by the apparatus, as will be discussed later in this chapter.

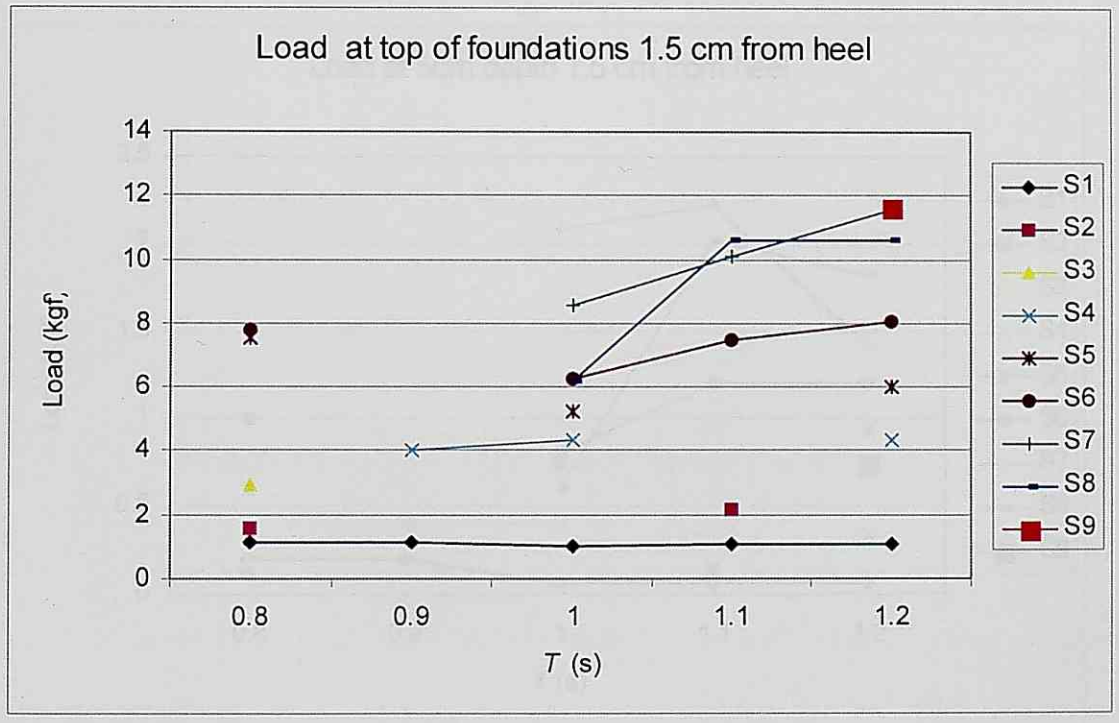

Fig. 3.13. Loads at the top of the foundation

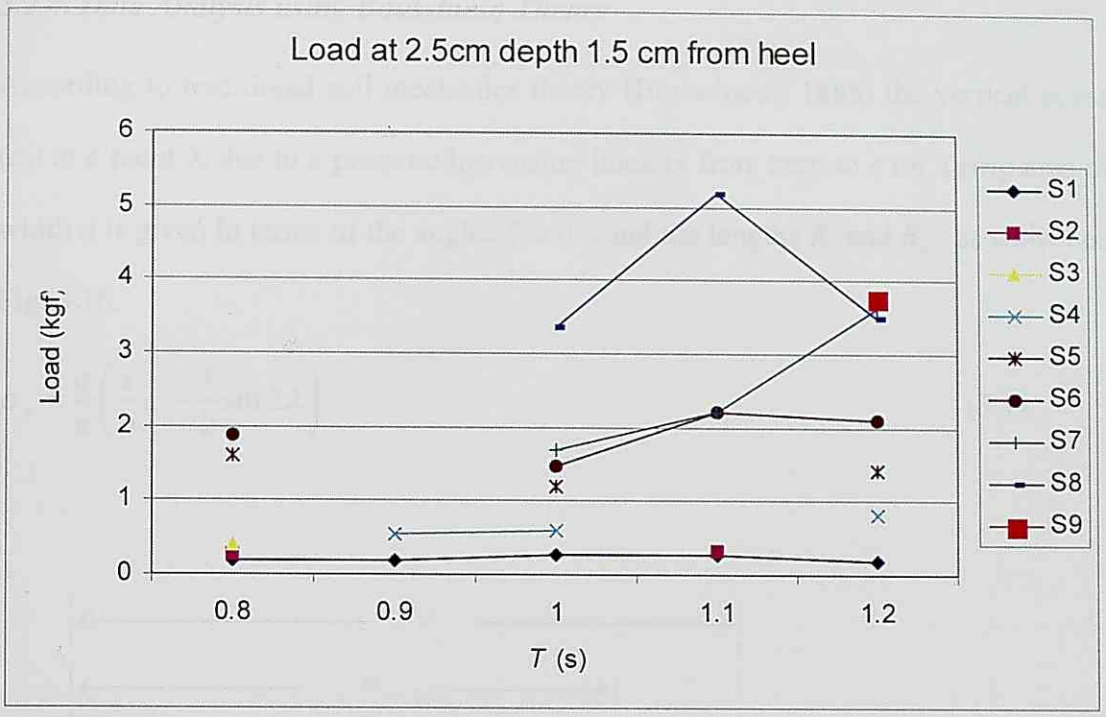

Fig. 3.14. Loads at 2.5cm depth

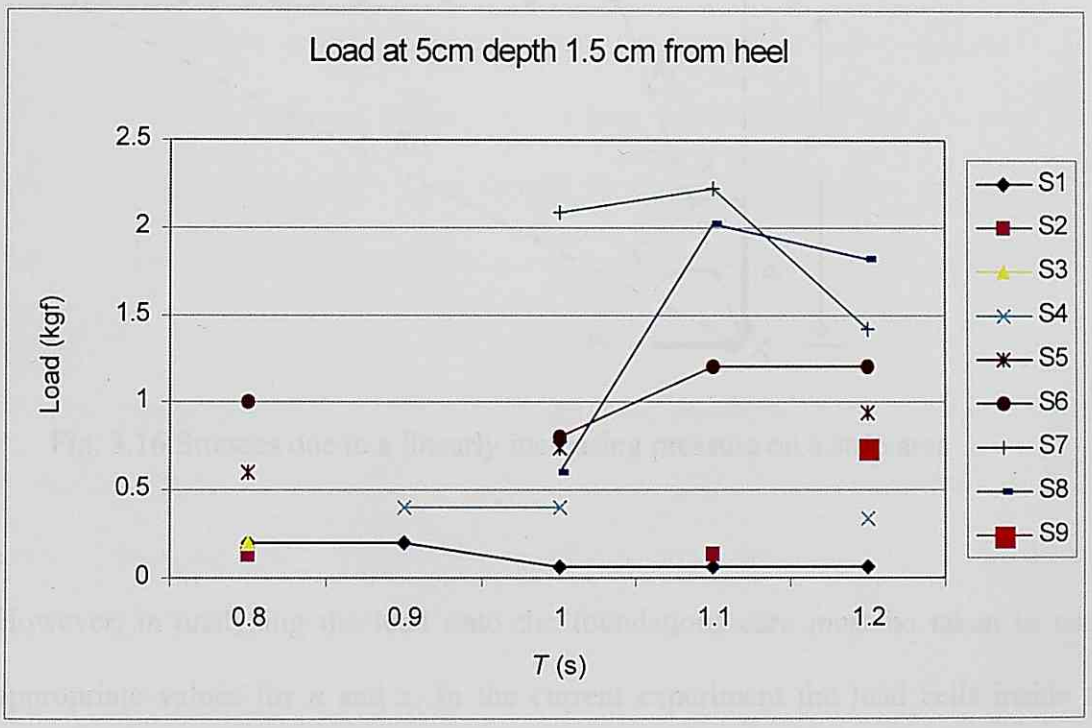

Fig. 3.15. Loads at 5cm depth

3.2.4. Data Analysis using Boussinesq Theory

According to traditional soil mechanics theory (Boussinesq, 1885) the vertical stress (σ_z) at a point X due to a pressure increasing linearly from zero to q on a strip area of width n is given in terms of the angles ζ and λ and the lengths R_1 and R_2, as shown on Fig. 3.16.

$$\sigma_z = \frac{q}{\pi}\left(\frac{x}{n}\zeta - \frac{1}{2}\sin 2\lambda\right) \tag{3.1}$$

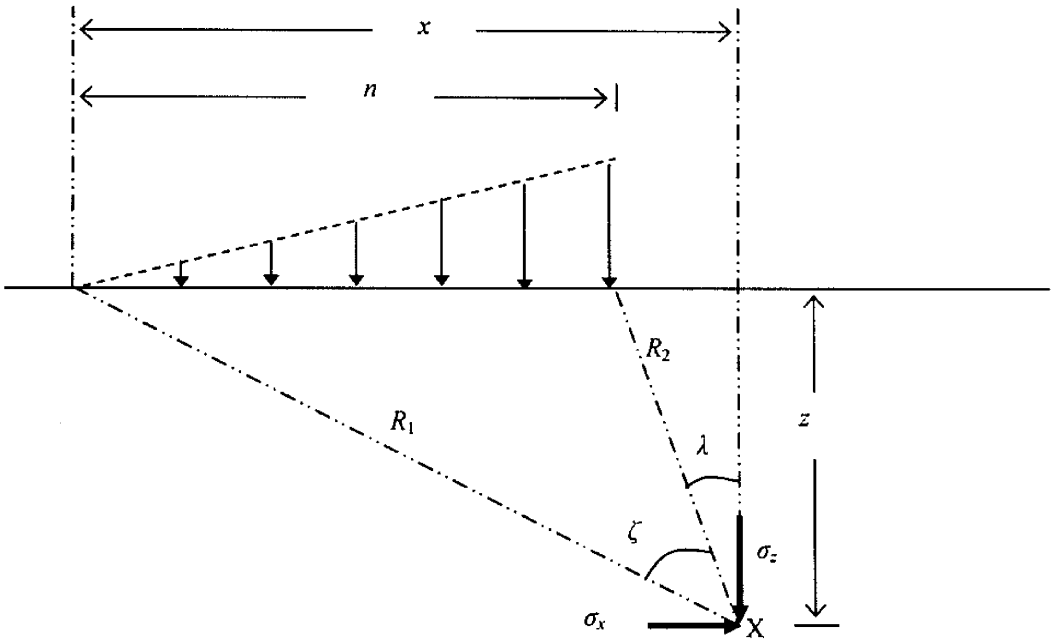

Fig. 3.16 Stresses due to a linearly increasing pressure on a strip area

However, in analyzing the load onto the foundations care must be taken in using appropriate values for n and x. In the current experiment the load cells inside the foundation were located 0.5 cm from the heel of the breakwater, although the location of the maximum load differed between experiments. For Conditions S1-S7 it was situated at m=1.5cm (see Fig. 3.17), though in S8 and S9 it was located at m=0.5cm.

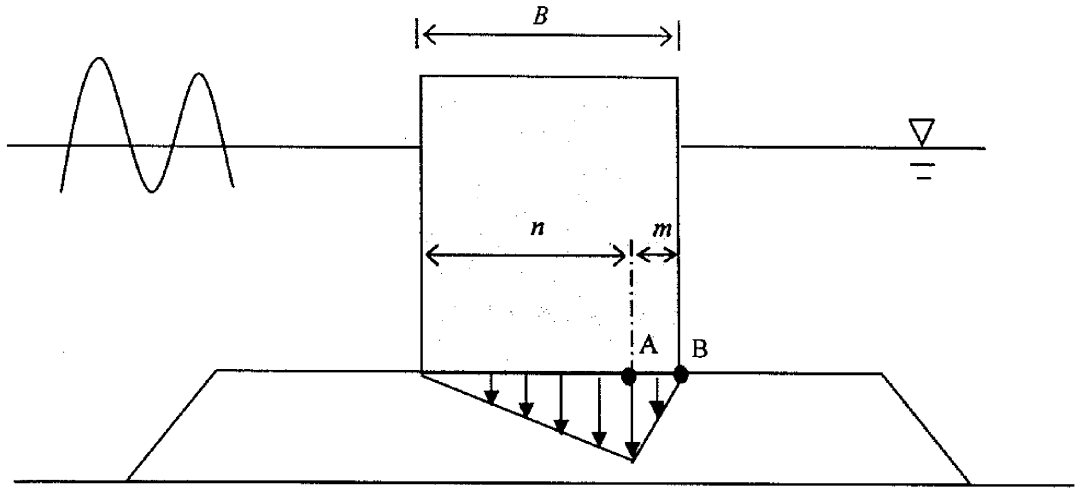

Fig. 3.17. Diagram of load on the foundations

As can be seen from Fig. 3.18 there is a good correlation between the values computed by Boussinesq's theory and the experimental values at a depth of 2.5cm, though the loads at the bottom of the gravel layer were somewhat overestimated (Fig. 3.19). The reason for this probably lies in the rapid cycles of loading and unloading that the waves apply to the soil, which contrasts with classical soil mechanics theory – which deals with loads that develop over a long period of time. It thus seems likely that under the present experimental conditions the loads do not have time to transmit themselves effectively to the deeper areas of the rubble mound, resulting in the loads in this area being lower than those predicted by the Bousinesq Theory. Another possible reason could be the effect of the pore pressures due to the loading and unloading cycles. This could be potentially increasing the pressure exerted in the top areas of the berm and would be lower as you go down through the berm. However it seems unlikely that such large pore pressure were developed in the present experiment to confound the results to this point.

Although the loads that are applied by the caisson onto the foundation appear to be dependent on T (Figs. 3.13 and 3.14), this parameter does not appear to influence the

propagation of load throughout the rubble mound foundation. However the range of T for which the experiment was carried out was quite small and it appears possible that if the wave pressures were applied for a longer time (i.e. higher T) the loads at the 5cm depth could become more similar to those predicted by the Bousinesq model. Also to be noted is how some of the loads recorded at this 5cm depth for the higher load cases (S9 and S8 specially) are lower than for some of the lower energy cases. This is unexpected, and possible explanations could include the movements of particles in the top of the berm affecting the transmission of loads so that the measurements at the bottom are somewhat confounded, or lack of contact with the measuring devices. The purpose of the present experiments however was not to measure the loads in this area, and hence no further investigations were carried out to ascertain what was the cause of this unexpected result.

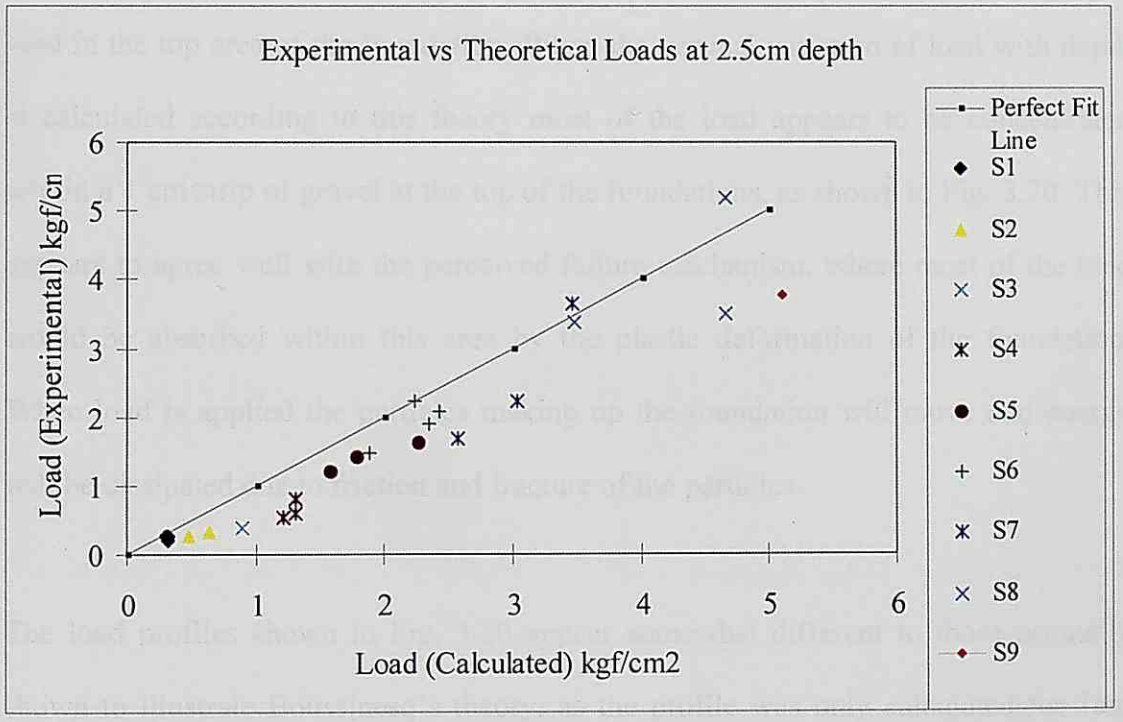

Fig. 3.18. Comparison between experimental and theoretical loads at 2.5cm depth

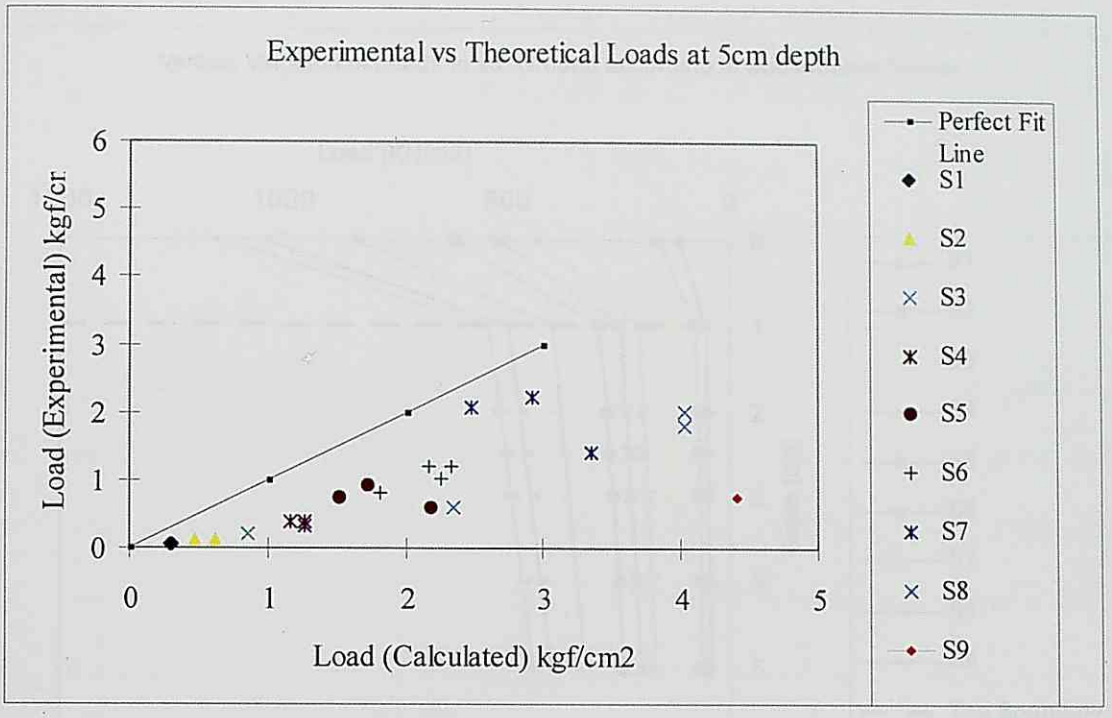

Fig. 3.19. Comparison between experimental and theoretical loads at 5cm depth

Therefore it appears that by using Boussinesq's theory it is possible to estimate the load in the top area of the foundation. When the vertical variation of load with depth is calculated according to this theory most of the load appears to be concentrated within a 1 cm strip of gravel at the top of the foundations, as shown in Fig. 3.20. This appears to agree well with the perceived failure mechanism, where most of the load would be absorbed within this area by the plastic deformation of the foundation. When load is applied the particles making up the foundation will move and energy will be dissipated due to friction and fracture of the particles.

The load profiles shown in Fig. 3.20 appear somewhat different to those normally shown to illustrate Boussinesq's theory, as the profile was only calculated for 1cm intervals. In the present experiment the gravel had a typical diameter of 1cm, and it would thus be meaningless to calculate the pressures at intervals lower than this.

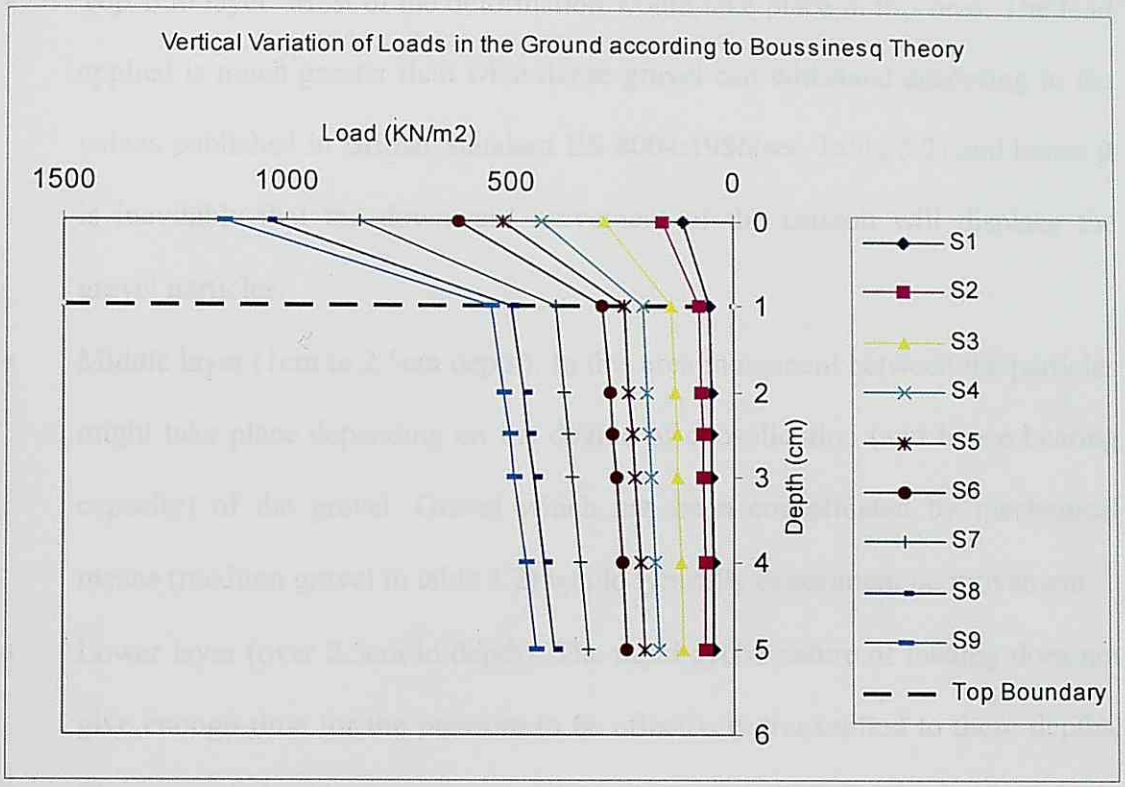

Fig. 3.20 Variation in vertical load according to Boussinesq Theory

At depths greater than 2.5cm Boussinesq's theory overestimates the loads registered during the laboratory experiments. In this case it would be necessary to apply a reduction factor and hence the following modification to Eq. 1 is proposed:

$$\left.\begin{aligned} \sigma_z &= \frac{q}{\pi}\left(\frac{x}{B}\alpha - \frac{1}{2}\sin 2\beta\right) && \text{for: } 0 \le z \le 2.5 \\ \sigma_z &= (-0.2z + 1.5)\left[\frac{q}{\pi}\left(\frac{x}{B}\alpha - \frac{1}{2}\sin 2\beta\right)\right] && \text{for: } 2.5 \le z \le 5 \end{aligned}\right\} \qquad (3.2)$$

The result of applying this reduction on the vertical variation of the load profile can be seen in Fig. 3.21. According to this graph, for the higher impulsive loads (S9 and S8), the soil would be responding to the applied pressure in three different ways according to depth:

- Top 1cm layer: Most of the deformation would take place in this area. The load applied is much greater than what dense gravel can withstand according to the values published in British Standard BS 8004:1986(see Table 3.2) and hence it is inevitable that the downward movement of the caisson will displace the gravel particles.
- Middle layer (1cm to 2.5cm depth): In this area movement between the particles might take place depending on the degree of consolidation (and hence bearing capacity) of the gravel. Gravel which has been consolidated by mechanical means (medium gravel in table 3.2) would typically experiment no movement.
- Lower layer (over 2.5cm in depth): The rapid cyclic nature of loading does not give enough time for the pressure to be effectively transmitted to these depths. The pressure in this area is lower than the expected according to Boussinesq theory and is generally below what non-consolidated gravel can withstand. Hence it appears unlikely that any movement would take place in this area.

Table 3.2: Presumed bearing values (BS 8004:1986)

Soil type	**Bearing value (kN/m^2)**	**Remarks**
Dense gravel or dense sand and gravel	>600	Width of foundation (B) not less than 1 m. Water table at least B below base of foundation.
Medium-dense gravel or medium-dense sand and gravel	200-600	
Loose gravel or loose sand and gravel	<200	
Dense sand	>300	
Medium-dense sand	100-300	
Loose sand	<100	

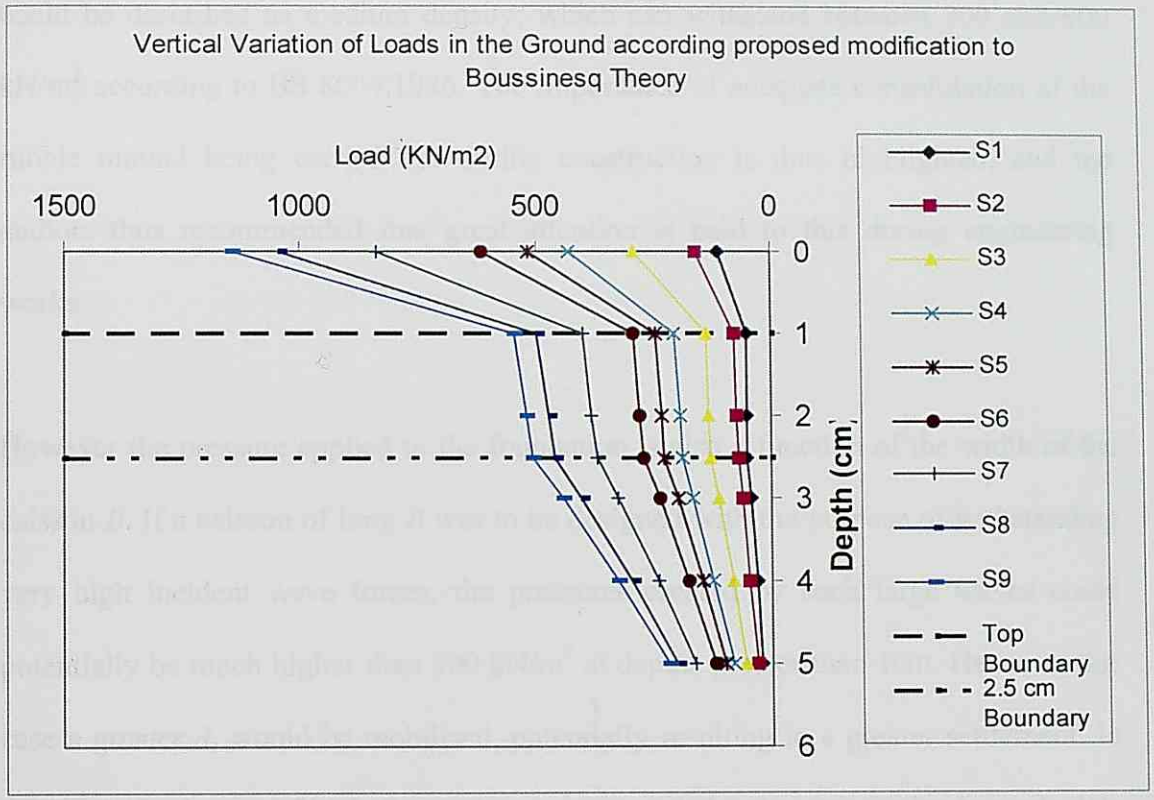

Fig. 3.21 Variation in vertical load according to proposed modification

3.3. Discussion of the Results

From the experimental results it appears adequate to use a depth of 1cm as the active depth of foundations for most caisson breakwater designs. The active depth depends on the force applied by the wave onto the foundations and on the bearing capacity of the ground, which in turn depends on the void ratio of the foundation. Although in the case of impact waves the pressure at depths of between 1 and 2.5cm depth can exceed 500 kN/m^2, it is probable that the bearing capacity of the gravel exceeds this quantity. This is justified due to the compaction process that the foundation is subjected to during breakwater construction and because of the natural settlement of the caisson through low-intensity wave action prior to the high intensity episodic wave event. It is likely that these two processes consolidate the gravel foundation into at least what

could be described as medium density, which can withstand between 200 and 600 kN/m^2 according to BS 8004:1986. The importance of adequate consolidation of the rubble mound being carried out during construction is thus highlighted, and the authors thus recommended that great attention is paid to this during engineering works.

However the pressure applied to the foundation is also a function of the width of the caisson B. If a caisson of long B was to be designed with the purpose of withstanding very high incident wave forces, the pressures created by such large waves could potentially be much higher than 500 kN/m^2 at depths greater than 1cm. Hence in this case a greater d_z would be mobilised, potentially resulting in a greater settlement. In the case of caissons of high B it is thus recommended not to use d_z=1m but calculate the pressure throughout the berm using Eq. 3.2 and thus compute d_z. As d_z is based on the bearing capacity of the foundations, which in turn depends on the void ratio (as explained in Chapter 5), d_z is not a constant value but will change dynamically according to the degree of consolidation of the gravel. Hence shortly after the construction of the breakwater a wave of certain H would mobilise a greater d_z. than after the caissons have undergone a certain number of storms. The choice of an appropriate d_z is very important in order to accurately estimate the expected deformation, and great care must be exercised in the choice of all gravel parameters based on the construction methodology employed.

In applying the results of the present experiments into a real life design the possibility of scale distortions occurring must be kept in mind. The present experiments were carried out on a 1/100 scale, and therefore the results obtained might deviate substantially to those in a prototype situation. The choice of whether to use Froude

scaling or Cauchy scaling would result in significant differences in the final analysis of the prototype breakwater. The European Research Project PROVERBS recommends that Cauchy scaling should be used for impact waves and Froude scaling should be used for standing waves. This approach appears sensible at this stage till large scale experiments can be carried out to further verify the present results.

The accuracy of the measurements of the loads throughout the foundation was also called into question. While all care was taken to ensure that the equipments was correctly placed and the various elements (caisson, gravel, load cells) were in contact at all times, the nature of the loading and the deformations that took place in the rubble mound meant this was not always possible. Due to the displacement of particles within the rubble mound contact was often lost between the measurement devices and the particles on top of them, resulting in no loads being recorded. Also, due to these deformations the measurement devices did not always return to 0 after one wave had passed. It is thus necessary to view these results with a certain element of caution, and though each one was analysed separately to try to find and remove these problems, there is a possibility that some of them do not accurately reflect the actual pressures in the ground. This could have resulted in some loads having an error of up to about 10%, judging from the analysed data, which would explain to some extent the variations observed in Fig. 3.18 and 3.19.

Also, in applying the results of the present experiment onto a prototype breakwater the influence of the shape of the gravel in the transmission of load must be taken into account. The present experiment used angular gravel of fairly constant size, which is probably similar in shape to the particles used in real life construction, often the result of crushing or blasting larger sized particles. However the properties of rounded

particles would differ somewhat from this and care should be taken in applying the results to this type of gravel in real designs.

3.4. Conclusion

The laboratory experiments that were carried out showed that the pressures exerted by a caisson breakwater on the top area of the foundation can be approximated using traditional Boussinesq Theory. Using this theory is appears likely that most of the deformation takes place within a narrow area 1cm deep at the top of the foundation, and thus this value is adopted as the active depth of foundations in the computation of the vertical displacement of the caisson. However, care must be exercised when determining this value, and for sections or loads that differ greatly to the caisson section studied in the present experiment it would be better to compute the depth by using the equations provided rather than using the simplified 1cm value.

CHAPTER 4

HYDRAULIC TESTS TO DETERMINE THE FAILURE MODE OF CAISSON BREAKWATER SUBJECTED TO IMPACT WAVES

4.1. Introduction

Breakwaters have been traditionally designed by applying safety factors to quasi-static (standing) wave loads and static calculations for the stability against the four main failure modes of sliding, overturning and circular slip. In order to obtain the wave loads a certain design wave height is chosen based on return periods determined by historical statistical data. However many researchers such as Shimosako and Takahashi (1998) or Goda (1999) have highlighted problems with this traditional approach and suggest that in the future maritime breakwaters should be designed using a reliability-based approach.

The main failure mode of caisson breakwaters is that of sliding along the top of the rubble mound foundation, which allows for does not prevent the breakwater from fulfilling its function as long as only limited movement takes place. This sliding is not normally allowed under traditional breakwater design, so Shimosako and Takahashi (2000) proposed a Level 3 design method for caisson breakwaters referred to as the

"deformation-based reliability design". This model can account for the sliding in the caissons, although it does not deal with the tilting of the caisson, and can thus not reproduce the actual displacement that takes place. Kim and Takayama (2005) modified this model to take into account the effect of caisson tilting on the computation of sliding distance. They identified two different kinds of tilting, which they referred to as variable tilting angle (θ_v) and residual tilting angle (θ_r). The former is due to the variation of the wave moment during one wave period (T) and the latter corresponds to the residual deformation (or settlement) of the rubble mound after the wave period is finished. In this method an assumption needs to be made regarding the final angle of tilting of the caisson, as Kim and Takayama provide no way of estimating it.

4.2. Laboratory Experiments

Experiments were carried out at Yokohama National University in Japan in order to understand the long-term deformation behaviour of caisson breakwaters and to verify the results of the deformation model that will be proposed in subsequent chapters of the current dissertation. The aim of these experiments was to ascertain how a caisson breakwater would behave after several storms of similar intensity in which impact waves were present.

4.2.1. Experimental Set-Up

The laboratory experiments were carried out in a wave flume of dimensions 15.3m long x 0.6m wide x 0.55m deep. Fig. 4.1 shows a schematic representation of the wave tank and apparatus used, which was modelled using a 1:100 scale.

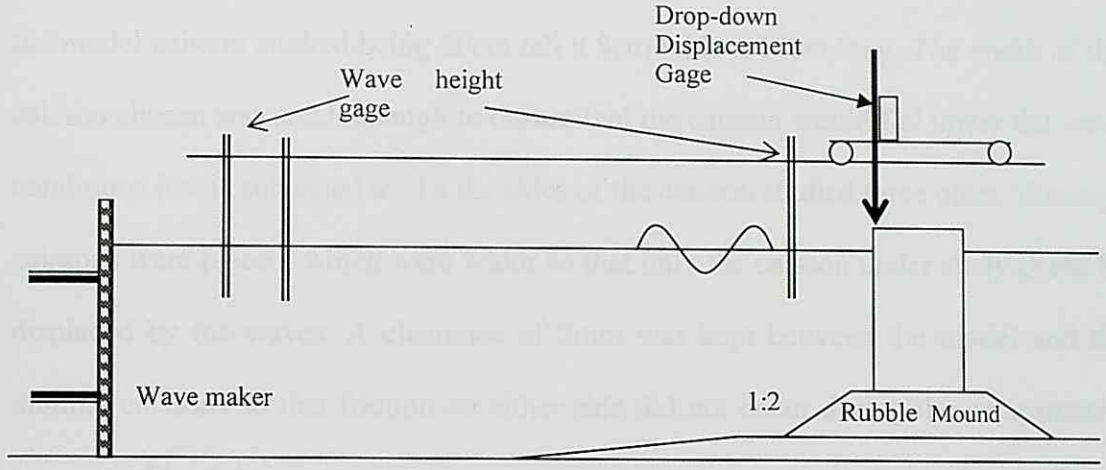

Fig. 4.1. Experimental Set-Up

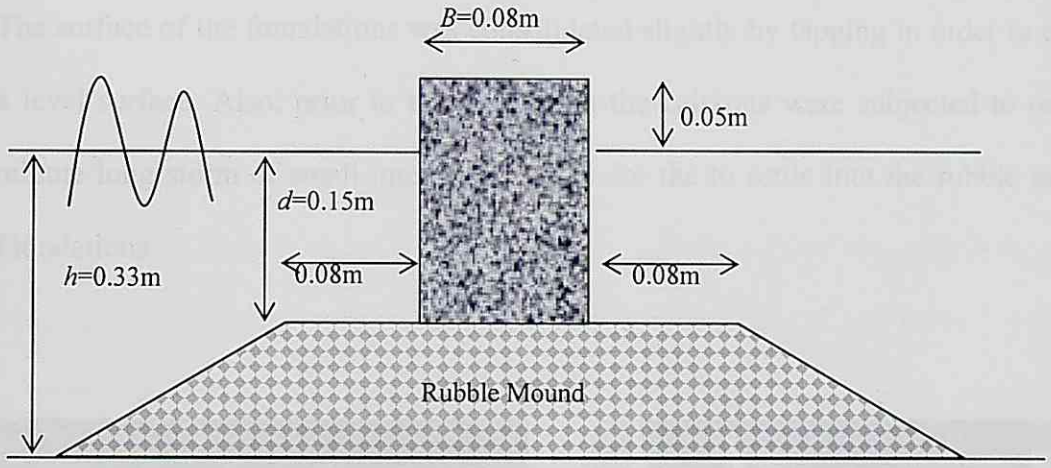

Fig. 4.2. Dimensions of the Model Caisson

The water depth in the tank was kept constant throughout the experiments at h=0.33m. A wave absorption beach was set at one end of the tank in order to dissipate the energy of the waves created by the overtopping of the caisson. The dimensions of the model caisson are shown in Fig. 4.2.

The caisson units were made of concrete in order to keep the density close to that of real-life caissons. A total of four concrete caissons were cast, with the dimensions of the model caisson studied being 20cm tall x 8cm wide x 18cm long. The width of the caisson chosen was small enough to ensure that the caisson would fail under the wave conditions it was subjected to. To the sides of the caisson studied three other 'dummy' caissons were placed, which were wider so that only the caisson under study could be displaced by the waves. A clearance of 2mm was kept between the model and the dummy caissons so that friction on either side did not occur during the experiments, as seen in Fig. 4.4

The surface of the foundations was consolidated slightly by tapping in order to create a level surface. Also, prior to the first storm the caissons were subjected to one 12 minute long storm of small intensity in order for the to settle into the rubble mound foundations.

Fig. 4.3 Hydraulics Laboratory at Yokohama National University

Fig. 4.4 View of Model Breakwater

The gravel used was generally formed of rounded elements –as opposed to angular elements obtained from crushing- having an average diameter D_{50} of 5mm, typical weight of 0.7g and density 2.002 tons/m^3. No toe armour was placed on top of the rubble mound gravel as it was heavy enough so that it could not be moved by the waves and hence did not require toe armour.

A total of 3 wave gages were placed, two roughly at the middle of the tank and one close to the caisson to measure the incident wave height, all of which were connected to a digital recorder. A drop-down displacement gage was mounted on rails above the tank to measure the vertical and horizontal displacement of the caisson.

The caisson units were subjected to three consecutive 12 minute long storms, with the position of the caisson recorded at the end of each storm. Irregular waves were used in the experiment, but the mean height, period and spectrum (Rayleigh distribution with deepwater significant wave height H_0'=6.5cm and T=1s) of the waves was kept constant throughout the tests. The Factor of Safety (F.S.) against the incident significant wave height of $H_{1/3}$=5.7cm was calculated to be 0.67 against sliding. A F.S. of 1.2 is common in breakwater design, and generally the breakwater will not move for any storm where the $H_{1/3}$ is lower than the design condition. Therefore, in order for movement to take place the caisson must be subjected to a storm of higher $H_{1/3}$ than what it was designed for, resulting in the caisson having a lower F.S. against that particular storm (indicating that failure will occur).

The experiment was repeated 48 times in order to obtain the probability distribution functions of sliding and vertical displacement at the back of the caisson.

4.2.2 Scaling issues

The issue of scaling is crucial in laboratory experiment dealing with impact waves. The amount of air bubbles and entrapped air has a huge effect on the final impact pressure. For example Peregrine & Kalliadasis (1996) showed that the presence of even a small amount of air in the water could lead to a reduction in the maximum pressure. Bullock et al. (2001) also found similar corrections when comparing wave impact between fresh and salt water in laboratory tests. This appears to be due to differences in the compressibility of the bubbles between fresh and salt water, with aeration levels being much higher in salt water than in fresh.

PROVERBS (1996-1999) suggests that in order for the results of impact waves to be interpreted correctly a combination of Froude and Mach-Cauchy scaling should be used. The choice of scaling law depends on the amount of aeration in the water, resulting in different parts of the wave pressure time history being scaled using different laws, e.g. the pressure part should be modelled according to Mach-Cauchy and the standing part according to Froude. However due to the difficulty in doing this and the size of the wave flume available the present experiments were analysed using Froude scaling only. According to these scaling laws in order to ensure that the waves outside the model breakwater are equal to real waves, the ratio of the fluid inertia forces to the gravitational forces must be equal in both situations.

Table 4.1 shows the scaling factors used for each parameter according to the equations provided in Chapter 2 for Froude scaling.

Table 4.1: Scale of model tests

Parameter	*Scale Used*
Time	1/10
Length	1/100
Weight	1/100
Wave pressure	1/100

3.2.3. Experimental Results and Data Analysis

As can be seen from Fig. 4.5 two different types of sliding distance (SD) can be measured depending on if it is measured at the top (SD_t) or at the bottom (SD_b) of the caisson. In the present work the sliding distance will be taken as SD_t as for small vertical deformations these two values are almost equal and hence the error incurred is small. The vertical displacement of the caisson is taken as that occurring at the shoreside edge of the caisson. Throughout the experiments the vertical position of the seaside edge of the caisson did not significantly change from its original position, as shown on Fig. 4.5.

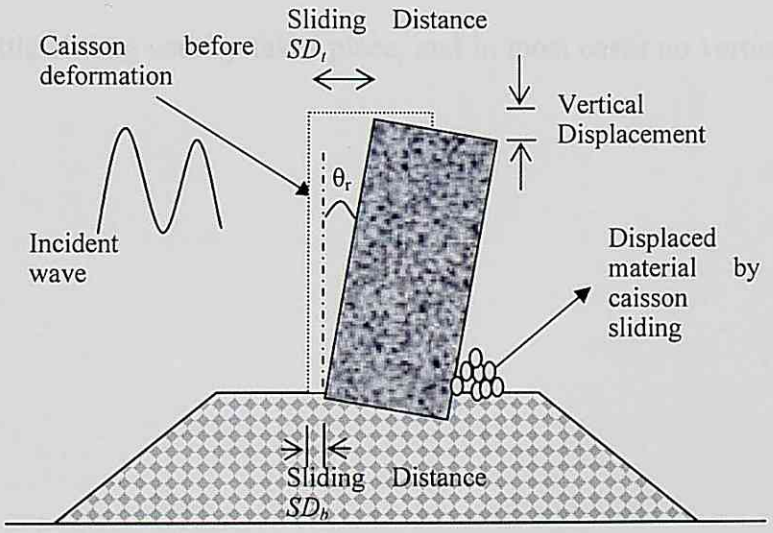

Fig.4.5. Sketch of various parameters

The laboratory experiments described were concerned only with the progression of damage in the caisson breakwater, and hence only the residual tilting angle (θ_r) was studied. The variable tilting angle (θ_v), corresponding to the oscillations in the caisson due to wave impact, was outside the scope of these experiments due to the small scale employed (1/100). The tilting angle itself was not calculated, so the results can be interpreted as horizontal and vertical deformations in the rubber mound.

As the caisson slid, and due to the fact that a certain part of the caisson becomes imbedded in the foundation due to the vertical displacement at the back, some of the foundation material was displaced. This material accumulated on the back of the caisson and a small but perceptible wedge of material was observed (see Fig. 4.5).

Figs. 4.6 to 4.11 show the probability distribution curves for sliding and vertical displacement at the end of the 1st, 2nd and 3rd storms. From these figures it can be seen that the mean value of the probability distribution function reduces after each storm, so that there is a general slowing down of caisson movement, with most of the movement taking place during the first storm. Between the end of the 2nd and 3rd storms very little sliding usually takes place, and in most cases no vertical movement was recorded.

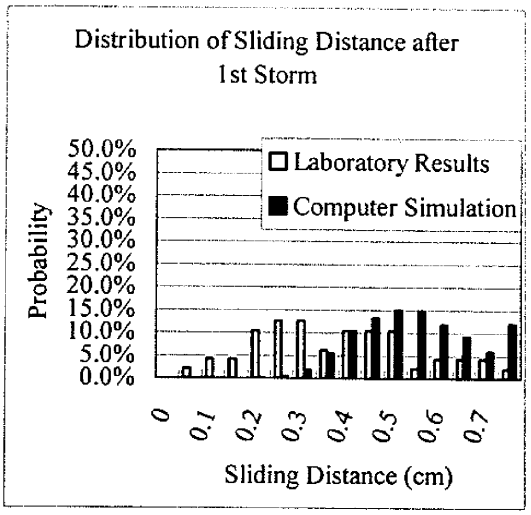

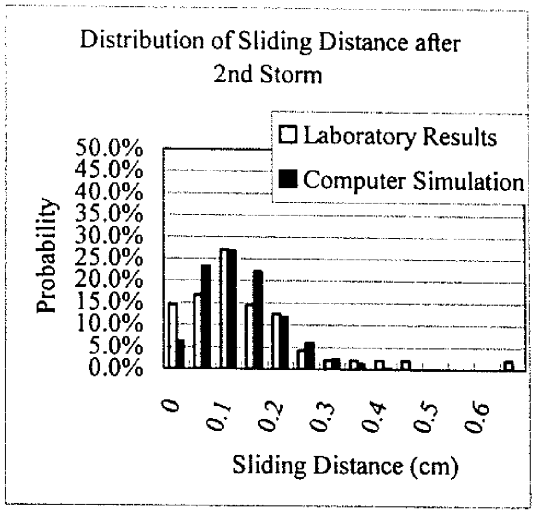

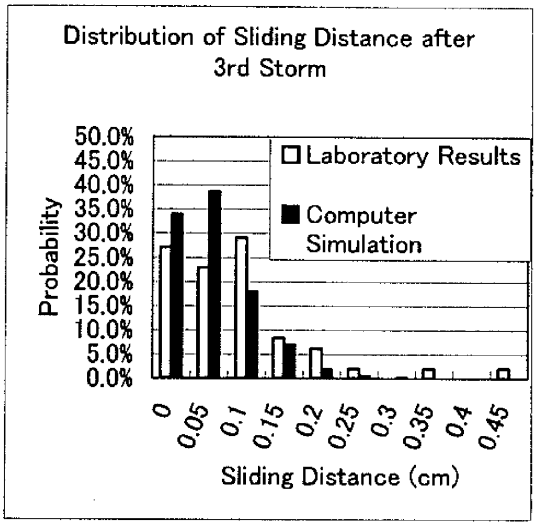

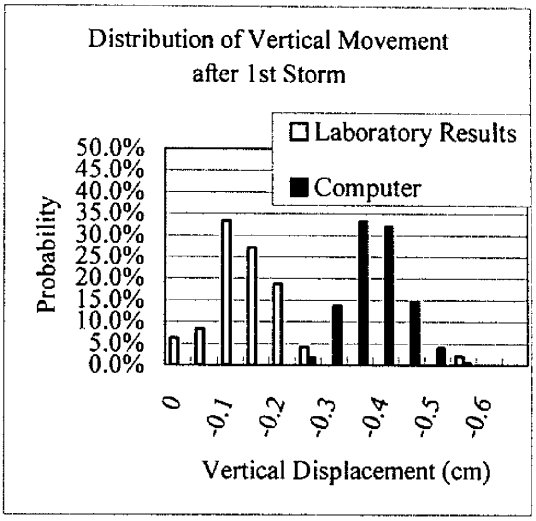

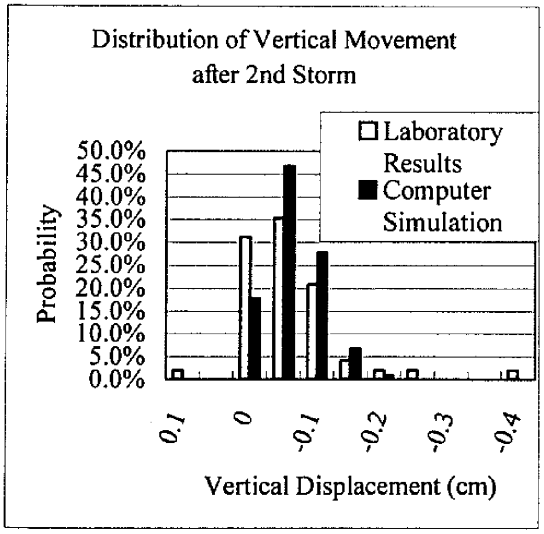

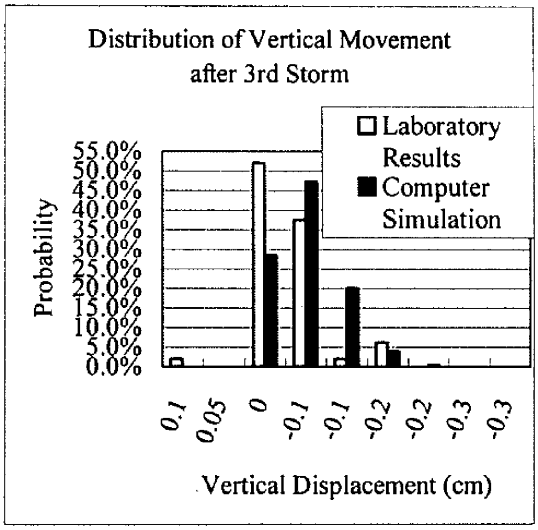

Figs. 4.6-4.11: Comparison of Computational and Laboratory Results Probability Distribution Curves

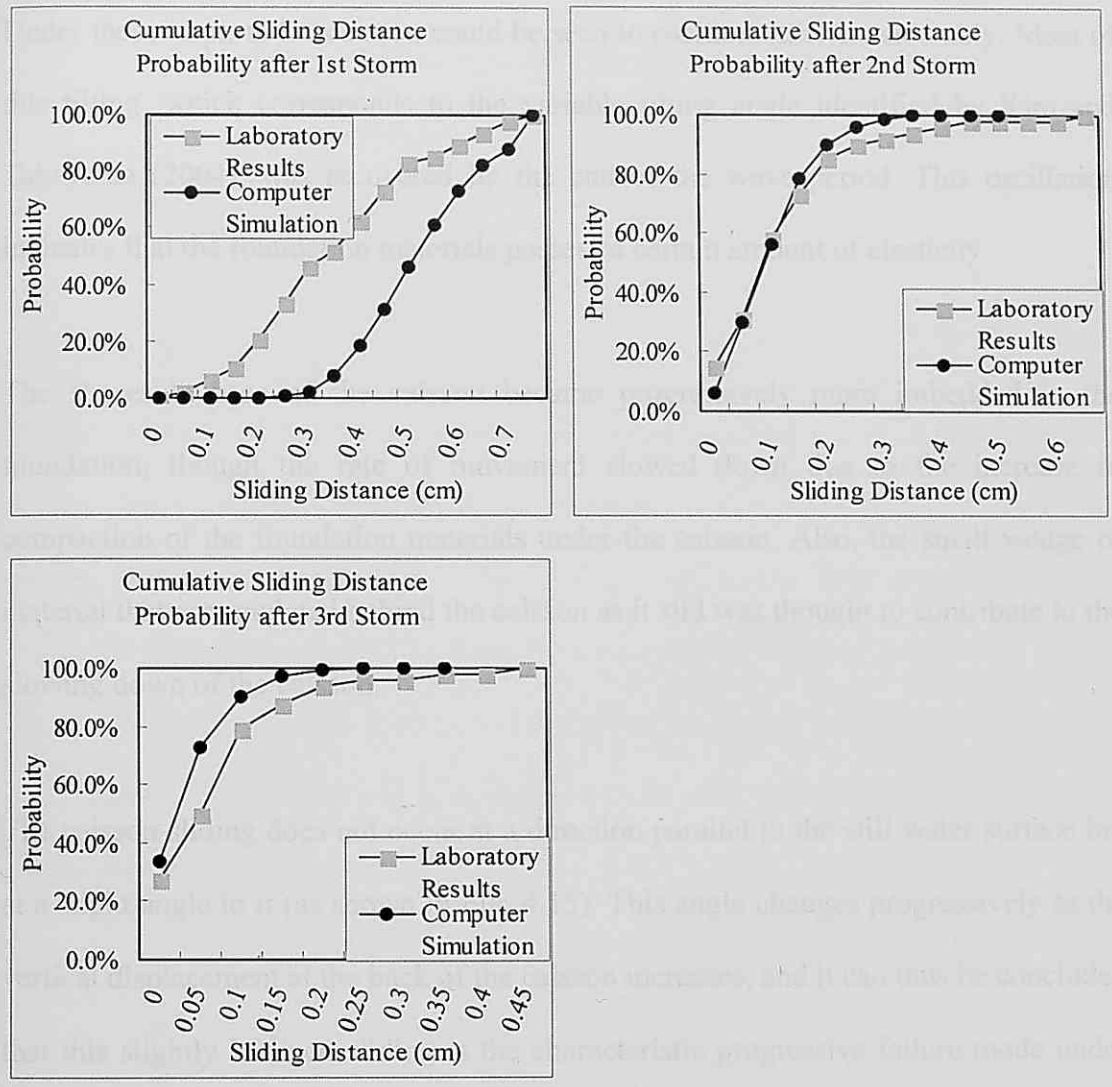

Figs. 4.12-4.14. Comparison of Cumulative Sliding Distance Probabilities

4.3. Discussion

The laboratory experiments were recorded using a video camera, which clearly showed the presence of impact loads. This agrees with the prediction of the parameter map in PROVERBS (see Fig 2.6 in chapter 2), as the caisson breakwater analysed in the present study had values of h_r^* =0.54 and H^* =0.43, which the parameter map classifies as 'Low Mound Breakwater' subjected to 'Large Waves' and indicating that Impact Loads will be present.

Under these impacts the caisson could be seen to oscillate (tilt) considerably. Most of this tilting, which corresponds to the variable tilting angle identified by Kim and Takayama (2004), was recovered by the end of the wave period. This oscillation indicates that the foundation materials possess a certain amount of elasticity.

The shoreside base of the caisson became progressively more imbedded in the foundation, though the rate of movement slowed down due to the increase in compaction of the foundation materials under the caisson. Also, the small wedge of material that accumulated behind the caisson as it slid was thought to contribute to the slowing down of the caisson.

The caisson sliding does not occur at a direction parallel to the still water surface but at a slight angle to it (as shown in Fig. 4.15). This angle changes progressively as the vertical displacement at the back of the caisson increases, and it can thus be concluded that this slightly inclined sliding is the characteristic progressive failure mode under impact waves.

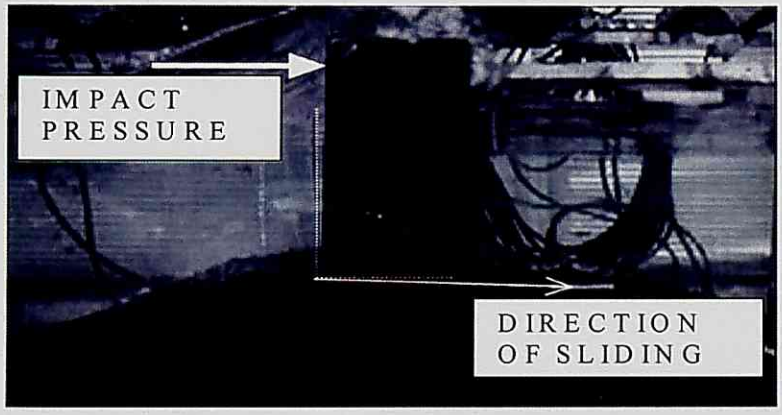

Fig.4.15: Photograph of wave impact showing the direction of sliding of the caisson.

The probability distribution curves obtained are not perfect due to the small number of experiments that were carried out. A much larger number of experiments should have been carried out in order to obtain better curves.

4.4. Conclusions

The failure mode of caisson breakwaters subjected to impact waves during a series of storms was established by the present experiments. The presence of impact waves was clearly established by using a video camera, which had been predicted by the Parameter Map shown in PROVERBS. By measuring the displacements at the back of the caisson the probability distribution functions for sliding and tilting at the end of each storm were obtained, which show that the rate of displacement slows down at the end of each consecutive storm.

CHAPTER 5

DEFORMATION BASED RELIABILITY DESIGN METHOD TO CALCULATE DEFORMATION IN THE FOUNDATION OF A CAISSON BREAKWATER

5.1. Introduction

Shimosako and Takahashi (2000) developed a Level 3 design method for caisson breakwaters referred to as the "deformation-based reliability design"(DBRD), which allows for a certain amount of sliding to take place before a caisson breakwater is deemed to have failed. This model uses the Goda formula (1974) as modified by Takahashi et al. (1994) in order to obtain the wave pressures at the wall. This modification simplifies the time history of wave pressure on the caisson into a triangular "churchroof" shape (impulsive wave force) and a sinusoidal part (standing wave force). In this approach the expected sliding distance of the caisson is a statistical average of the sliding distance over the service lifetime of the structure as computed by a Monte-Carlo type simulation. The European Report PROVERBS (1999) offers a comprehensive review of the state-of-the art probabilistic breakwater technology. It includes guidance on how to design breakwaters by using a probabilistic approach and recommendations on how to calculate the various forces acting on the breakwater and foundations.

More recently research by Kim and Takayama (2003) and Takagi and Shibayama (2006) proposed different improvements to the basic model of Shimosako and Takahashi. However, in all these models the displacement caused by a certain wave pressure is assumed to stay constant throughout the caisson's life. Kim and Takayama (2004) modified this model to take into account the effect of caisson tilting on the computation of sliding distance. In this method an assumption needs to be made regarding the final angle of tilting of the caisson, as Kim and Takayama provide no way of estimating it.

It is thus necessary to develop a method to compute the vertical deformation of the breakwater berm so that the sliding distance can be accurately estimated.

5.2. Deformation-Based Reliability Design Considering Sliding and Tilting

A new deformation model was developed based on that of Shimosako and Takahashi (2000). This model basically replicates the original model for the calculation of the sliding distance, but includes an additional restraining force due to the caisson's rotation. As can be seen in Fig. 5.1 the tilting of the caisson will push its shoreside edge into the foundation, with the foundation material exerting an additional restraining force F_w on the caisson sliding. In order to calculate the vertical movement of the caisson basic soil mechanics stress-strain theory is used. However, the parameters used in the calculation of the deformation will change progressively with time due to the compaction effect that successive waves will have on the foundation material. This compaction process will decrease the void ratio and thus increase the

bearing capacity and Young's Modulus of the gravel, making further deformation more difficult.

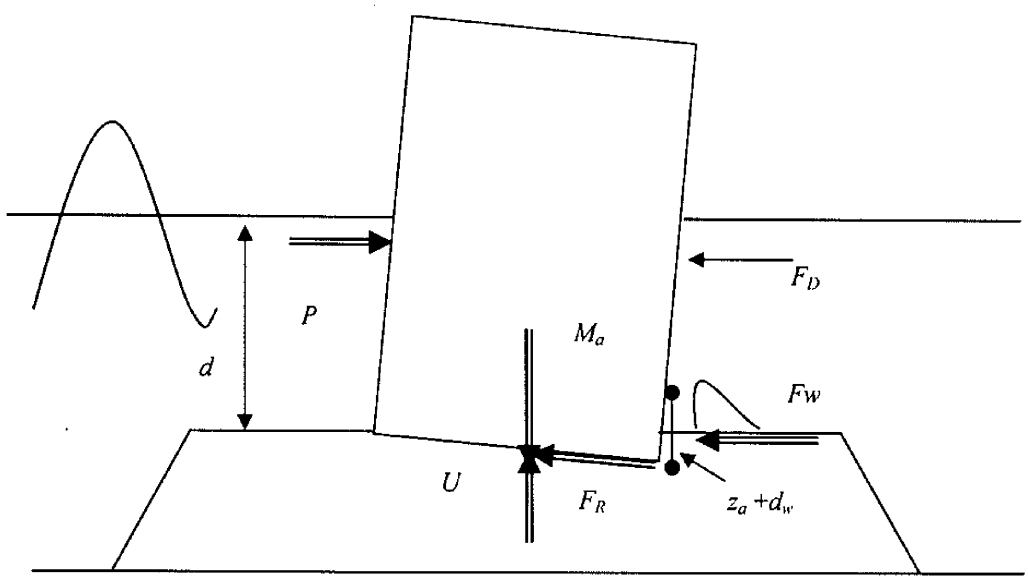

Fig.5.1. Forces acting on the caisson

5.2.1. Outline of the computational procedure

Using the methodology described in the next sections a FORTRAN program was written to evaluate the sliding and tilting of the caisson using the same parameters as those used in the laboratory experiments. Probability distribution functions for the sliding and tilting of the caisson were computed and these curves were then compared to the ones obtained from the laboratory experiments detailed in section 4 below (see Figs. 4.5 to 4.10 in chapter 4). The computational procedure is summarised in Figs. 5.2 and 5.3.

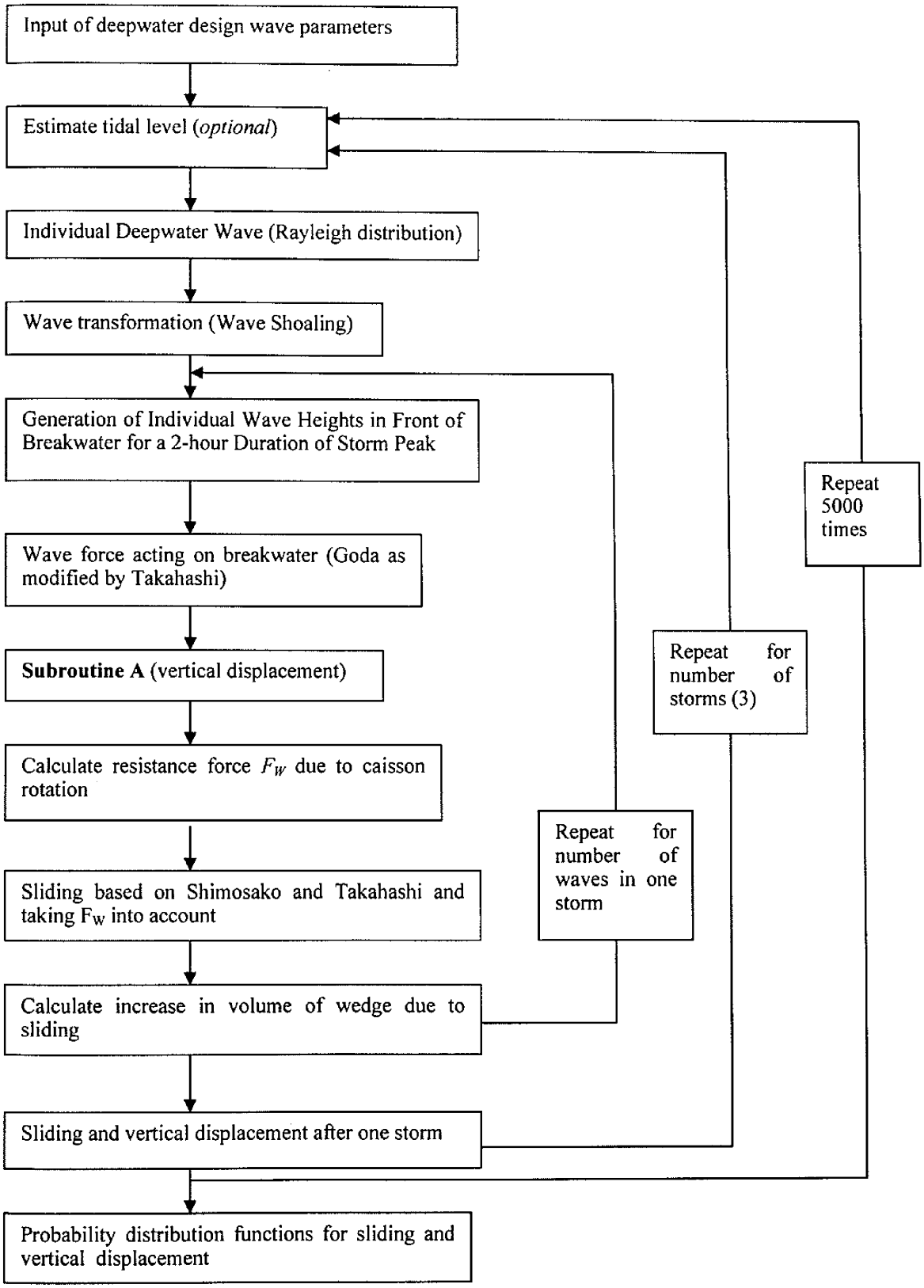

Fig. 5.2. Block diagram of computation procedure

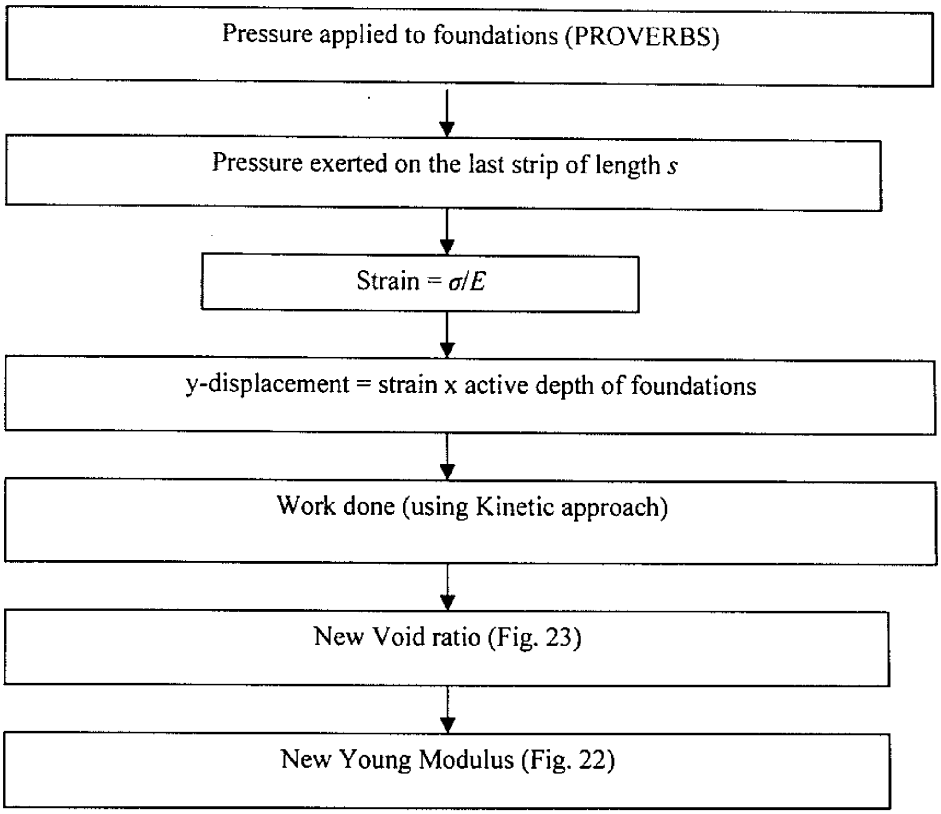

Fig. 5.3. Details of block diagram for computation of vertical

The computational procedure divides the movement of the caisson into two different components, sliding and tilting, with the vertical position of the caisson influencing the sliding motion but not vice-versa. As the caisson becomes increasingly more imbedded in the foundation the magnitude of the additional resistance force induced by the tilting increases, thus progressively slowing down the caisson sliding.

5.2.2. Sliding Equation of Motion

The forces that act on the caisson during the sliding motion can be seen on Fig. 5.1. Shimosako and Takahashi (2000) proposed that the equation of motion that describes the sliding should be:

$$(\frac{W}{g} + M_a)\ddot{x}_G = P - F_R - F_D \tag{5.1}$$

where P is the horizontal wave force, $\ddot{x}_G$ the acceleration at the centre of gravity of the caisson, M_a the added mass, F_R the frictional resistance force, F_D the force related sliding velocity including the wave-making resistance force, W the caisson weight in air and g the gravity.

In addition, a force F_W induced by the rotation of the caisson and the wedge of material accumulated behind the caisson due to sliding must be included:

$$(\frac{W}{g} + M_a)\ddot{x}_G = P - F_R - F_D - F_W \tag{5.2}$$

This F_W is similar to the force $R(\theta(t))$ first introduced by Kim and Takayama (2005), which was proportional to the weight of the material above the hypothetical sliding plane of the caisson.

In the simplified model of Shimosako and Takahashi (2000), it is assumed that the friction coefficient μ takes a constant value i.e. it represents both the static and dynamic coefficients. Takagi and Shibayama (2006) showed quantitative evidence that F_D can be neglected if the duration of the effective impact is small enough. Consequently the above equation can be rewritten in the form:

$$(\frac{W}{g} + M_a)\ddot{x}_G = P + \mu U - \mu W' - F_W \tag{5.3}$$

where W' is the caisson's weight in water and U is the uplift force.

5.2.3. Wave Forces on the Caisson

The procedure proposed by Tanimoto et al. (1996) describes how the wave force acting on the caisson can be calculated. The time history model, as shown on Fig. 5.4, is made of the superposition of an impulsive "churchroof" shaped wave force $P_2(t)$, and a slowly varying standing one $P_1(t)$, as given by Eq. 5.4:

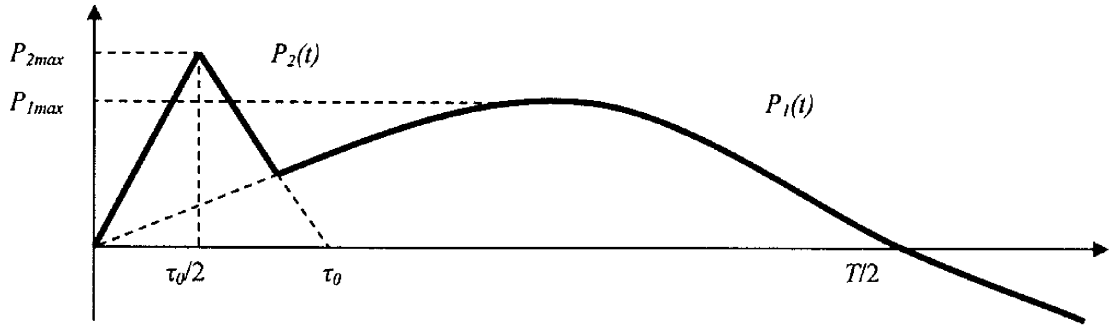

Fig.5.4. Wave force profile for sliding calculation

$$P(t) = \max \{ P_1(t), P_2(t) \} \tag{5.4}$$

These parameters are defined by the following equations,

$$P_1(t) = \gamma_P P_{1\max} \sin\frac{2\pi t}{T} \tag{5.5}$$

$$P_2(t) = \frac{2t}{\tau_0} P_{2\max} \qquad for : (0 \le t \le \frac{\tau_0}{2}) \tag{5.6}$$

$$P_2(t) = 2(1 - \frac{t}{\tau_0}) P_{2\max} \qquad for : (\frac{\tau_0}{2} \le t \le \tau_0) \tag{5.7}$$

$$P_2(t) = 0 \qquad for : (t \ge \tau_0) \tag{5.8}$$

$$\gamma_P = 1 - \frac{\pi}{P_{1\max} T} \int_{t_1}^{t_2} (P_2(t) - P_{1\max} \sin\frac{2\pi t}{T}) dt$$

$$for : P_2(t) - P_{1\max} \sin\frac{2\pi t}{T} \ge 0 \tag{5.9}$$

P_{1max} denotes the horizontal wave force estimated from the Goda formula (1974) neglecting the coefficient that indicates the effect of an impulsive pressure (α_2). The symbol P_{2max} represents the horizontal wave force exerted by the Goda formula considering an impulsive pressure coefficient defined as:

$$\alpha^* = \max\{\alpha_1, \alpha_2\} \tag{5.10}$$

where α_1 is the impulsive pressure coefficient proposed by Takahashi et al. (1994). The symbol γ_P denotes a modification factor that indicates the reduction in the standing wave force due to the occurrence of the impulsive wave force and t_1 and t_2 the beginning and end of the impulsive wave force, respectively.

The uplift pressure $U(t)$ is defined as:

$$U(t) = \max\{ U_1(t), U_2(t) \} \tag{5.11}$$

where,

$$U_1(t) = \gamma_0 U_{\max} \sin\frac{2\pi t}{T} \tag{5.12}$$

$$U_2(t) = \frac{2t}{\tau_0} U_{\max} \qquad for: (0 \le t \le \frac{\tau_0}{2}) \tag{5.13}$$

$$= 2(1 - \frac{t}{\tau_0}) U_{\max} \qquad for: (\frac{\tau_0}{2} \le t \le \tau_0) \tag{5.14}$$

$$=0 \qquad for: (t \ge \tau_0) \tag{5.15}$$

$$\gamma_U = 1 - \frac{\pi}{U_{\max} T} \int_{t_1}^{t_2} (U_2(t) - U_{\max} \sin\frac{2\pi t}{T}) dt$$

$$for: U_2(t) - U_{\max} \sin\frac{2\pi t}{T} \ge 0 \tag{5.18}$$

where $U_{\max}$ is the uplift force calculated from the Goda formula.

When $(P+\mu U) > \mu W'$ the caisson starts sliding. The peak values of $P(t)$ and $U(t)$ are obtained using the Goda formula and the duration of the impulsive wave τ_0 is given by:

$$\tau_0 = k\tau_{0F} \tag{5.19}$$

$$k = \left(\frac{1}{(\alpha^*)^{0.3}+1}\right)^2 \tag{5.20}$$

$$\tau_{oF} = \left(0.5 - \frac{H}{8h}\right)T \qquad for: (0 \le \frac{H}{h} \le 0.8) \tag{5.21}$$

$$=0.4T \qquad for: (0.8 < \frac{H}{h}) \tag{5.22}$$

where H denotes the wave height and h the water depth.

5.2.4. Vertical Displacement Equation of Motion

In order to evaluate the vertical displacement at the back of the caisson a similar principle to that used in the sliding calculation is followed. In this analysis only the shoreside edge of the caisson is considered, as this is the area that will suffer the greatest deformation.

It is thought that the wave force acting on the caisson induces a triangular distribution of pressure underneath the breakwater, as shown in Fig.5.5. This triangular distribution is responsible for the tilting of the caisson as it slides, as the shoreside of the foundation will take a much higher load and deform more significantly than the seaward part. Taking into account this triangular distribution, the total pressure applied to the entire foundation is given by the formula:

$$P_{foundations} = \frac{B \cdot P_{foundations.\max}}{2} \tag{5.23}$$

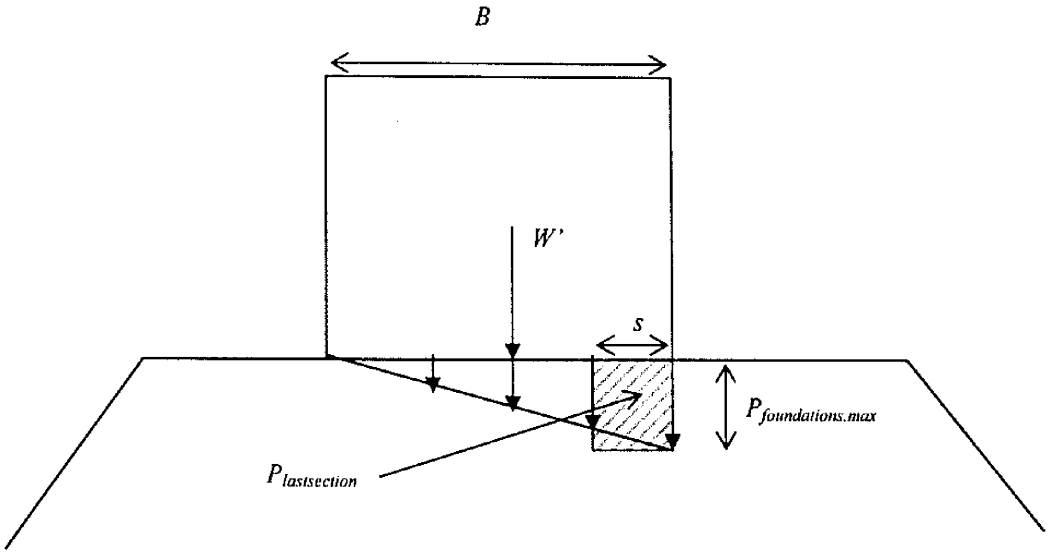

Fig.5.5. Diagram of Vertical Movement Parameters

where B is the width of the caisson, $P_{foundations}$ is the total pressure applied to the foundation by one wave, and $P_{foundations.max}$ is the maximum pressure applied to any one point of the foundation (corresponding to the shoreside edge of the caisson).

Therefore,

$$P_{foundations.\max} = \frac{2 \cdot P_{foundations}}{B} \tag{5.24}$$

The total pressure acting on the last section (a strip of length s) of the breakwater foundation will be given by:

$$P_{last\ section} \approx \left(\frac{2 \cdot P_{foundations}}{B} + \frac{W'}{B} \right) \cdot s \tag{5.25}$$

In order to obtain the motion inducing force acting on this strip of soil, the bearing capacity of the foundation needs to be deducted from the pressure applied. The equation of movement in the vertical direction thus becomes:

$$\left(\frac{W}{g} + M_a \right) \ddot{x}_E = \left(\frac{2 \cdot P_{foundation} + W'}{B} s \right) - q_U \cdot s \tag{5.26}$$

where $\ddot{x}_E$ is the acceleration at the edge of the caisson and q_U is the bearing capacity of the foundation. Or,

$$\left(\frac{W}{g}+M_a\right)\ddot{x}_E=\left(\frac{2\cdot P_{foundation}+W'}{B}-q_U\right)s \tag{5.27}$$

By integrating the acceleration with respect to time the velocity can be obtained, and by integrating twice the vertical movement of the caisson can be calculated.

5.2.5. Pressure to the Foundation

The pressure to the foundation was evaluated using the method described in Chapter II of PROVERBS. This procedure models the foundation of the caisson as a series of linear elastic springs, thus allowing the transformation of the oscillating pressure which the wave produces on the foundation into an equivalent static pressure $F_{stat,eq}$ defined as,

$$F_{stat,equ}=\nu_D F_{dyn,\max} \tag{5.28}$$

where ν_D is the dynamic response factor and $F_{dyn,max}$ is the peak of the hydraulic load to the wall.

This mass-spring system is characterised by its natural period T_N. The load/time curve can be simplified into the characteristic churchroof shape shown in Fig. 5.4. Only the short duration "churchroof" impulsive part of the wave pressure is considered in this method, leaving the standing part out. The dynamic response factor of the mass-spring system loaded by such a wave is a function of T_N, t_d (total impact duration) and t_r (time rise) as seen in Fig. 5.6.

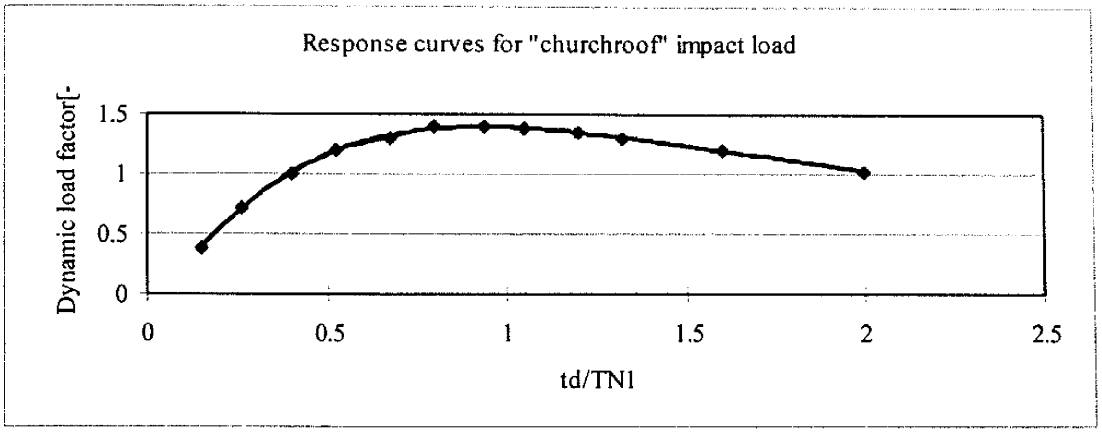

Fig.5.6. Response curves for "churchroof" impact load: dynamic response

PROVERBS recommends that the mass-spring system should be approximated as a two-degree of freedom system with 2 natural periods T_{N1} and T_{N2}. The largest of the two natural periods (T_{N1}) is usually close to the natural period of the single degree of freedom system in the horizontal direction and should be used for obtaining the response curve. On the other hand T_{N2} is close to the natural period of the rotation of the structure.

T_{N1} and T_{N2} are functions of the two components of the stiffness matrix, k_x and k_φ, and the two components of the mass matrix, m_{tot} and Θ_{tot}. When a caisson that is subjected to an impulsive wave load is forced to oscillate the body of water and soil adjacent to the caisson is forced to move along with the structure. The total mass of the system m_{tot} is obtained by considering the mass of the caisson m_{cai}, the added mass of water m_{hyd}, and the geodynamic mass, m_{geo} ,

$$m_{tot} = m_{cai} + m_{hyd} + m_{geo} \tag{5.29}$$

In the same way the total moment of inertia around the centre of gravity, Θ_{tot}, is given by,

$$\Theta_{tot} = \Theta_{ca} + \Theta_{hyd} + \Theta_{geo} \tag{5.30}$$

De Groot et al.(1996) provides the following equations to find these various components:

$$m_{hyd} = 1.4\,\rho\, d^2\, L_c \tag{5.31}$$

$$m_{geo} = \frac{0.14\rho_s (BL_c)^{1.5}}{(2-\Gamma)} \tag{5.32}$$

$$\Theta_{cai} = \frac{m_{cai}(B^2 + h_h)}{12} \tag{5.33}$$

$$\Theta_{hyd} = 0.063\,\rho\, d^4\, L_c \tag{5.34}$$

$$\Theta_{geo} = \frac{0.039\rho_s (B^3 L_c)^{1.25}}{(1-\Gamma)} \tag{5.35}$$

$$k_x = 3\,G\,(B\,L_c)^{0.5} \tag{5.36}$$

$$k_\varphi = 0.8\,G\,B^2\,L_c \qquad \text{for } 0.1 < B_c/L_c < 1 \tag{5.37}$$

$$k_\varphi = 0.8\,G\,B^{2.5}\,L_c^{0.5} \qquad \text{for } 1 < B_c/L_c < 10 \tag{5.38}$$

G is the shear modulus, h_h is the height of the caisson, L_c is the caisson length, ρ the density of water, ρ_s the density of the foundation material and Γ is the Poisson ratio. If a thick rubble foundation is considered then the average values of the (drained) rubble can be used whereas if a thin foundation is present PROVERBS recommends that undrained parameters be employed.

The two natural periods can then be found using Eq. 5.39,

$$T_{N1,2} = \frac{2\pi}{\omega_{1,2}} \tag{5.39}$$

where,

$$\omega_{1,2}^2 = \frac{\psi}{2} \pm \sqrt{\frac{\psi^2}{4} - \frac{k_x \cdot k_\varphi}{m_{tot} \cdot \Theta_{tot}}} \qquad \psi = \frac{k_\varphi}{\Theta_{tot}} + \frac{k_x \cdot (a_x^2 + a_z^2)}{\Theta_{tot}} + \frac{k_x}{m_{tot}} \tag{5.40}$$

a_x and a_z are the distance from the centre of gravity to the point where the resistance forces from the foundation in the x and z co-ordinates are applied.

In a first approximation ω_1 can be assumed to be very small in comparison to ω_2 and hence,

$$T_{N1} \approx T_{Nx} = 2\pi\sqrt{\frac{m_{tot}}{k_x}} \quad and \quad T_{N2} \approx T_{N\varphi} = 2\pi\sqrt{\frac{\Theta_{tot}}{k_\varphi}} \tag{5.41}$$

5.2.6. Bearing Capacity

In order for the equation of motion to be solved the major problem lies in determining the value of q_U, which is thought to change throughout the life of the structure due to the consolidation of the foundation material. Table 3.2 in Chapter 3 gives some presumed bearing capacity values according to British Standard (BS) 8004:1986, showing how the bearing capacity of the foundation is greatly affected by the degree of consolidation in the foundation material. The limit to which the foundation materials can be compacted depends on the void ratio of the gravel used and there is a limit to the compaction level that can be achieved for a certain type of gravel. During the construction phases the foundation of caisson breakwaters is usually consolidated by different means though it appears unlikely that the consolidation limit is reached during this time. Furthermore, although there is a theoretical limit to the void ratio that can be achieved for a given foundation particle diameter, further compaction is still possible as high energy impacts can break the gravel into smaller particles capable of achieving higher densities.

In order to determine q_U, it is necessary to first determine the properties of the gravel.

5.2.7. Plastic Young's Modulus

The strain ε which occurs in a soil when a load is applied can be divided into elastic (ε_e) and plastic (ε_p) strain:

$$\varepsilon = \varepsilon_e + \varepsilon_p = E \cdot \sigma \tag{5.42}$$

where E is the Young's Modulus of the soil and σ is the pressure applied to the gravel. Thus,

$$\varepsilon_p = E \cdot \sigma - \varepsilon_e = E_p \cdot \sigma \tag{5.43}$$

Fig.5.7 illustrates the different strain curves that can be obtained when a foundation material is loaded. Each time the caisson is subjected to wave loading a strain will be observed in the foundation, corresponding to the E curve. However when the load is removed –at the end of each wave cycle- part of the strain is recovered due to the elasticity of the foundation. The non-recovered part behaves as if a slightly different E had been applied from the start and none of it had been recovered, corresponding to the E_p curve.

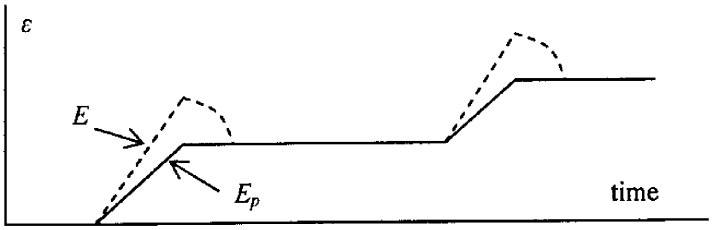

Fig.5.7. Graph of Plastic and normal Young's Modulus

In order to determine E_p laboratory experiments were carried out at the soil mechanics laboratory of Yokohama National University. These consolidation experiments were conducted in accordance with the Japanese Code JIS A1210:1999 and the results are shown in Fig. A.3 of Appendix A.

To determine the reduction in the void ratio due to the compaction energy applied by the caisson to the gravel foundation a "Test Method for Soil Compaction using a Rammer" (JIS A 1210:1999) was carried out, with the results shown in Fig. A.5 of Appendix A. In this test the void ratio of the gravel decreased rapidly when a relatively small amount of compaction energy was applied, but then the rate of decrease in the void ratio slowed down progressively and after a certain point the material was completely compacted. From this point any further reduction in void ratio was caused by the breakdown of the gravel into smaller particles. During the soil compaction tests this breakdown of particles was clearly observed, with the higher energy tests producing significant amounts of fine sand and dust.

By using Figs. A.3 and A.5 of Appendix A it is possible to determine the plastic Young's Modulus E_p of the foundation material if the amount of energy that has gone into the foundation is known.

5.2.8. Compaction Energy

To estimate the energy done by the caisson on the foundation a kinetic approach is used. The time history of the pressure exerted by a single wave on the foundation can be calculated following the procedure described in Section 5.2.4 and then by using Eq. 5.27 the time history of the acceleration can be calculated. The maximum velocity that

the caisson would achieve **if it was not constrained** by the foundation can be found by integrating Eq. 5.27. This can then be used to obtain the total kinetic energy (*K.E.*) that is transmitted by the caisson onto the foundation:

$$K.E. = \frac{1}{2} m_S V_{unconstrained}^2 \tag{5.44}$$

where m_s denotes mass and $V_{unconstrained}$ is the unconstrained maximum velocity. The philosophy of the analysis carried out up to this point was to examine only the behaviour of a section of width *s* situated at the shoreside of the caisson. It is not completely clear what fraction of the mass of the caisson should be used in calculating the *K.E.* that goes into the last section of the foundation. In order to simplify the procedure only the vertical strip directly above the section being studied –a mass corresponding to the strip of width *s*- is considered i.e. this last section becomes a 'rammer' going into the foundation. Hence:

$$m \approx m_{last.section} = \frac{W'}{B} \cdot s \tag{5.45}$$

where $m_{last.section}$ is the mass of the rammer section of width *s*.

The *s* value used would depend on the size of the caisson, however for normal caisson widths an *s* value equal to two times the average diameter of the foundation gravel (0.5cm in the present experiment, corresponding to a real size rock of 0.5m in diameter giving *s*=1m) is proposed.

5.2.9. Strain

The plastic strain in the last section of the foundation can be calculated by using

$$\varepsilon_p = \frac{P_{last\ section}}{E_p} \tag{5.46}$$

Once ε_p is known the total vertical displacement (z_a) caused by each wave can be obtained by

$$z_a = \varepsilon_p \times d_Z \tag{5.47}$$

where d_z is the active depth of foundation.

The choice of an appropriate active depth of foundation is difficult, though it is believed that most of the consolidation at the shoreside of the caisson takes place in the top region of the foundation material. Chapter 3 of the present dissertation justifies how for most caisson sections the value of d_z =1cm is adequate, and this value will be adopted in the present computations.

5.2.10. Additional horizontal resistive force on sliding caused by tilting of caisson

Fig. 5.8 shows how the tilting of the caisson slows down the sliding motion by inducing an additional restraining force F_W. This force is the result of two related phenomena:

1. As the caisson tilts it becomes imbedded in the foundation. In order for further sliding to take place the caisson must push towards the shore the material (area B in Fig. 5.8) directly adjacent to it.

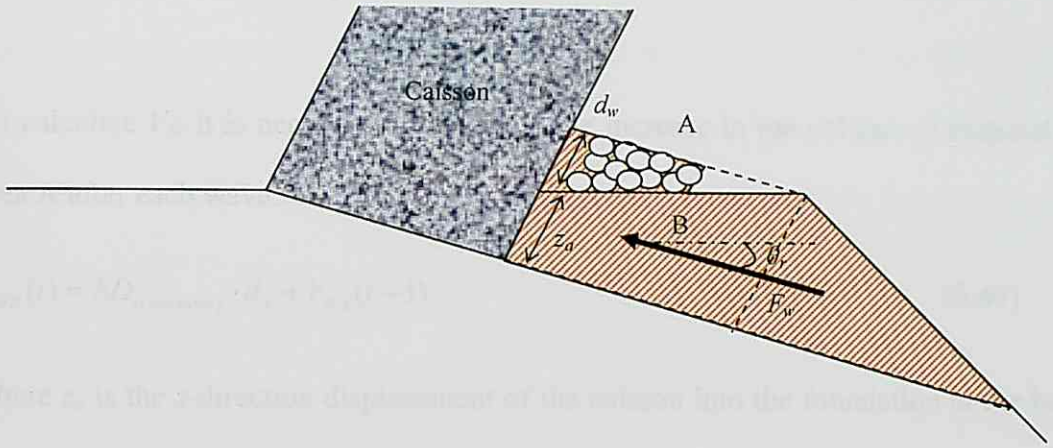

Fig. 5.8: Restraining forces on caisson sliding

2. Then, as the caisson moves towards the shore it will displace material from area B upwards. This material will accumulate as a 'wedge' of gravel on top of the existing foundation (area A) and will also resist any further shoreside sliding of the caisson.

The force that resists the movement of the caisson acts along the sliding plane of failure as shown on Fig. 5.8. Thus F_W can be defined by using,

$$F_w = \rho_s \cdot g \cdot V_w \cdot \tan\phi \qquad (5.48)$$

where ρ_s is the density of the foundation gravel stones ,ϕ is the angle of friction of the gravel, V_W is the volume of material resisting the sliding movement (shown in yellow in Fig. 5.8.) and g the acceleration of gravity. According to Mizukami and Kobayashi (1991) ϕ should have a value of 35 degrees.

In order to be consistent with Eq. 5.2 the horizontal component of F_W should be used,

$$F_w = (\rho_s \cdot g \cdot V_w \cdot \tan\phi)\cos\theta_r \qquad (5.49)$$

where θ_r is the residual tilting angle, though in the present simulation θ_r is small and Eq. 48 can be used as a simplification.

To calculate V_W it is necessary to calculate the increase in the volume of material in area A after each wave:

$$V_{WA}(t) = SD_{t(onewave)} \cdot d_z + V_{WA}(t-1) \tag{5.49}$$

where z_a is the z-direction displacement of the caisson into the foundation at the back of the caisson, $V_{WA}(t)$ is the volume of the wedge of accumulated material at the shoreside of the caisson after a certain number of waves, $V_{WA}(t-1)$ is the volume of accumulated material by previous waves and $SD_{t(onewave)}$ is the sliding distance caused by each individual wave.

5.4. Comparison between computer simulation and laboratory results

Figs. 4.6 to 4.11 in Chapter 4 show the comparison between the probability distribution curves obtained using the proposed computational model and those plotted from the laboratory experiments. Figs. 4.12 and 14 show the expected probability of a certain sliding taking place. From these figures it can be seen how although the present model appears to be able to predict the sliding and tilting values for the 2nd and 3rd storms it tends to overestimate the deformation during the first storm. This is specially the case for the vertical movement, as the soil mechanics tests do not give a very reliable indication of the strength of the soil for high void ratios. Also there are uncertainties regarding the true value of d_z, which can affect the final results.

Consideration also has to be given to the fact that the probability distribution curves for the laboratory tests are based only on 48 experiments and hence although they give an indication of the shape of the curve it cannot be considered as definite The shape of this probability distribution changes with each subsequent storm due to the average displacement reducing in each subsequent storm, thus skewing the shape of the curve.

Finally, the results are shown in intervals of 0.05cm (0.5mm) so in the case where small displacements occur (such as after the 2^{nd} and 3^{rd} storms) it is not clear that the results displayed constitute a real probability distribution curve. In this case a smaller interval would probably have been more appropriate, but this was difficult due to the small scale (1/100) used in the experiments.

5.5. Discussion

Normal soil mechanics theory does not deal with the long-term plastic deformation of gravel foundations. Moreover, in the case of impulsive loading of the caisson the crucial part of the load applied which causes the deformation lasts for fractions of a second, and most soil mechanics theories deal with loads being applied over a long period of time (not rapid cycles of loading and unloading). Also to be noted is that the entire soil is submerged in water and can be considered to be in the fully drained condition. All these points raise questions as to the validity of using normal soil mechanics theories in the model proposed. However, although a more complex theory might be more appropriate, it is believed that the simple approach given is enough to give an approximate value for the vertical deformation of the caisson.

The accuracy of the soil mechanics parameters that were used in the derivation of the model proposed above is also not clear. The experiments that were carried out were small in scale and hence it appears likely that due to boundary effects there were large errors in the final gravel parameters obtained. The parameters used have a big effect in the final computed deformation of the rubble mound, and hence the choice of appropriate ones is of paramount importance if the model is to be accurate.

Scale effects could also be a possible significant source of discrepancy between the results of the model and real life behaviour. The bearing capacity of the foundation is governed by the amount of friction between gravel, and thus the shape and contact area between particles can greatly affect this parameter. It is not clear to what extent the values used in the experiment can translate into the real life values due to these differences. Moreover, real rubble mound foundations are made from a variety of rock sizes and shapes, which are often angular in nature due quarry extraction procedures. The rock used in the experiment was of a rounded shape and hence the method proposed should be treated with caution if used for angular rock.

When applying the current model to prototype breakwaters careful consideration has to be given to the issue of compaction of the foundation. The present experiments were conducted with light compaction to the gravel (in the form of light tapping of the gravel and a preparatory "storm" to "settle" the caisson). In real construction it is not clear to what extent the foundations are compacted and its possible that due to different working practices there could be a significant difference in the observed deformations in prototype breakwaters.

It appears probable that if more accurate soil mechanics parameters could have been obtained better results could have been produced. However, as the results tend to overestimate slightly the deformation during the first storm they can be considered to be conservative. Nevertheless they are of the right order of magnitude to those observed in the laboratory tests and it thus seems that the model can be used to obtain an estimate of the final tilting and sliding of the caisson.

5.6. Conclusions

A new methodology was proposed for the estimation of the deformation in the rubble mound of a caisson breakwater due to the sliding/tilting failure nature of impact waves acting on its vertical face. This model uses a simple soil mechanics theory to evaluate the vertical displacement at the back of the caisson, which depends heavily on the degree of consolidation of the rubble material. The model is heavily influenced by the choice of the gravel parameters, and hence care taken to use accurate values if the methodology is to be applied to a prototype breakwater.

CHAPTER 6

SOLITARY WAVES

6.1. Introduction

Tsunamis are extremely powerful waves caused by large undersea disturbances such as earthquakes, landslides, volcanoes or meteorites. The most common type, representing probably 95% of occurrences, is that caused by earthquakes –usually under the ocean floor but occasionally near shore. Because the volume of water in the sea is essentially constant, an upward or downward movement of the sea floor will raise or lower the water above it, causing a wave to occur. These waves are sometimes incorrectly called tidal waves, which are in fact long-period waves associated with the tide-producing forces of the moon and the sun and which are identified with the rising and falling of the tide.

Tsunamis are distinguished from normal sea waves by their wavelength, which can extend more than hundreds of kilometres from crest to crest. A tsunami in deepwater is considered a shallow-water wave, and as the celerity of these waves is determined by the ratio of the water's depth to the wavelength of the wave, a tsunami can travel at high speeds over great transoceanic distances with limited energy loss. However once a tsunami leaves the deep water of the open sea and moves into the shallower water of the coastal areas it undergoes a transformation. Its speed and wavelength will decrease

and its amplitude will increase, dramatically sometimes. The shape of the tsunami as it reaches the shore will depend on the area's topography and bathymetry. It might appear as a rapidly rising or falling tide that rushes up onto the beach without breaking, as a turbulent wall of water with higher water behind it (bore-type) or as a soliton, as seen in Fig. 6.1.

The increase of the tsunami's waveheight as it enters shallow water is given by:

$$\frac{H_s}{H_d} = \left(\frac{h_d}{h_s}\right)^{1/4} \tag{6.1}$$

where H_s and H_d are waveheights in shallow and deep water and h_s and h_d are the depths of the shallow and deep water. So a tsunami with a height of 1 m in the open ocean where the water depth is 4000m would have a waveheight of 4 to 5 m in a water depth of 10 m.

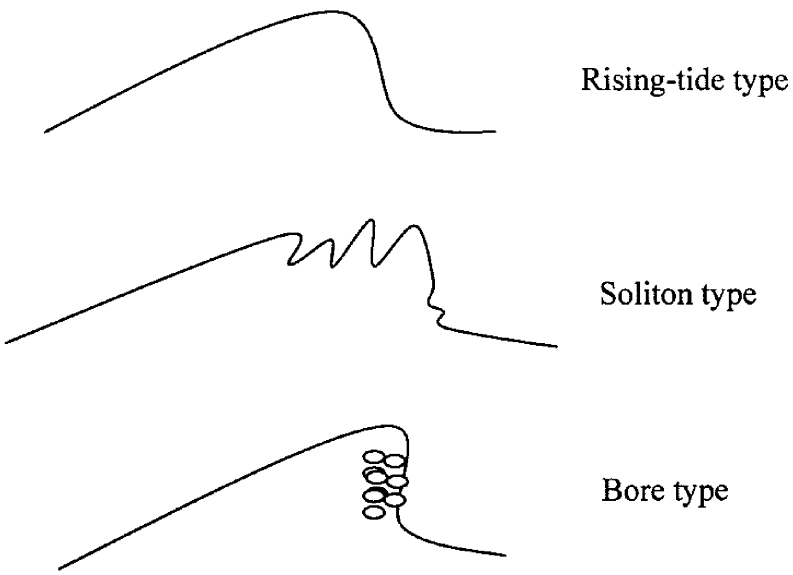

Fig. 6.1: Tsunami types

Following a number or recent tsunamis in the Asia-Pacific area there has been an increased awareness about the destructive potential of these phenomena. The development of countermeasures is of paramount importance in order to prevent the loss of life and property that might occur as a result of these waves. Various researchers such as Shibayama et al, (2006), Sasaki (2006) or Jayaratne et al. (2006) have noted the effects that various types of coastal terrain have on the attenuation or magnification of the damage due to tsunami attack. However the degree of protection that the various natural or artificial coastal structures offer against tsunami attack is not yet properly understood. The 2003 Banda Aceh tsunami has highlighted how coastal forests do not always offer effective protection against tsunami attack as previously thought (it appears that if the tsunami height exceeds the height of the trees these are ripped from the ground and carried by the force of the wave). Hence it is not clear which is the best method to protect against tsunami attack and what degree or risk is related to the different methods of defence.

In Japan, sea dikes have been built along the coast to protect against tsunamis, high waves and storm surges, and numerous records (such as that of Naksuksakul (2006) for Kanagawa Prefecture) can be found of the construction of such structures. However, expected tsunami heights are often higher than the existing defences, and hence the damage due to a tsunami should be comprehensively estimated in order to formulate a correct disaster prevention policy.

Naksuksakul (2006) developed a risk based safety analysis for a coastal area against tsunami and storm surges. The methodology he proposed can estimate the loss of life for an urban coastal area provided that the topography, city layout and population

density are known. This method does not however consider the possibility of constructing counter-measures and what effect would these have on the loss of life. In order to incorporate these into the model the behaviour and characteristics of a tsunami attack must be further researched. In particular, the interaction and possible damage by the tsunami on possible defensive mechanisms must be clarified.

The stability of coastal dikes and breakwaters against tsunamis must be ascertained in order to understand the degree of reliability of these structures. The wave force induced by the tsunami, along with the scouring of breakwaters foundations are two of the major factors relating to the failure of coastal dikes. The force exerted by the tsunami would depend strongly on the shape of the wave, which in term depends on the depth of water and other factors.

Tanimoto et al. (1984) performed large-scale experiments on an vertical breakwater by using a sine wave and developed a formula for the calculation of the wave pressure. Ikeno et al (2001) conducted model experiments on bore type tsunamis and modified Tanimoto's formula by introducing an extra coefficient for wave breaking. Subsequently Ikeno et al (2003) improved the formula to include larger pressures around the still water level, where the largest wave pressure was observed to occur. Mizutani and Imamura (2002) also conducted model experiments on a bore overflowing a dike on a level bed and proposed a set of formulae to calculate the maximum wave pressure behind a dike. These formulas are however based on fixed structures, and no research has been done on the pressures applied to the rubble mound foundation and the deformation that would be suffered as a consequence. This research is important for the development of an effective risk management policy, as the reliability of the structures must be determined against a variety of tsunami heights

and types. As tsunamis are extreme rare events it is possible to design a structure allowing for it to deform substantially –which would be considered as a traditional engineering failure- if it is still able to significantly protect the area behind it.

The experiment detailed in the current chapter will attempt to reproduce the damage that a tsunami would cause on a caisson breakwater by using solitary waves.

6.2. Laboratory Experiments

6.2.1. Definition of solitary wave

A solitary wave or soliton is an isolated wave that propagates without dispersing its energy over a large region of water, and can thus maintains its shape while it travels at constant speed. They were first described by John Scott Russell, who first observed such a wave in the Union Canal in England.

6.2.2. Apparatus and Methodology

Laboratory experiments were carried out in order to try to obtain a picture of the failure mode of caisson breakwaters under solitary wave attack. The wave flume used measured 15.3m long x 0.6m wide x 0.55m deep and is located at the Hydraulics laboratory of Yokohama National University in Japan. Fig. 6.2 shows a schematic representation of the wave tank and apparatus used, which was modelled using a 1:100 scale. The experiments were conducted for a range of water depths between h=15 and 20cm. At one end of the wave tank a wooden gate was placed to create a water reservoir (2.25m long x 0.6m wide x 0.55m deep) behind it, with ductile clay placed around the edges to ensure that water did not escape. At the other end of the

tank a low crest rubble mound breakwater and a wave absorption beach were constructed in order to dissipate the energy of the waves created by the overtopping of the caisson. Figs. 6.3 and 6.4 show the gate and a view of the wave tank.

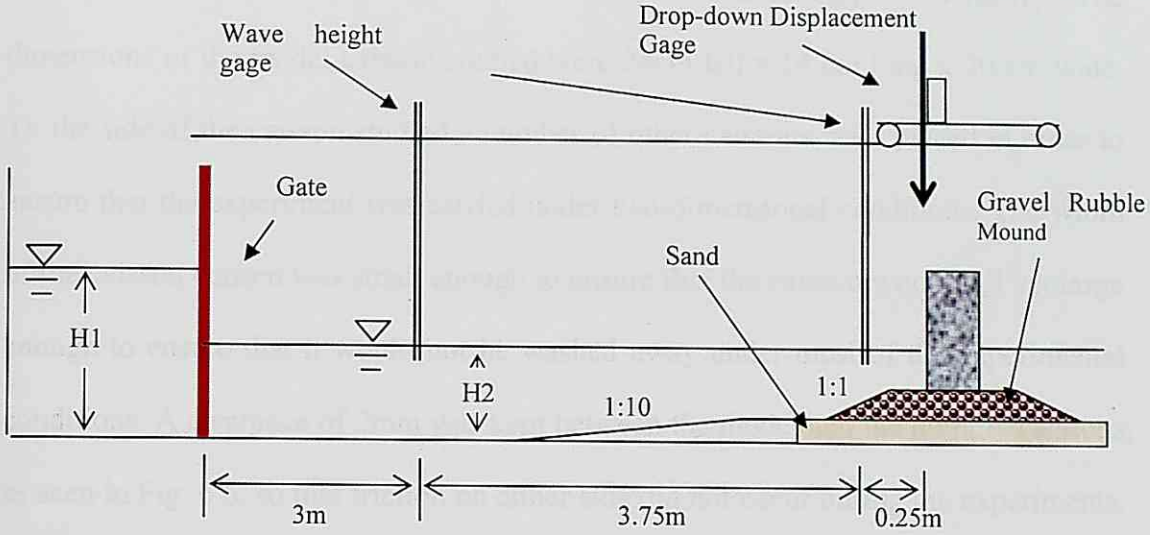

Fig.6.2. Experimental Set-Up

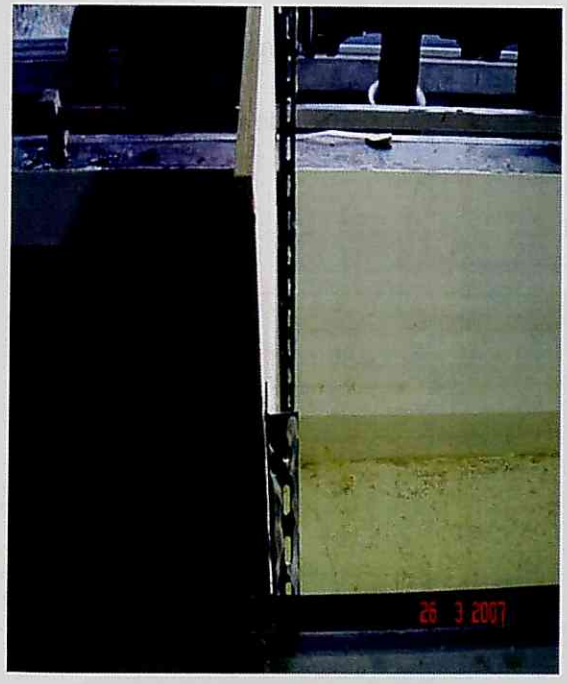

Fig. 6.3: View of gate

Fig. 6.4: View of wave tank

The dimensions of the model caisson are shown in Fig. 6.5. The mean diameter of the underlayer particles used was 10mm. The caisson units were made of an outer shell of glass filled with a mixture of iron sand and normal sand to ensure that the final density was similar to that of a real life concrete caisson (ρ_c=2.0 tons/m^3). The dimensions of the model caisson studied were 24cm tall x 14 cm long x 20 cm wide. To the side of the caisson studied a number of other caissons were placed in order to ensure that the experiment was carried under two-dimensional conditions. The width of the caisson chosen was small enough to ensure that the caisson would fail yet large enough to ensure that it would not be washed away under most of the experimental conditions. A clearance of 2mm was kept between the model and the dummy caissons, as seen in Fig. 6.6, so that friction on either side did not occur during the experiments. No toe armour was placed on top of the rubble mound gravel, and although some limited scouring took place due to the solitary wave attack it was clear that this was not the predominant mode of failure. Nevertheless, the exclusion of armour allowed for the potential damage due to scouring to be assessed and so it was felt that valuable information could be gained from its exclusion.

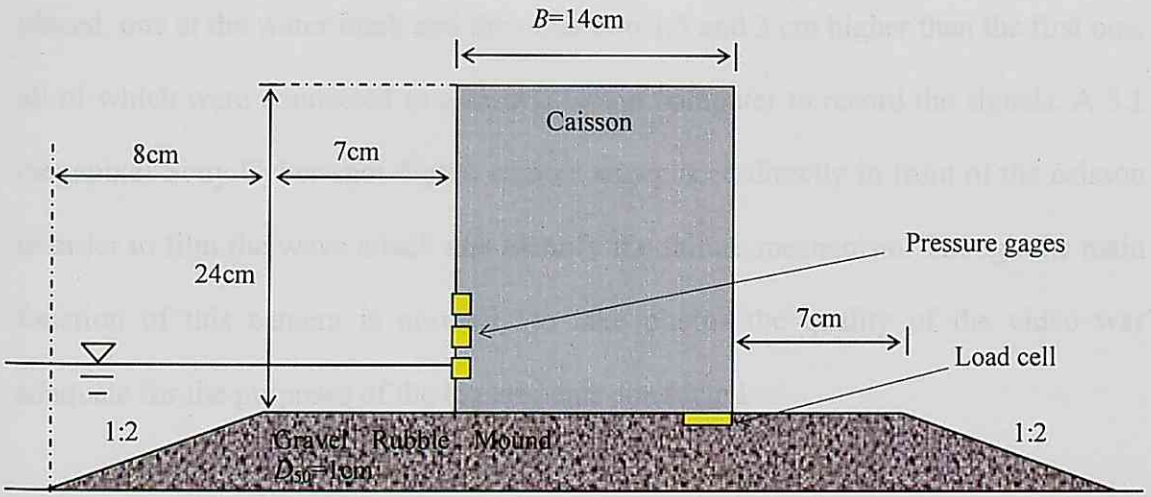

Fig.6.5. Experimental set up and location of measuring devices at the breakwater model

Fig.6.6. Experimental Set-Up

Two wave gages were placed, one around the middle of the tank and one before the caisson to measure the incident wave height. The wave gages were connected to a PC, which recorded the waves as voltage signals that were later analysed to obtain the wave profiles. A drop-down displacement gage was mounted on rails above the tank to measure the vertical and horizontal displacement of the caisson. A single load cell was placed at the top of the foundations, with the measuring head of the device situated 1.5cm from the back heel of the caisson. A total of 3 pressure gages were placed, one at the water mark and the other two 1.5 and 3 cm higher than the first one, all of which were connected to a second labtop computer to record the signals. A 5.1 megapixel Sony Cyber-shot digital camera was placed directly in front of the caisson in order to film the wave attack and identify the failure mechanism. Though the main function of this camera is normally to take photos the quality of the video was adequate for the purposes of the experiments conducted.

At the beginning of each experiment the rubble mound was slightly compacted to reproduce the compaction process that would be applied to the foundations during the

construction of a breakwater. This created a level foundation on top of which the caisson was placed, with its location determined by means of the drop-down gage.

6.2.3. Experimental Conditions

The reservoir situated at one extreme of the tank was filled to create the required water step according to the conditions set in Table 6.1 and was then opened rapidly so that a solitary wave was created. Two people, standing on either side, opened the gate manually. Care was taken to try to raise the gate in the same manner each time, although slightly lower or higher rising times would produce waves of slightly different characteristics.

The waves thus created had a celerity of between 3.9 and 4.16 m/s, a typical height of 7-10 cm at the first wave gage which increased due to shoaling to 17-20 cm as they hit the caisson, as can be seen from Fig. 6.7.

There was a clear limitation to the number of experimental conditions that could be carried out in the wave tank available. A number of different conditions outside the ones outlined in Table 6.1 were tried, but resulted in either almost no pressure acting on the breakwater (for h<15cm the wave broke quite early in the tank and arrived as a "bore" to the breakwater) or the complete failure of the caisson (for h>20cm or when h>17 with a step of 20cm). Generally speaking for the higher h the incident wave looked like a standing wave, but as h decreased the arriving wave front was more eccentric and eventually looked like a breaking wave (for conditions T2 and T3 for example). For conditions T1-T3 many of the waves broke in the mid-section of the

tank and the incident wave looked like a bore-type tsunami. Representative photos of the various wave shapes are shown in Appendix B.

Each of the conditions was repeated a certain number of times to ensure that the results were reliable, though not all the experiments carried out were valid due to the incorrect installation of the measuring instruments. The number of repetitions shown in Table 6.1 is the number of experiments with valid data that were obtained. Conditions T1 and T8 were considered to be the limit of what could be carried out using the available installations. The bore type waves were not so interesting for the present results due to the low amount of energy that they applied onto the vertical face, whereas anything more onerous than condition T8 caused the caisson to fail. As the failure of the caisson strained the cables that connected the instrumentation to the computers the experiments were not repeated many times for this condition.

Table 6.1. Experimental Conditions

Condition	Water level h (cm)	Water Step (H2-H1) cm	No. Repetitions	Classification
T1	15	15	1	bore type
T2	16	15	6	bore type/breaking on caisson
T3	17	15	7	bore type/breaking on caisson
T4	18	15	8	almost breaking on caisson
T5	19	15	5	almost breaking on caisson
T6	20	15	5	non-breaking
T7	16	20	2	bore type/breaking on caisson
T8	17	20	3	Caisson failure

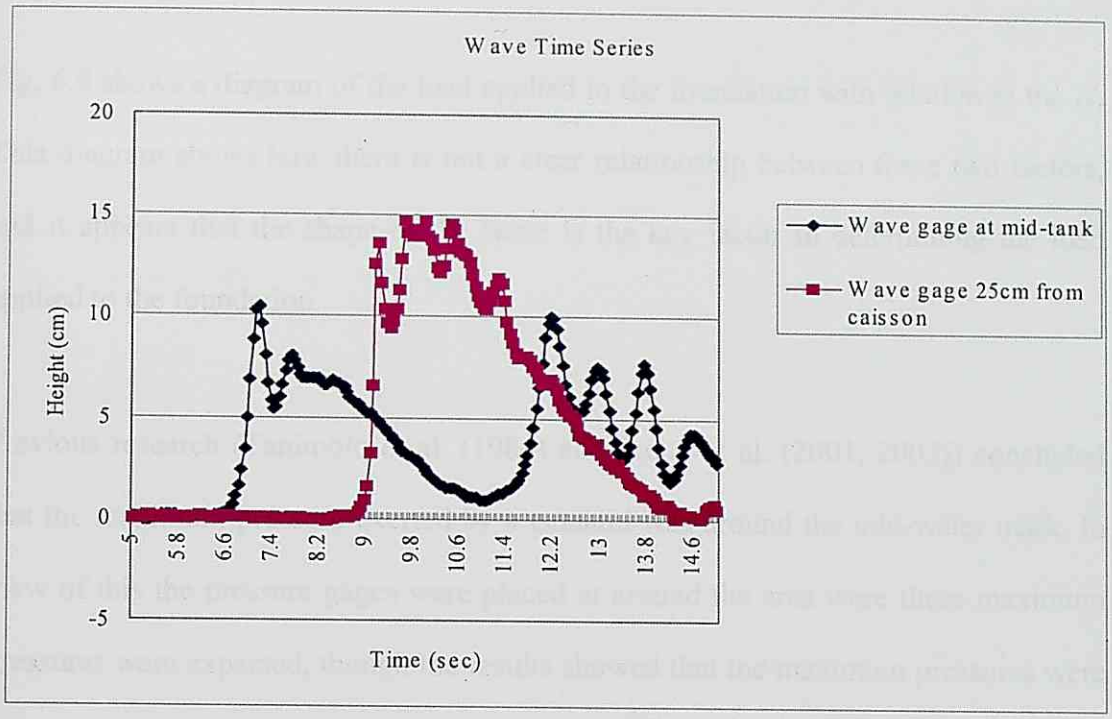

Fig. 6.7. Typical Wave Time Series (Condition T5)

6.2.4. Experimental Results

The loads exerted by the caisson onto the foundation for the various wave conditions and wave shapes can be seen in Fig. 6.8. Generally it can be said that the bore type waves did not appear to exert a great load onto the foundations, as the force of the wave was dissipated through turbulence before it reached the caisson. Condition T4 was also shown not to exert a significant load onto the caisson. This was unexpected as the breaking or almost breaking waves of conditions T2, T3 and T5 exerted much higher loads, though the breaking mechanism did not appear to be different judging from the video analysis. The laboratory equipment was tested repeatedly to ensure that all the apparatus was working correctly but high loads were never recorded for this condition. The highest loads recorded were for condition T6, were the large volume of water applied a massive quasi-static force on the caisson, often resulting in large displacements.

Fig. 6.9 shows a diagram of the load applied to the foundation with relation to the *H*. This diagram shows how there is not a clear relationship between these two factors, and it appears that the shape of the wave is the key factor in determining the load applied to the foundation.

Previous research (Tanimoto et al. (1984) and Ikeno et al. (2001, 2003)) concluded that the maximum pressure exerted by a tsunami was around the mid-water mark. In view of this the pressure gages were placed at around the area were these maximum pressures were expected, though the results showed that the maximum pressures were not located around this area. Due to laboratory and time constraints it was not feasible to place pressure gages throughout the height of the caisson face in order to establish the pressure profile. It was thus not possible to obtain an accurate picture of the incident wave loads on the caisson face. This research should be carried out in future in order to try to establish the time history of the tsunami wave force on the caisson, which is of vital importance for the computation of the sliding distance of the caisson. As it was not possible to compute this time history the computation of the sliding distance was not attempted in the present research.

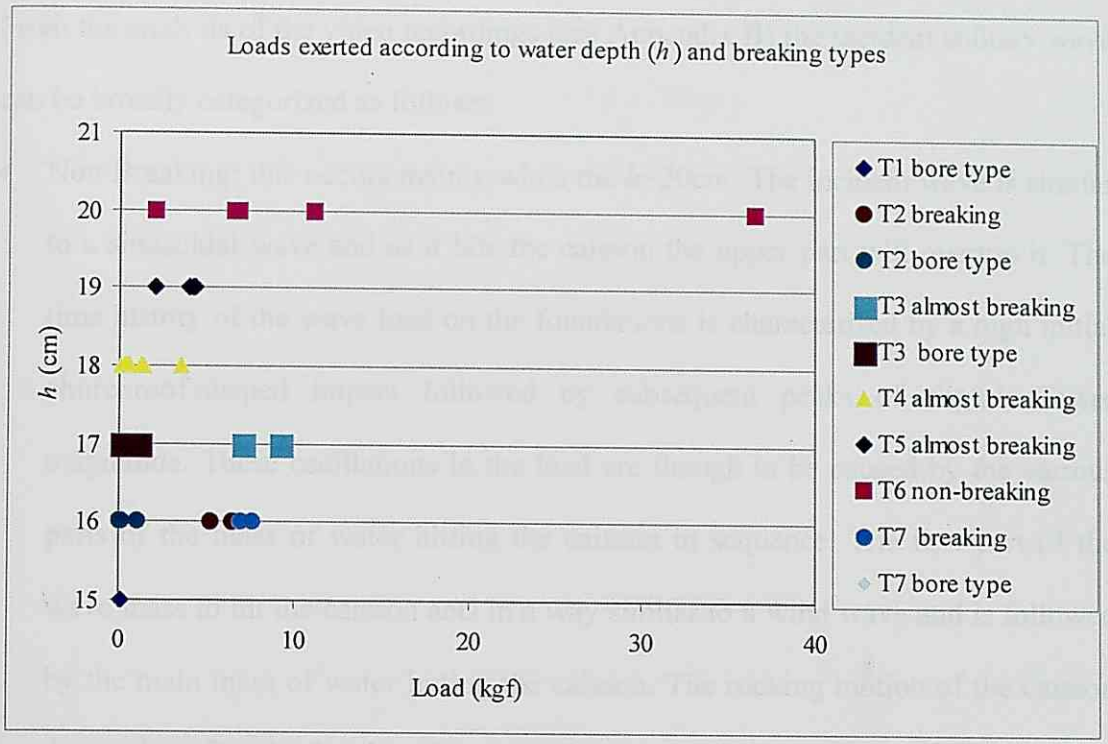

Fig. 6.8. Loads exerted by the caisson on the foundation according to h and breaking type

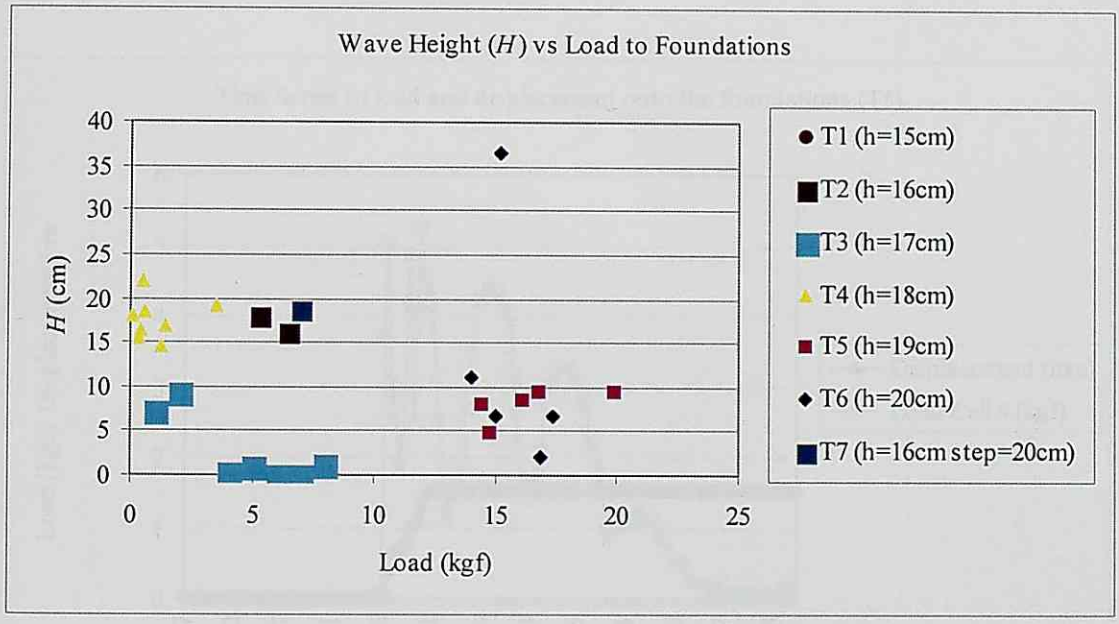

Fig. 6.9. Load to Foundations according to Incident Wave Height

6.2.5. Classification of waves

From the analysis of the video recordings (see Appendix B) the incident solitary wave can be broadly categorized as follows:

- Non Breaking: this occurs mainly when the h=20cm. The incident wave is similar to a sinusoidal wave and as it hits the caisson the upper part will overtop it. The time history of the wave load on the foundations is characterised by a high initial churchroof-shaped impact followed by subsequent peaks of slightly lower magnitude. These oscillations in the load are though to be caused by the various parts of the mass of water hitting the caisson in sequence. The first part of the wave mass to hit the caisson acts in a way similar to a wind wave and is followed by the main mass of water hitting the caisson. The rocking motion of the caisson due to this effect is also though to contribute to this effect. (a typical load profile is shown in Fig. 6.10)

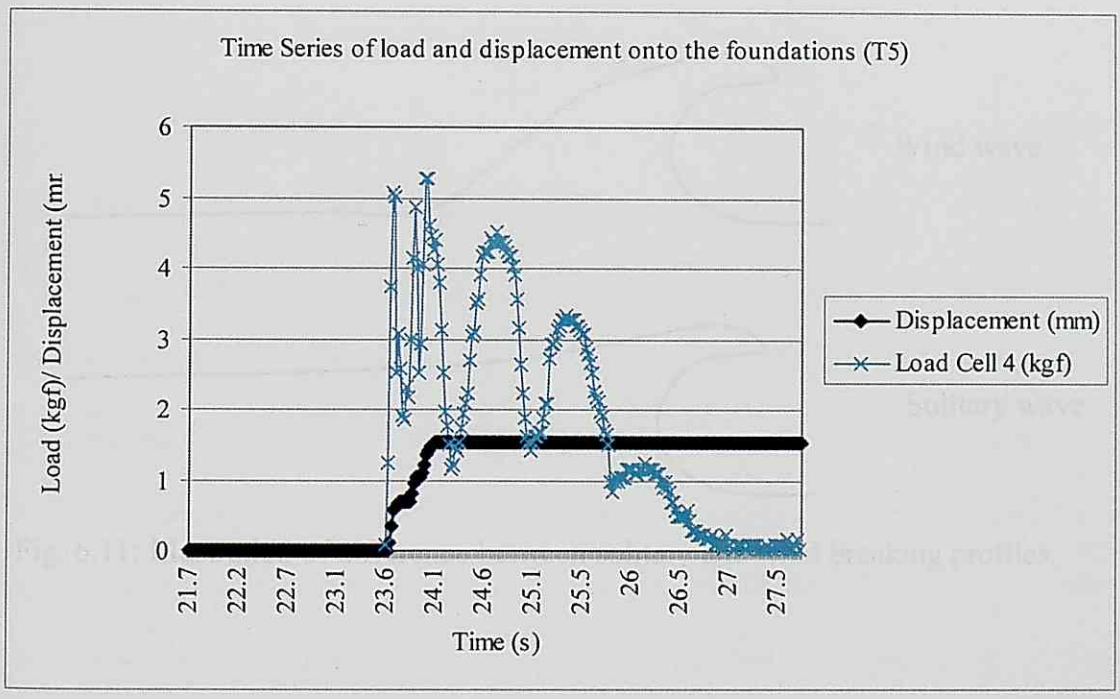

Fig. 6.10. Time Series of load and vertical displacement at the heel of the caisson for one wave for condition T5.

- Almost breaking: as the incident wave approaches the caisson it starts to deform prior to impact. The load profile is similar to the non-breaking part but with a higher initial peak and smaller subsequent oscillations.
- Breaking wave: the front of the solitary wave appears similar to a breaking wind wave, though the period of the wave is much longer and hence it differs due to the large amount of water at the back (see Fig. 6.11)
- Bore type: the wave breaks before it arrives at the breakwater. The wave front that arrives is characterised by a high turbulence, though due to this turbulence the impact component of the wave force is completely lost and thus mostly hydrostatic pressure is applied to the caisson. In most of the recorded cases almost no load is placed on the foundations by these waves, which would imply that caisson breakwaters should be relatively safe against this type of wave attack.

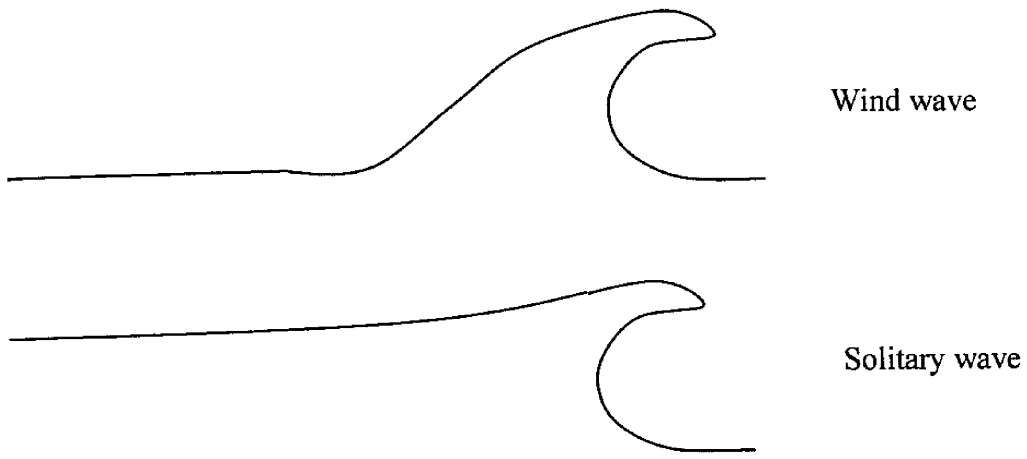

Fig. 6.11: Illustration of difference between solitary and wind breaking profiles.

6.2.6. Failure Mode

Two main failure modes were identified during the experiments:

1. Caisson overturning: for the caissons situated in deeper water (h>20cm for 15cm step and h>16 for a 20cm step) this was the predominant mode of failure. In this case the caisson overturned around its heel and was completely washed away.
2. Caisson sliding/tilting: in the other cases the caisson was seen to tilt and slide along a similar failure plane as that observed for wind waves (see Chapter 4 of the present thesis).

6.3. Computer Simulation

In order for engineers to be able to effectively design a caisson against tsunami attack it is necessary to attempt to analyse the deformations that would take place against various scenarios to choose the most appropriate cross-section.

6.3.1. Methodology for calculating the vertical deformation

The vertical deformation at the back of the caisson was estimated by using the method outlined in Chapter 5 of the present dissertation, which was originally intended to calculate the deformation in the rubble mound due to wind waves. This method uses the history of the wave force acting on the caisson to analyse the pressure exerted on the foundation using the procedure described in PROVERBS. Though at present the force time history applied by a solitary wave on the face of a caisson has not been fully clarified, the load cell situated at the back of the caisson provided data on the loads at the heel of the caisson. Hence it was possible to use these loads as the starting

point of the calculation of the vertical deformation, as outlined in Chapter 5. The calculation procedure becomes quite simple and can be achieved using a simple EXCEL spreadsheet.

One of the main problems of adapting the model proposed in Chapter 5 is the choice of appropriate parameters to describe the initial characteristics of the gravel. The gravel used in the experiment was slightly consolidated to create a level surface by gently tapping the surface using a wooden board, a process which attempts to mimic the consolidation to which the foundation of a real caisson would be subjected to. A bearing capacity of 200 kN/m^2 (corresponding to the lower bound of medium-dense gravel as described in BS 8004:1986, as shown in Table 3.2 in Chapter 3) was thus chosen, which would be on the lower end of what could be expected. Fig. 6.10 shows a typical load profile for the non-breaking or almost breaking wave types. The vertical displacement at the heel of the caisson caused by the applied load is also shown in the graph. It shows how the initial impact "peaks" are responsible for most of the displacement caused by the solitary wave. These original peaks are responsible for the most of the consolidation of the ground under the caisson, which thus limit the displacement that is caused by the rest of the wave.

6.3.2. Simulation results

Fig. 6.12 shows a comparison between the simulated results using the methodology proposed and the observed laboratory displacements at the heel of the caisson. Generally the results compare well though the simulation sometimes overestimates the displacement, by up to a factor of 2 in some occasions. The reason for this probably lies in part in the difficulties in measuring the load action on the foundation.

The load measured by the load cell does not always return to 0 at the end of the wave, indicating that the displacements in the rubble mound are subjecting the load cell to a higher pressure than it was originally withstanding. It is quite difficult to know from what point the instrument started to over-estimate the pressure which is applied by the wave. Also, there is the possibility that the instrument was over-recording during part of the wave and the returned to its original condition due to further deformation in the rubble mound. A number of experiments were the load cell clearly did not function properly were removed from the final graph, but some of the ones included in Fig. 6.12 could also be slightly inaccurate. By analysing load time history graphs it is believed that the load values subsequent to the first peak could have an error of up to 20%. This error is probably not present in the first measured peak in the time history as prior to this time there has been no deformation in the rubble mound. This error can thus result in a certain deviation from the observed results and could partially explain the scattering of values shown in Fig. 6.12.

Another source of error is the choice of the initial gravel parameters. These are based on an "engineering" guess, though in the case of high loads the choice of a low initial bearing capacity value will result in a very large acceleration of the caisson into the ground. The model introduced in Chapter 5 deals with a large number of consecutive wind waves, and hence it is unlikely that the highest waves will occur at the beginning of the storm, thus allowing the simulation to slowly consolidate the ground due to smaller waves. However in the present simulation no such computational procedure takes place, and hence a wave which exerts a high initial load into the ground can somewhat confound the results. Furthermore, it is likely that in many of the experimental cases the ground had a bearing capacity greater than the 200 kN/m^2 used

in the simulation, which would result in lower deformations that those predicted by the model.

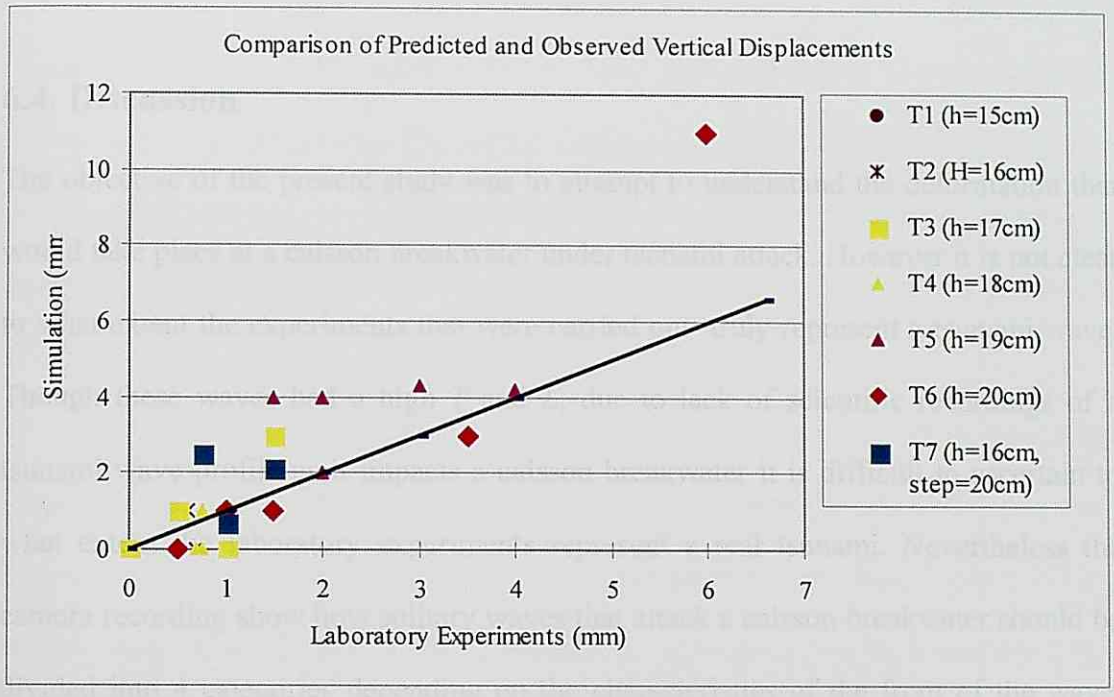

Fig. 6.12. Comparison of simulated and observed vertical displacements

6.3.3. Methodology for calculating the sliding

It was not possible to calculate the sliding distance of the caisson due to uncertainties in the time history of wave pressure on the caisson. Further laboratory experiments should be carried out to ascertain the various parameters involved, verify the various formulas available -such as that of Ikeno et al (2003)- and obtain the wave time history.

The author would like to refer readers to the doctoral dissertation of Thao Nguyen Danh (2007) for a computational simulation of the pressures at the vertical face of a breakwater due to solitary wave attack. These computational results could be

eventually used in an integrated model for the prediction of the sliding of the breakwater.

6.4. Discussion

The objective of the present study was to attempt to understand the deformation that would take place at a caisson breakwater under tsunami attack. However it is not clear to what extent the experiments that were carried out truly represent a tsunami wave. Though these waves had a high T and L, due to lack of scientific recordings of a tsunami wave profile as it impacts a caisson breakwater it is difficult to ascertain to what extent the laboratory experiments represent a real tsunami. Nevertheless the camera recording show how solitary waves that attack a caisson breakwater should be divided into 4 categories depending on the characteristics of the front of the wave. Each of these has a characteristic load time history, with some applying far more load (such as the breaking type) than others (bore-like type).

Due to the small water depth used in the laboratory it is also not clear to what extent the waves in the experiment can be truly called solitary waves, as it is clear that they "shoal" as they approach the caisson. Hence there is a clear interaction between the bottom of the tank and the wave, meaning that the wave does not conserve its energy as it travels. Nevertheless this effect is a desirable one as it reproduces the tsunami shoaling effect, though the actual classification of the wave used is somewhat ambiguous.

The measurements obtained allow the evaluation of the deformation in the rubble mound foundation of a caisson breakwater due to solitary wave attack. The proposed

computational model appears to be able to predict the magnitude of the vertical displacement of the caisson into the ground, although it sometimes overestimates the displacement by up to a factor of 2. The reason for this appears be an over-recording of the pressures on the foundation by the load cells and a low choice of starting bearing capacity parameters. The results obtained by the simulation thus provide a conservative estimate of this displacement and could be used by engineers to determine what would be the maximum vertical displacement that could be expected.

The sliding displacement of the caisson could not be calculated, as the load time history on the face could not be measured correctly. In order for the model to be used in practice this time history must be clarified, though at present there appears to have been no research in this area. It thus represents an interesting area for future research.

Also, the exact nature of the vertical distribution of force pressure on the face of the caisson is not properly understood at present. As shown by the experiments carried out it depends on the type of wave that arrives at the breakwater, which would result on different pressure time histories. Further experiments to verify the formula of Ikeno et al (2003) should be carried out, in order to ascertain at what height the maximum pressure is applied and what is the rise time that can be expected to the top of the first pressure peak.

When applying the present results to a prototype caisson the issue of scaling is of paramount importance. Though PROVERBS recommends the use of Cauchy scaling for impact waves, and a part of the solitary wave time history appears to be similar to that of impact wind waves, it is not clear at present if the use of Cauchy scaling would

also be adequate. Thus, caution is recommended at this stage in the application of the present model till larger scale model tests are carried out.

When designing the caisson breakwater against the possibility of a tsunami attack engineers should take extreme care in assessing what type of tsunami could possibly arrive at the location to be protected. A relatively small cross-section might resist the force of a bore type tsunami but could be completely washed away by a tsunami that breaks upon it. As tsunamis are extremely infrequent events that typically do not occur during the service life of a breakwater it should be adequate to design the breakwater so that it will take extensive damage while dissipating enough wave energy to protect the area behind it. By allowing for deformation to take place it would thus be possible to design a more slender structure than what would otherwise be required if the caisson was not to move. The present model appears adequate to give an initial estimation of what magnitude of deformation can be expected.

6.5. Conclusions

Solitary waves were employed in laboratory experiments to try to understand the failure mode of caisson breakwaters under different types of tsunami attack, which influenced the loads exerted at the heel of the structure. By adapting the methodology introduced in Chapter 5 of the current dissertation it was possible to roughly estimate the vertical displacement that could be expected for a given wave.

CHAPTER 7

ANALYSIS OF REAL LIFE CAISSON FAILURES

7.1. Introduction

There are many documented cases of failures of caisson breakwaters in recent times, with sliding of the upright section representing the majority of these failures (Goda 1999). One of the most well documented cases according to this author is that of the Mustafa breakwater at Algiers Harbour in Algeria. This structure was built at a water depth of 18 to 20m using cyclopean blocks designed to resist waves 5.0 m in height and with a T of 7.4s. A large storm in February 1934 (with a peak wave height of 9m and period of 13.5s) damaged a 400m section of the breakwater. Interestingly three quarters of the failed sections fell towards the seaside and only a quarter towards the harbour side. The reason for this according to Oumeraci (1992) lies in the possibility of a slip failure through the seabed. However this type of failure is relatively rare, with Takahashi et al. (2000) citing how in more than half of the major breakwater failures that occurred between 1983 and 1991 in Japan sliding was recorded. These authors also cite a survey of damage to major caisson breakwaters conducted by the Bureau of Ports and Harbours (BPH), which indicates how 23 caissons were damaged in the period 1991-2000, with 75% of them suffering meandering sliding, and 25% being damaged due to wave-induced strong currents. As a total of 9644 caissons existed in Japan during this time only about 0.2% suffered some type of problem,

which led these authors to conclude that the probability of encountering sliding over a 50-yr lifetime is about 1%.

Takahashi et al. (2000) cite several case studies of typical failures of caisson breakwaters, such as that at Sendai Port after Typhoon 9119, which caused several caissons to slide towards the shore.

Recently Takagi (2007) studied the failure of the breakwater at Hakodate Port in Hokkaido in 2004, believed to have failed due to bearing capacity failure attributed to standing wave pressures at key points along the breakwater. This author also introduced a new concept called the "Expected Occurrence in Frequency (EOF)" to asses the degree of potential risk of a given storm against each of the main 4 types of failure mode (sliding, overturning, bearing capacity and circular slip).

7.2. Case Study: Susami West Breakwater

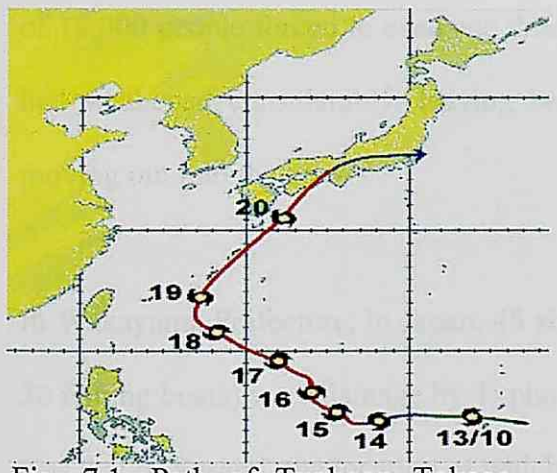

Fig. 7.1. Path of Typhoon Tokage over the Japanese Islands

Susami West Breakwater, in Japan, was damaged by high waves caused by typhoon Tokage on the 20th of October 2004. The failure was reported by Kim et al. (2005), who recorded the displacement of the caisson breakwaters and analysed the failure mode. By using the method of Kim and Takayama (2004) they were able to

reproduce the sliding distance of the caisson, though the method used could only be applied as the tilting at the end of the storms was know (this method provides no way to forecast the tilt in a caisson).

By using the data provided by Kim et al. (2005) it is possible to reproduce the deformations experimented in the rubble mound foundation of Susami West Breakwater by using the method introduced in Chapter 5.

7.2.1. Location and background of typhoon Tokage.

Tokage is the Japanese word for lizard. The typhoon started forming on October 12th 2004 around 480 miles east-southeast of Guam. The storm eventually made landfall over Tosa-Shimizu on the 20th of October 2004, near the southern tip of Shikoku. The highest measured wind gust was 142 mph (63.7 m/s) at Unzendake, Nagasaki. News reports indicated Tokage was the worst storm to strike Japan since Typhoon Mireille thirteen years before, and resulted in 80 dead, 20 missing and 350 injured, with a total of 18,000 people forced to evacuate their homes. By the time it passed over Tokyo it had weakened considerably, leaving behind very little damage in this area before moving out into the sea.

In Wakayama Prefecture, in Japan, 45 sites and 25 fishing ports (including more than 30 fishing boats) were damage by Typhoon Tokage. One of the fishing ports damaged was that of Susami, the location of which is shown in Fig. 7.2.

(a) Map of Japan showing the location of Wakayama Prefecture

(b) Map Wakayama Ken

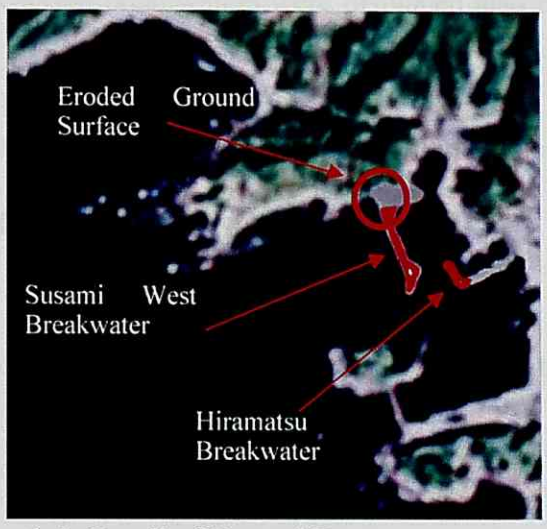

(c) Detail of Susami Port area

Fig. 7.2. Location of Susami West Breakwater

7.2.2. Overview of Damage at Susami Port

Fig. 7.2 (c) shows the three main damaged areas at Susami port:

- The West Breakwater suffered damaged in about 60m of the total 254m it was composed of. The main area of damage was around the head of the breakwater, with the caissons sliding and tilting into the rear of the rubble mound. The wave-dissipating concrete units, which covered the caisson front, collapsed into the foundation due to the large waves resulting from the typhoon action.

Kim et al. (2005) do not provide any details of the shape of these units, though by looking at the photographs they do not appear to be cubes but possible accropodes. The sliding distance of the breakwater caissons surveyed was between 6 and 10m. By looking at the photographs provided by Kim et al. (2005) it is possible to estimate that the greatest vertical movement at the heel of the caisson is of the order of 3.3m. Fig. 7.3 shows a typical cross-sectional view of the breakwater before and after the typhoon.

- The Hiramatsu Breakwater constructed inside the West Breakwater was also significantly damaged and several caisson breakwaters were displaced also in this area.
- In the area where the West Breakwater joins the land the footing of the caisson breakwaters was eroded by overtopping .

However, the present simulation will focus only on Susami West Breakwater due to the lack of availability of data for the other two areas of failure.

7.2.2. Estimation of wave climate during Typhoon Tokage

Kim et al (2005) used GFS (which stands for "Global Forecast System", http://www/met.utah.edu/jimsteen/gfs/framesGFS/html) and SWAN ("Simulating Waves Nearshore") in order to estimate the heights of the offshore waves due to caisson Tokage. Based on this data they used the EBED model by Mase (2001) to estimate the incident wave at Susami West Breakwater, obtaining a $H_{1/3}$ of between 6 and 6.3m and a T=14s around the breakwater head and in the area were the breakwater joins the land. For the central area of the breakwater they obtained $H_{1/3}$<6m, which explains why this area was not as badly damaged as the other areas.

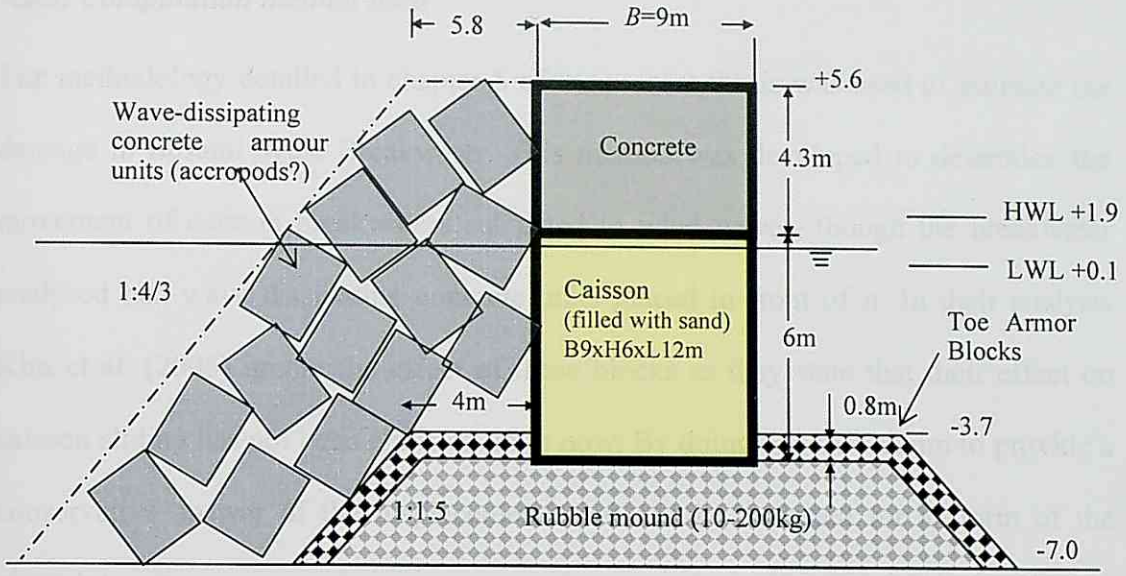

Fig. 7.3(a). Design Cross Section of Susami West Breakwater

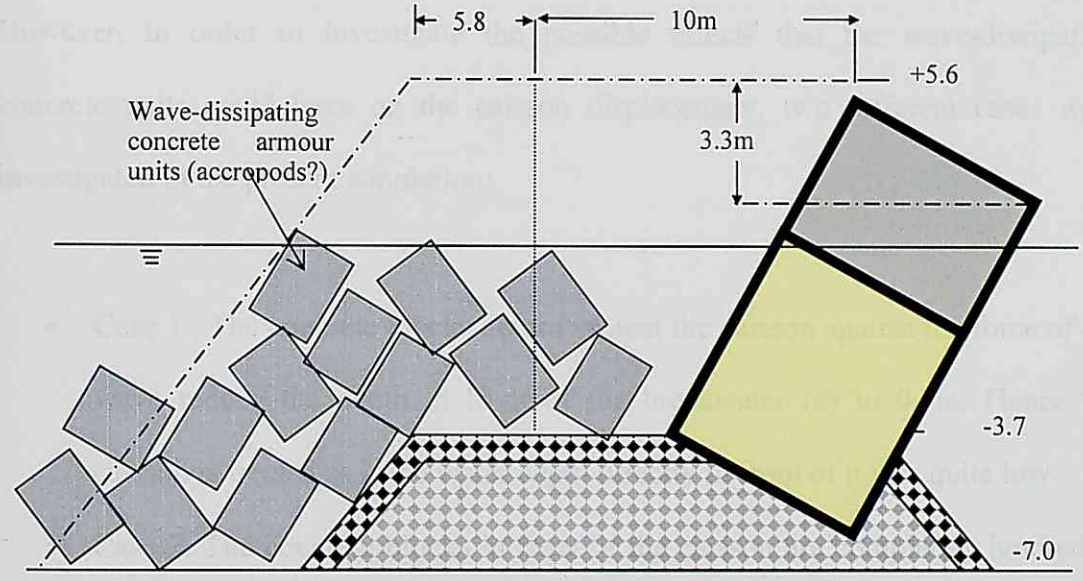

Fig. 7.3(b). Cross Section of Susami Breakwater after the storm.

As the design H of the breakwater was 3.8m (4.9m for the head section) it is normal that the caisson suffered significant damage.

7.2.3. Computation method used

The methodology detailed in chapter 5 of the present thesis was used to estimate the damage to Susami West Breakwater. This method was developed to determine the movement of caisson breakwaters subjected to wind waves, though the breakwater analysed had wave dissipating concrete units placed in front of it. In their analysis Kim et al. (2005) ignore the effect of these blocks as they state that their effect on caisson sliding has not been clarified up to now. By doing this they claim to provide a conservative answer of the displacements that can be expected for a storm of the given intensity.

However, in order to investigate the possible effects that the wave-dissipating concrete units could have on the caisson displacement, two different cases were investigated in the present simulation:

- Case 1:. The concrete blocks do not protect the caisson against the force of the wave reduce the depth in front of the breakwater (d) to 0.7m. Hence the caisson is treated as if the water depth directly in front of it was quite low.
- Case 2: The concrete blocks in front of the caisson are completely ignored in the simulation.

Tables 7.1. and 7.2. show a summary of the parameters used in the computation of the caisson deformation.

Table 7.1. Basic Parameters of Simulation

Parameter	Symbol	Value	Unit
Water depth	h	7	m
Incident Significant Wave Height	$H_{1/3}$	0	m
Weight of caisson in air	W	180	t/m
Duration of storm	-	2	hrs
Unit mass of sea water	ρ	1.03	t/m^3
Incident angle of wave to normal of breakwater	-	0	degrees
Friction factor	μ	0.6	-
Density of caisson	ρ_c	2.177	t/m^3

Table 7.2. Soil mechanics Parameters

Parameter	Symbol	Value	Unit
Active depth of foundations	d_z	1	m
Initial void ratio of gravel	e	0.6641	-
Density of gravel	ρ_s	2.002	t/m^3
Angle of friction of gravel	ϕ	35	degrees

7.2.4. Computational Results

Figs. 7.4. and 7.5. show the probability distributions of sliding and vertical movement at the back of the caisson, respectively, for each of the two cases considered. From these it can be seen how the deformations expected in Case 1 are lower than those for Case 2. Although with regards to sliding both cases provide an accurate estimation of the range of displacement that actually took place, in terms of vertical displacement Case 1 cannot predict displacements of 3.3m. Case 2 (ignoring the wave-dissipating concrete units) produces a range of vertical displacement with an average of around

0.6m and a maximum value of 2m, which appears to be of the right order of magnitude to that observed in the photographs.

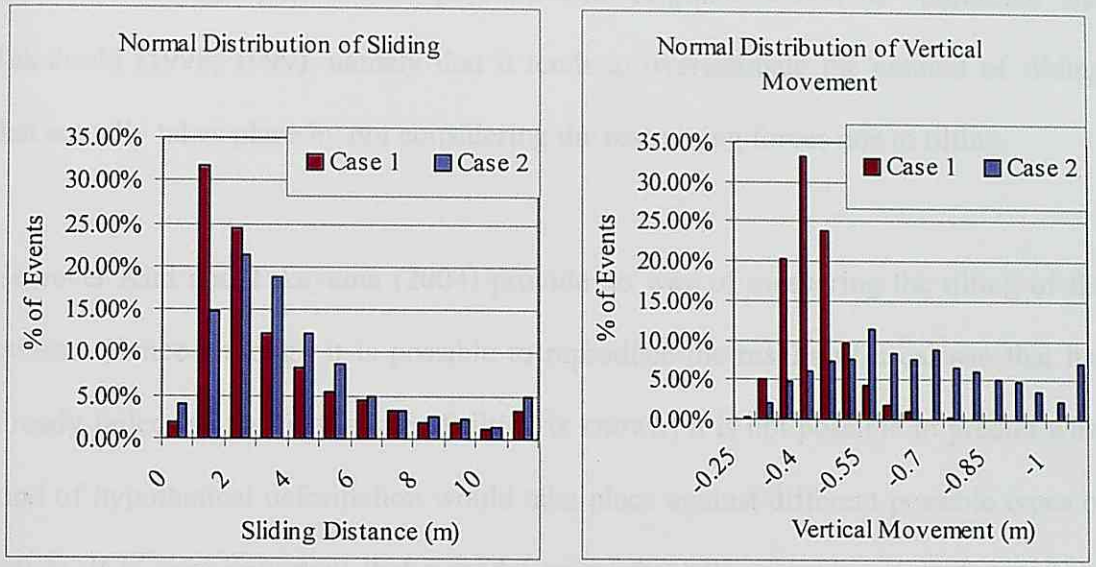

Fig. 7.4. and 7.5. Probability distributions for sliding and vertical displacement of Susami West Breakwater.

7.2.5. Comparison with results of Kim and Takayama (2004)

Kim and Takayama (2005) computed the expected sliding distance using two different methods:

1. Kim and Takayama (2003), is a simple modification of the method of Shimosako and Takahashi (1998, 1999) but with the introduction of a doubly-truncated normal distribution
2. Kim and Takayama (2004), which considers the effect of caisson tilting on the sliding distance.

The results obtained for each of the two methods are reproduced in Fig. 7.6. This figure clearly shows the importance of including tilting in the computation of the

sliding distance. If tilting is not included the computation gives sliding values of over 20m, indicating that the caisson should have been washed away, which clearly did not happen. This highlights a clear problem with original method of Shimosako and Takahashi (1998, 1999), namely that it tends to overestimate the amount of sliding that actually takes place by not considering the restraining forces due to tilting.

However Kim and Takayama (2004) provide no way of measuring the tilting of the caisson. Hence although it is possible to reproduce the results of a caisson that has already failed (as the final angle of tilting is known) it is not possible to predict what kind of hypothetical deformation would take place against different possible types of waves. It is very important that a model exists that allows engineers to forecast the deformation that could take place in order to correctly assess the risk to the population and areas a caisson is built to protect.

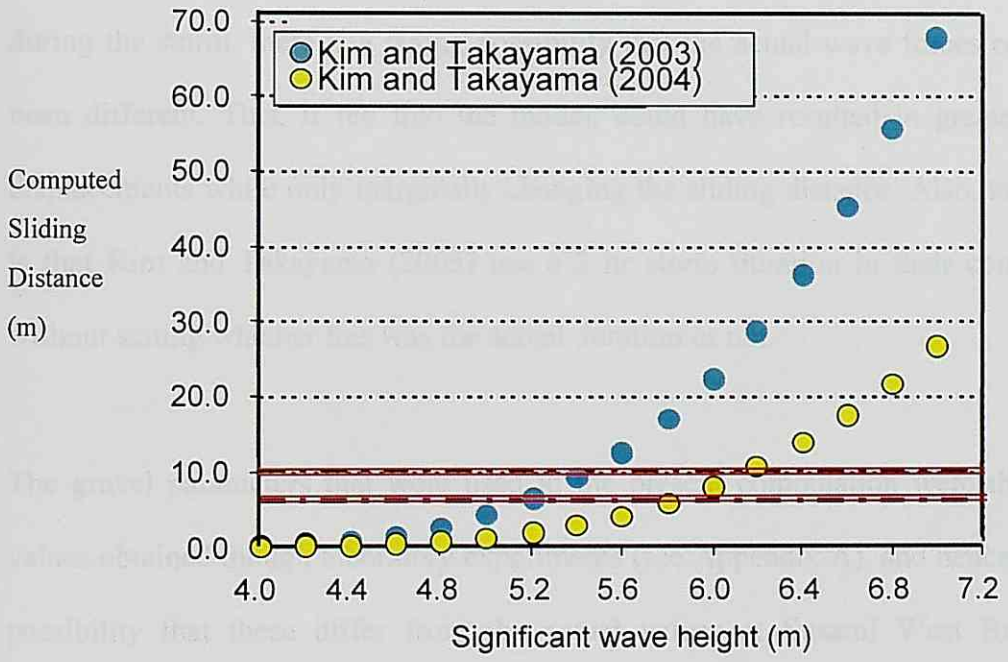

Fig. 7.6. Comparison between the surveyed and computed sliding distance according to Kim and Takayama (2005)

The model proposed in this thesis is able to predict both the range of sliding and tilting that can be expected. Each of the caissons that made the breakwater slid by a different amount, falling within the probability distribution curves shown in Fig. 7.4. Though by looking at the photographs the maximum vertical displacement appears to be almost 3.3m, most of the caissons had much more limited vertical deformation, agreeing well with the result in Fig. 7.5. It thus appears that although the model failed to predict the maximum vertical deformation observed, it was able to predict adequately the range of most of the vertical deformations that took place.

7.2.6. Discussion

There are a number of sources of uncertainty in the present analysis. First and foremost is the value of $H_{1/3}$ that was used, which was derived from a computer model based on the deepwater wave height. As there was no recording of the actual $H_{1/3}$ during the storm, there is a strong possibility that the actual wave forces could have been different. This, if fed into the model, could have resulted in greater vertical displacements while only marginally changing the sliding distance. Also, to be noted is that Kim and Takayama (2005) use a 2 hr storm duration in their computation, without stating whether this was the actual duration or not.

The gravel parameters that were used in the present computation were the generic values obtained though laboratory experiments (see Appendix A), and hence there is a possibility that these differ from the actual values at Susami West Breakwater. However, it is unrealistic to attempt to carry out tests on the type of foundation material present at the breakwater due to the cost involved in doing so. As the parameters used were based in small scale laboratory experiments it is possible that

there are significant scale effect involved, as the degree of friction between laboratory and prototype particles could be different.

The most crucial uncertainty lies however in what effect the wave-dissipating concrete units have in the simulation. It is not clear at what stage of the storms these blocks failed, though it could be assumed that the failure was progressive throughout the storm. Laboratory tests should be carried out to ascertain what protection these blocks still offer to the caisson after they have failed.

All these factors explain why the present results should be viewed with a degree of caution, although the sliding distances of all blocks and the majority of the tilt angles were successfully predicted by the model proposed in Chapter 5 of the present thesis.

7.3. Conclusions

The model described in Chapter 5 of the current dissertation was able to replicate the damage that actually took place at Susami West Breakwater in 2004. Though one of the caissons suffered greater vertical movement that what the model could predict, all the other caissons appeared to fit into the computed probability distribution functions. All of the caisson's sliding distances fell within the obtained distributions, and thus it appears that the model is adequate for forecasting the damage that would take place on a breakwater that was subjected to $H_{1/3}$ higher than it was designed for.

CHAPTER 8

METHODOLOGY FOR THE RISK ASSESSMENT OF A CAISSON BREAKWATER DURING THE CONSTRUCTION PHASE

8.1. Introduction

In traditional design safety factors are used to evaluate the stability of caisson breakwaters against various modes of failure. Goda (1999) highlights problems with the traditional method of design and suggests that 'The reliability-based design of maritime structures is the direction we should take'.

Though under traditional breakwater design caissons are not allowed to slide, a limited amount of movement does not prevent the structure from fulfilling its purpose. Hence Shimosako and Takahashi (2000) proposed a Level 3 design method for caisson breakwaters referred to as the "deformation-based reliability design". Kim and Takayama (2005) provided a way to take into account the effect of caisson tilting on the computation of sliding distance. By using simple soil mechanics consolidation theory Esteban and Shibayama (2006) proposed a method to calculate the amount of settlement at the heel of the caisson, thus allowing for the calculation of the tilt in the breakwater.

Reliability-based risk design has recently become more important in the planning and design stages of civil engineering works. Hillyer et al. (1997) first stated the need for the evaluation of the benefit-cost ratio in coastal projects by taking into account the risk factors inherent to the construction phase.

The main justification for the use of Reliability Design in breakwaters is that the cost and risks associated with the entire life of the breakwater can be more precisely identified than under traditional design procedures. Shimosako and Takahashi (1998, 1999) quantitatively clarified the risk of failure, but they used a pre-determined design wave height for a return period equal to the lifetime of the breakwater. In contrast Goda and Takagi (2000) proposed to design the breakwater with a FoS of 1.0 and to apply the reliability design method by temporarily varying the design significant wave height over a range of return periods. Both these approaches are useful to estimate the life-cycle costs of the breakwater but fail to take into account the possible damage to the breakwater during the construction phase. During this phase a wave height lower than the design wave height can cause significant damage to the breakwater and thus affect the life-cycle costs.

Balas (1998) developed a risk management approach that can be used to optimise the construction operations by minimizing the time and budget of a coastal project and depreciating the structural damage risk by network planning. In this case the uncertainties were confined to environmental design conditions and methodologies, with human and organizational uncertainties not taken into account. More recently Balas and Ergin (2002) developed a Reliability Model for rubble mound breakwaters during the construction phase by taking into account both the structural risks of

construction (derived from the wave climate) and other risk parameters arising from problems particular to the construction industry in Turkey. However they did not include delays due to accidents during construction, which can be a significant source of delays, particularly in developed countries.

The purpose of the present paper is to propose a new methodology for the evaluation of the risk –in terms of estimated cost and time to complete- related to the construction of a caisson breakwater. This model would allow engineers to estimate the machinery needed to complete the construction in a certain amount of time and the risk associated with various machinery combinations and start dates of construction.

In Japan contractors have no responsibility for failures during construction due adverse wave climate, as the government normally assumes most of the responsibility. However the situation is not the same in other countries, with different stakeholders usually assuming different levels of responsibility. The development of such a method can allow project planners and stakeholders to make an informed judgement as to what would be the best time to start construction.

Though in Europe breakwaters are sometimes insured during the construction process this is rarely the case in Japan. The methodology proposed allows for a better estimation of the insurance premiums to be made, which at present in Europe are typically calculated as a fraction of the total cost of the breakwater without taking into account other variables.

8.2. Proposed Methodology for the Risk Assessment of a Breakwater during the Construction Phase

The simulation of an activity as complex as a construction process is a daunting task. Construction is an activity prone to many problems inherent to human nature and is also heavily influenced by other factors (such as weather) that are difficult to predict and plan for. In order to be able to simulate the construction of a breakwater the methodology used should take into account as many of these variables as possible, and yet be able to be solved in a relatively short amount of time to make it practical for designers. In order for this to be possible the scope of the simulation must be clear from the onset, i.e. which variables will or will not be considered. The limitations of the computer model must also be understood to be able to qualify how precisely the computation reflects the reality of the construction process.

The methodology proposed will attempt to reproduce the construction of the breakwater by simulating the placement of the various materials that form the breakwater according to the machinery available to the Contractor. The wave climate is simulated in 6-hour intervals and the caisson sections are checked for damage during each of these periods (a total of 120 periods per month). The methodology thus provides a clear picture of the state of the breakwater at any given time during its construction, with the amount of materials placed at each section and the amount of damage (if any) recorded. It is thus possible to see how the construction evolves from the beginning to the end, and can allow engineers to determine which sections are particularly vulnerable at certain times of the year or bottlenecks during the construction process.

8.2.1. Scope

In the present simulation the **main** source of risk is considered to be the wave climate. This will affect the rate of construction (i.e. the rate at which the Contractor can place the various materials needed to build the breakwater) and possibly damage the breakwater during high wave periods.

Regarding damage the following failure modes have been included:

- Displacement of the large rubble stones or concrete blocks armouring the foundation material of the caisson (toe armour).
- Erosion of the foundation material if it is not protected by toe armour units or if these are removed by a storm. This can lead to the collapse of the caisson if a sufficiently large amount of the foundation gravel is eroded.
- Sliding/Tilting of the caisson
- Overturning of the caisson

Generally overturning will not take place for the shallower section as normally the caisson will slide and tilt before the overturning limit is reached. Goda and Takagi (2000) explain how owing to the Japanese practice of keeping the bearing capacity at the heel below 500kPa few overturning failures have been recorded in this country. However Takagi (2007) gives an example of overturning caisson failure and explains how as the water depth increases there is an increased probability of this failure mode occurring (i.e. the Expected Occurrence in Frequency (EOF) would go up)

Another form of failure that is sometimes reported after exceptionally violent storms is the rupture of the caisson walls. This is thought to be due to the generation of

impulsive breaking wave forces and due to adverse breakwater geometric configurations. Goda and Takagi (2000) express the view that "this event should be avoided through the improvement of the design methodology for the concrete members of breakwater sections. It should be dealt with separately from the overall design of breakwater sections with the reliability method".

The other main failure modes include circular slip and other failures of the foundation and subsoil. Takagi (2007) included this failure mode in the computation simple cross-sections, its inclusion in the present methodology would raise the computational time to the order of weeks or possibly months. As the sliding/tilting failure mode comprises the majority of recorded failures in literature it is believe this failure mode can be ignored without incurring in major errors.

The second source of risk considered is that of accidents during construction. These will lead to delays in the construction due to workers staying away from the construction site to recover, health and safety inspections and possibly site closures. The delays can be quite severe in the case of loss of life, though this tends to be rare in developed countries. In the Japanese case the compensation paid to workers due to these accidents is born directly by the Japanese government, which subsidises it through premiums paid by the Contractor (see Section 2.14.1)

Other factors that would affect breakwater construction in real life include labour strikes, lack of availability of construction materials, financial hardships and acts of force-majeure. Balas and Ergin (2002) list other delay sources inherent to coastal engineering in Turkey:

- Funding problems (29.8% of cases)

- Project revisions (21.6%)
- Site conditions (18.9%)

Other secondary delay sources inherent in projects that may concurrently occur with the main sources are listed as:

- Quarry problems, including quarry efficiency (5.5%)
- Access to quarry (5.3%)
- Official and regulatory agencies (5.4%)
- Structural damage (5.2%)
- Project organisations (2.7%)
- Logistics (2.6%).

However the methodology proposed has been devised in order to be applied to the Japanese island of Honshu, where due to the nature of the Japanese construction industry these factors are not deemed to be critical. For the model to be adapted to a different country some of these factors would have to also be included in the simulation by analysing the construction industry in the required area.

8.2.2. Description of Case Study Breakwater

In order to test the proposed methodology the construction of a fictitious breakwater will be simulated. This "case study" breakwater consists of ten caisson sections going from 16 to 20.5 meters in water depth as shown on Fig.8.1. The direction of wave attack is perpendicular to the breakwater and the wave climate used will be similar to that of Kanagawa Prefecture in Japan.

Figs. 8.2 and 8.3 show two typical cross-sections of the breakwater. The caisson dimensions are assumed not to change throughout the breakwater, and as the water depth increases the height of the rubble mound foundation will increase gradually.

The breakwater proposed is quite an extreme case of breakwater construction as it is situated in a region of relatively deep water and will be subjected to the direct attack of ocean waves.

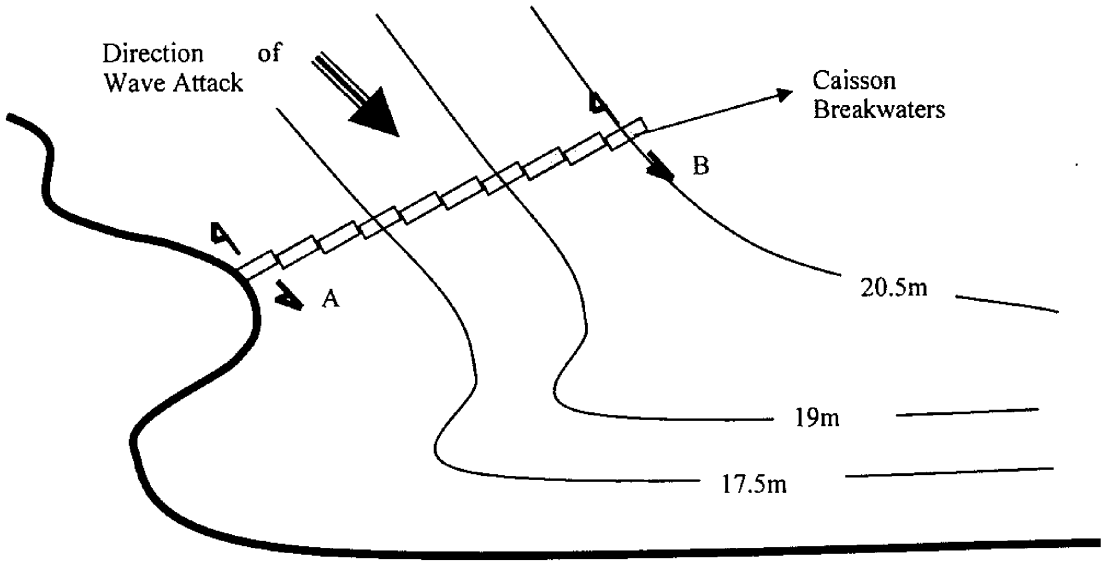

Fig. 8.1. Plan View of Proposed Port.

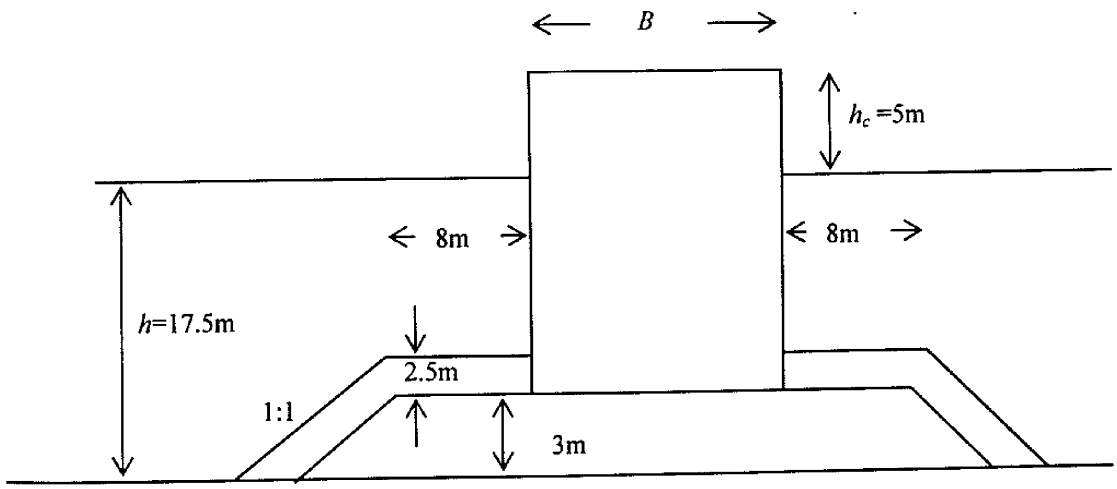

Fig. 8.2. Cross-Section A

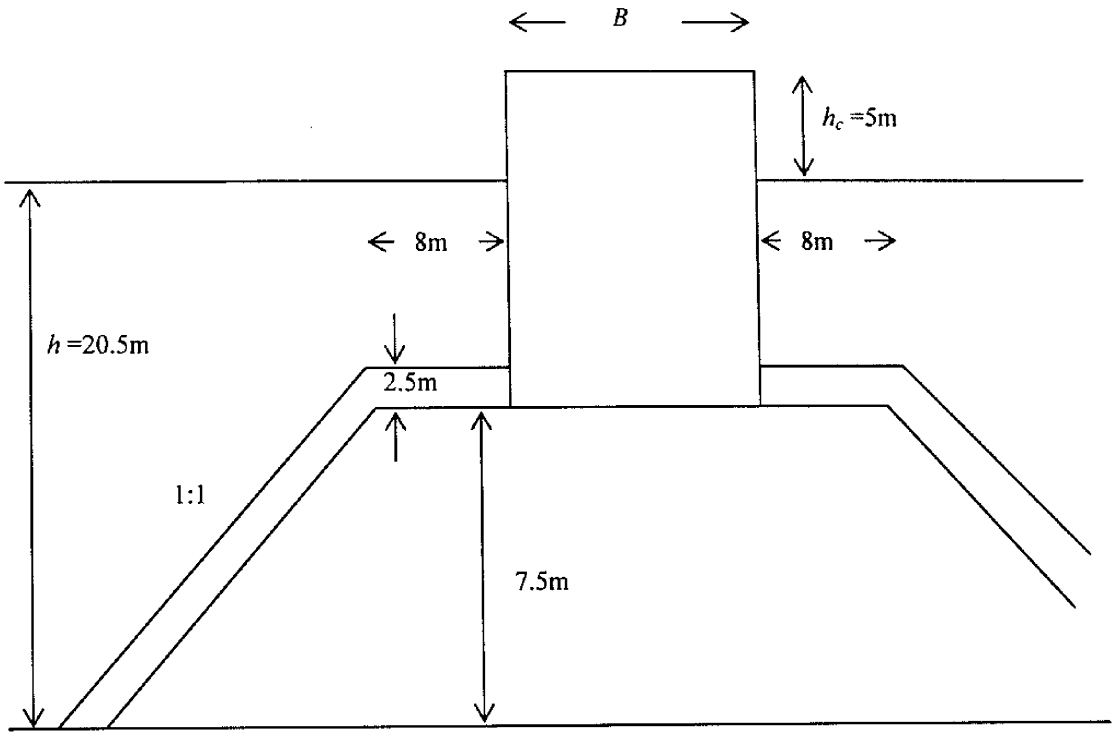

Fig. 8.3. Cross-Section B

8.2.3. Methodology

In order to determine the construction duration and cost a computer program was developed, the main loop of which is given by Fig. 8.4. First, a preliminary design significant wave height is picked by considering the wave climate in the area where the breakwater will be placed. For the present simulation the service lifetime is considered to be 50 years and hence a 1 in 50 years return wave will be chosen. By using the deterministic, conventional design method a caisson cross-section with a Factor of Safety (F.S.) of 1.2 is chosen, corresponding to a width B=18m. Though the F.S. actually changes with depth all caissons must meet the minimum requirement, resulting in the shallower water caissons having a FS much greater than the deeper water caissons.

The program will then simulate the construction of the breakwater by placing each month the various materials according to the construction machinery that the contractor has made available. Each month will then be divided into 6-hour intervals and the wave climate for each of these periods will be simulated at random using the probability distribution curves of wave heights for the given area (which vary throughout the year). Each of the breakwater section is checked for damage during each of these periods, and if any damage takes place the program will repair it in subsequent months as would happen in a real construction. By adding the cost of all materials and overheads used the cost to complete the breakwater can be calculated.

$$\hat{\mathcal{G}}(c) = \frac{\sum_{1}^{5000} \mathcal{G}(c)}{N} \qquad (8.1)$$

where,

$\hat{\mathcal{G}}(c)$ Expected cost of construction

$\mathcal{G}(c)$ Cost obtained from one simulation

N Number of simulation runs

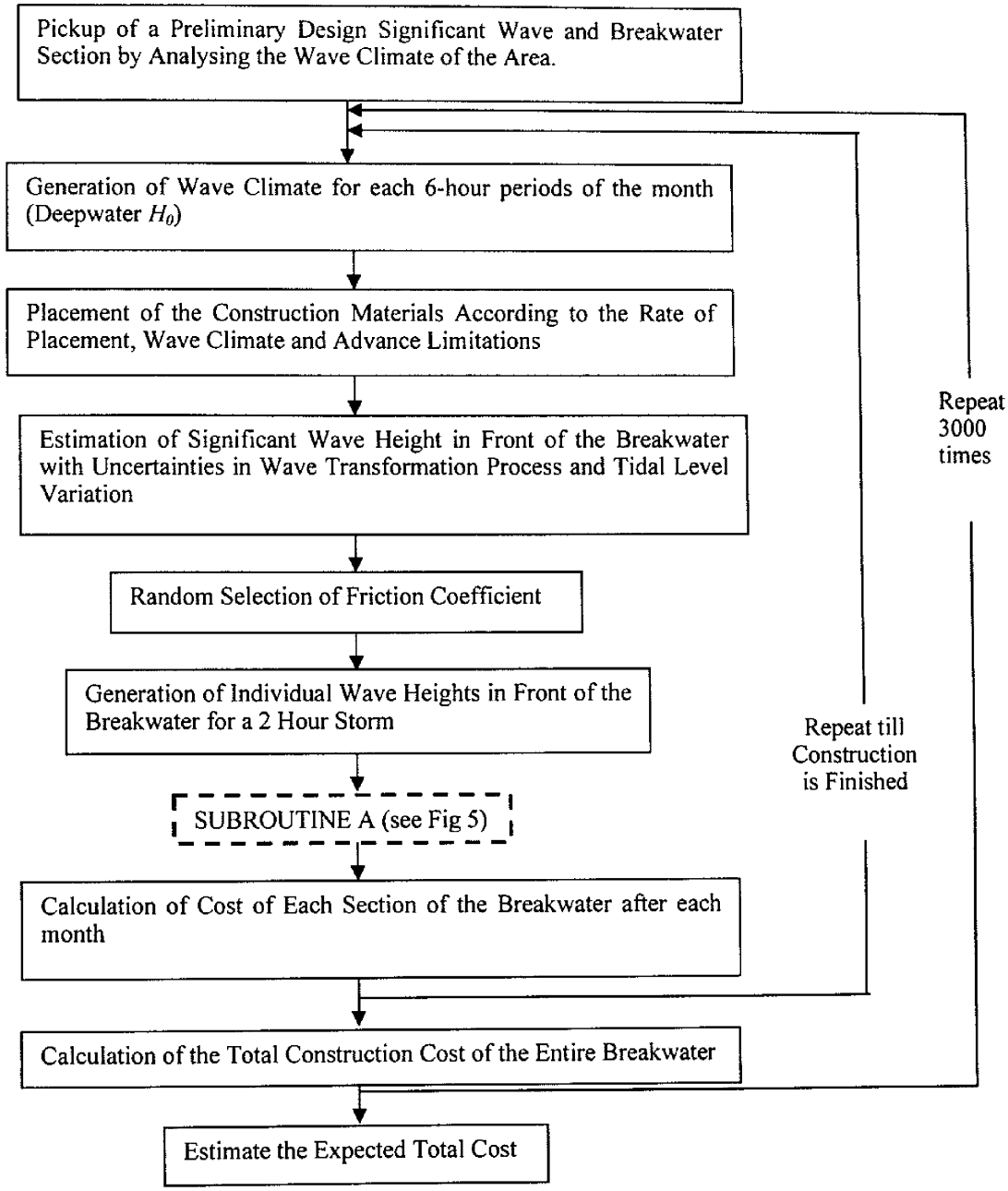

Fig. 8.4: Main Loop of Computation

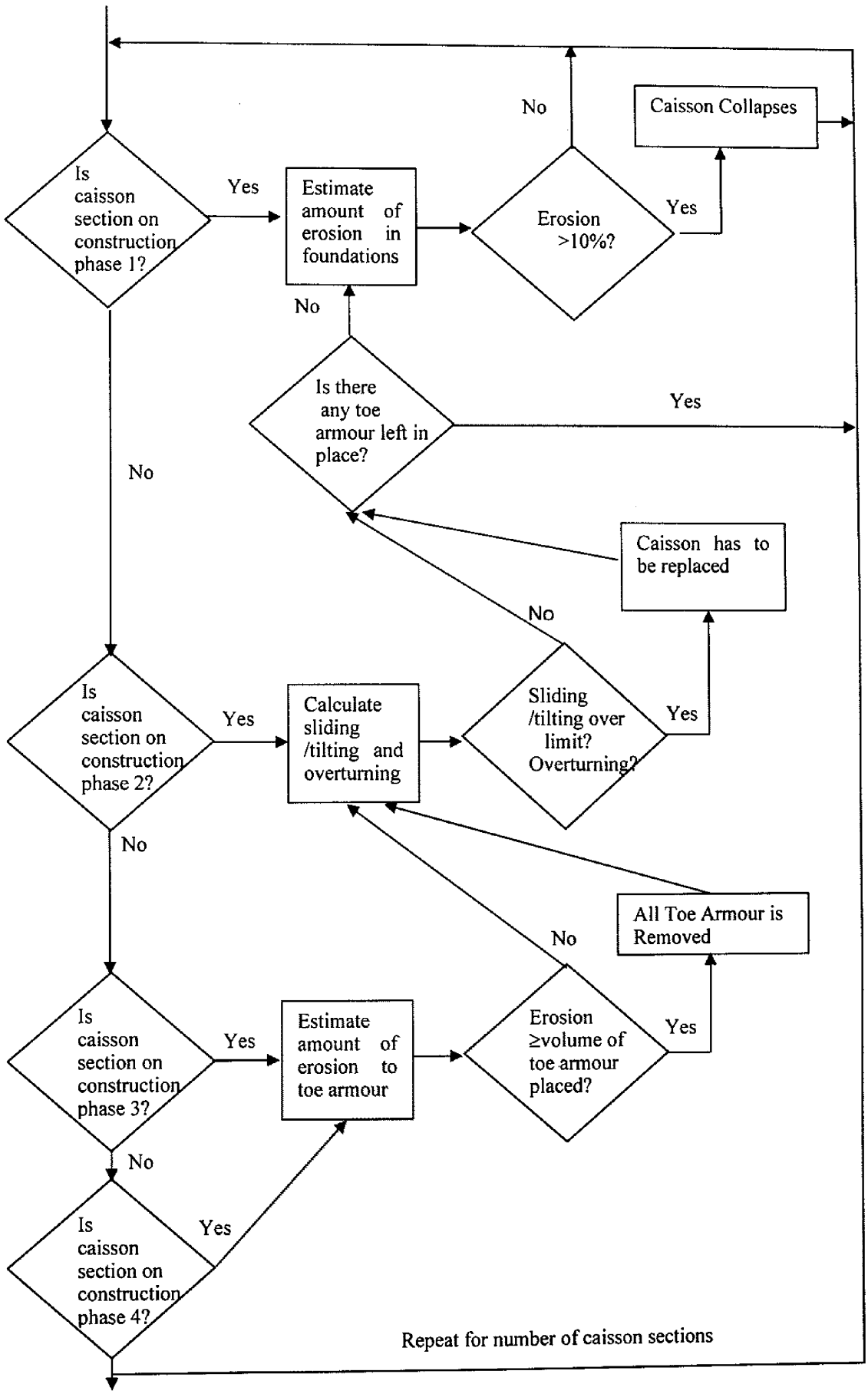

Fig. 8.5: Subroutine A

A Monte Carlo (Level III Reliability Design Method) simulation was carried out by repeating the simulation 3000 times, with the average of computed results for the entire breakwater giving the expected construction cost and time. The estimation errors of the design parameters used are the same as those used by Shimosako and Takahashi (2000).

Shimosako and Takahashi (1998 and 1999) demonstrated that by repeating the simulation 5000 times an error of less than 3% can be obtained. However due to computational restrictions the present simulation was only repeated 3000 times, though the results are considered sufficiently reliable for the present purpose.

8.2.4. Wave Climate

The Wave Climate was modelled using data obtained from the NOWPHAS Report published by the Japanese Ports and Airports Research Institute (P.A.R.I). This information is derived from 27 years of recordings of the wave climate around the Japanese Islands. The deepwater recording station situated at Habu Island (South of Tokyo Bay) was chosen as representative for the Kanagawa area. The NOWPHAS Report provides the statistics to reproduce the wave climate in a certain area based on a normal distribution of wave heights. Table 8.1 shows the values the deepwater significant wave height (H_0') and standard deviation that were used in the simulation. Though it would have been more desirable to use a different type of distribution (such as Rayleigh) allowing for the simulation of the more extreme events, these were not available in the NOWPHAS Report. This is not believed to be a significant source of error as during the construction phase the breakwater will fail even without these

extreme wave events being simulated. In order to simplify the computational procedure the deepwater significant period of all storms was kept constant (though the period of each of the individual waves that made up the storms was varied). This is not believed to be a significant source of error in the case of the present methodology as most of the damage that takes place is due to erosion of the foundation materials (estimated by the method of Madrigal and Valdes (1995), which does not take the wave period into account).

Table 8.1: Parameters to generate probability distributions of H_0' for each month

Month	Mean H_0	H_0 Standard Deviation
January	1.6	0.59
February	1.64	0.61
March	1.73	0.68
April	1.59	0.63
May	1.41	0.61
June	1.29	0.52
July	1.21	0.49
August	1.34	0.74
September	1.48	0.74
October	1.62	0.73
November	1.57	0.65
December	1.48	0.57

8.2.5. Determination of H_0'

For the purposes of the computation, each month was divided into a total of 120 six-hour periods (30 days/month x 4 period/day) and a random H_0' was chosen for each period using the probability distribution parameters given in Table 8.1. The duration of each of the storms however was limited to 2 hours in keeping with Japanese design

custom. As the highest wave heights are only reached for a small duration of time (see Fig. 8.6) this is believed to be a realistic approximation.

By using this method the wave climate for each given month can be reproduced statistically as discussed previously, but it cannot be reproduced in a sequential manner. Though in real life the values of H_0' follow a trend (as seen in Fig. 8.6) in the present simulation a large value can be followed by a very small value or vice-versa. This is not believed to be a significant source or error as most of the damage will be due to the highest H_0' values in each month and hence the order in which they occur will not have such a big effect on the final outcome.

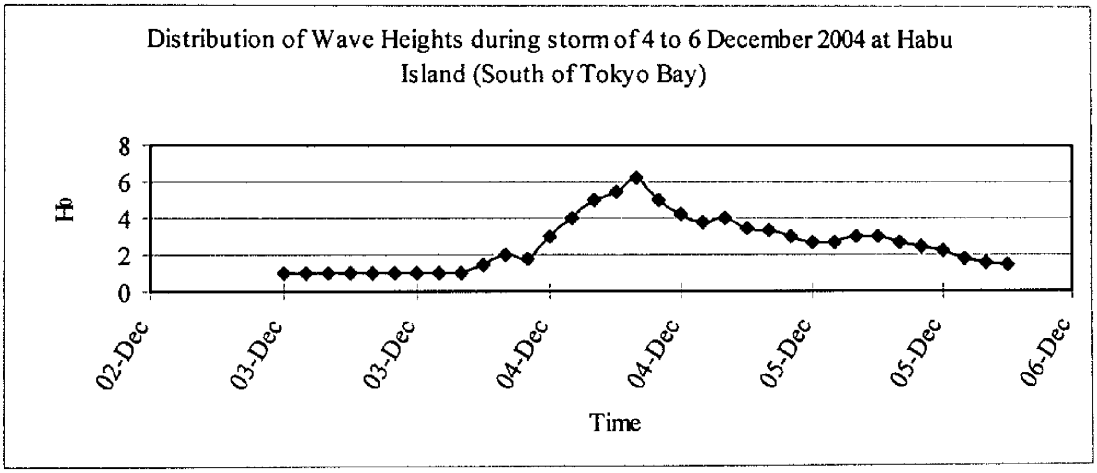

Fig. 8.6. Typical Storm at Habu Monitoring Station

8.2.6. Construction Stages

Under the methodology proposed each of the caisson sections that form the entire breakwater is classified each month as being under one of the following stages of construction:

- Stage 0: No work has been made on the section or the foundation material has not been completely placed.

- Stage 1: The rubble mound foundation of the breakwater has been completely placed.
- Stage 2: The caisson has been placed and filled with sand.
- Stage 3: The toe armour on the seaside of the caisson has been completed
- Stage 4: The toe armour on the shoreside of the caisson has been completed.

In the present methodology there is no separate stage for the caisson immediately after being placed (before it is filled with sand) as this is not deemed to be critical due the low number of caisson sections in the breakwater. It seems unlikely that a contractor would place a caisson unless he knows the weather in the following few days would be good enough for the filling to be completed. Also, as a limit of 5 caissons is set for each month it is considered that the Contractor would have enough time to comfortably complete this activity. If the placement each month of a large number of caissons was to be allowed then the methodology should be revised to add another stage between stages 2 and 3 to take into account the possibility of the caisson being washed away during the time it has no sand inside it.

8.2.7. Construction Sequence

The construction of a breakwater is a process involving many separate activities. However, in order for the model to become manageable these activities have been incorporated into four major groups:

- Placement of Foundation Material. During the construction of breakwaters the contractor will place the foundation –which usually consists of quarry run - material before the positioning of the caisson itself. This foundation material may be placed by a bottom-dump or side-dump barge. Usually the

construction specifications will limit the advance to certain distance in order for only a limited part of the foundation to be unprotected, and a value of about 50m could be considered typical of this limitation. So the advance of the foundation is considered to be limited by a certain distance $A_{foundation}$ in front of the caissons. The foundation material is often compacted by vibration after being placed.

- Placement of Caissons. The placement of the caissons is a complicated operation that requires the placing of a leveling course of gravel over the foundation material, the densification of this gravel (using a vibratory screed, an operation which often requires the use of divers) to a typical tolerance of 20 mm, and the placing of the caisson itself. Concrete box caissons are usually designed as self-floating. A typical box will have been fabricated at a nearby casting yard, moved forward on rails by sliding or transporter jacks, and then set into the water by a large sheer legs crane barge. This transfer from land to water is a critical operation that depends on things such as the tidal range and seasonal variations in water height. The caissons are then towed to their final location and launched by using a ballasting process. The caisson is then filled with sand to achieve its final weight.
- Placement of Seaside Toe Armour. After the caissons have been placed the toe armour on the seaside of the caisson can be placed. These armour units are usually placed with the help of a crane by using slings, so that the unit may be oriented and placed with precision working from the lower end upward. This process also often makes necessary the use of divers. Again, specifications would limit the advance of the caissons to a certain distance $A_{caisson}$ in front of the toe armour.

- Placement of Shoreside Toe Armour. The final stage, placing the toe armour on the shoreside of the caisson is not the most critical, so it is considered that once the seaside toe armour is placed the cranes would move back to the beginning of the breakwater and start this phase of the construction. The placement of the shoreside toe armour will greatly improve the resistance against sliding of a caisson breakwater and hence the caisson is especially vulnerable to this failure mode before this phase is completed.

Once all these four stages have completed the breakwater head and other features – such as a wave returning wall for example- would be placed. Though these features can be important for the stability of the breakwater as a whole they have been omitted in this model for simplification.

8.2.8. Placement Times and Costs

Generally speaking there are two main ways of prizing works in civil engineering, the use of a Bill of Quantities (BoQ) or a Bulk Sum for the entire project. Neither of these is adequate for the objective of the present study, hence for the purposes of the present methodology the costs incurred by a Contractor will be divided into three groups:

- Cost of the Construction Materials: this includes the cost of the materials plus their manufacturing (transport of raw materials, storage, casting, etc). In the case of the caissons it is assumed to include also the preparation of the top of the foundations by divers to create a level surface.
- Cost of the Placing Equipment: this is independent from the cost of the materials in order to simulate the effect that a delay in the construction will have on the Contractor's finances. The values shown in Table 8.2 are

representative of construction costs in Japan. In the simulation it is assumed that the dump barge will be retained throughout the duration of the project as it will be used for various other duties by the Contractor. However, the Caisson Launching Barge is a very specialized an expensive piece of equipment which is typically only at the construction site for the duration of the caisson placement. The present simulation assumes it will be on site for a week each month when any caisson operations would be executed (placement of caissons or removal of the ones that have fallen out of position).

- Contractor Overheads: the computer simulation includes an allowance for the contractor's site office costs and the salary for two engineers (assuming to include a junior engineer working full time and a senior engineer half-time).

Table 8.2. shows the placement rates and costs of the various pieces of machinery and materials involved in the construction. It also gives an estimation of the Contractor overheads for the breakwater considered, and provides some additional restrictions and notes on how the construction is assumed to progress. This includes a limit on the allowable advance, which is typical of the specifications required for breakwater construction. All these rates, number of machines and personnel involved and restrictions can be altered by the engineer to see what effect a different configuration would have on the risk associated with the project.

Table 8.2: Typical Rates and Performance of Materials and Equipment.

Item	Unit Rate	Maximum Rate of Placement	Placement Equipment	Number of pieces of equipment used	Workforce	Notes
Foundation Material	30 US$/m^3	N/A	Dump Barge	N/A		Maximum Advance 50m in front of caissons
Toe Armour	50 US$/m^3	N/A	Crane	N/A		After seaside is finished shoreside toe placement starts
Caissons	1,000 US$/m^3	N/A	Caisson Launching Barge	N/A		Maximum Advance 50m in front of toe
Dump Barge	90,000 US$ /month	15000 m^3 /month	N/A	2	6 per barge	Assumed to work throughout the construction
Armour Placing Crane	40,000 US$ /month	2000 m^3 /month	N/A	2	6 per crane	
Caisson Launching Barge	150,000 US$ /month	5 caissons /month	N/A	1	20 on ship + 20 onshore (making caissons, etc)	Assumed to work only one week each month
Contractor Overheads	150,000 US$ /month	CONSTANT	N/A	N/A	2 engineers + 10 workers	Includes engineers, site office, etc

The rates given on Table 8.2 would thus be the maximum rate of placement that the Contractor could be able to achieve if the weather conditions are absolutely perfect. However the effect of adverse weather has to be taken into account by deducting from this quantity a proportion relative to the periods when high waves occur. In the

present case study the minimum H_0' that is considered by the computation as a storm is 1.5m. Anything under this value will not affect the breakwater and hence the damage subroutine will be ignored in order to save computational time. It will be assumed that in each of the periods when H_0'>1.5m the Contractor will not be able to do any work. To be noted is how Japanese construction regulations estipulate that work is to stop when the wave height is higher than 1m and generally contractors abide by this rule. However the *present case study* would constitute a difficult working site (as it face waves from the open sea and is situated in deep water) and hence it is felt that a 1m height restriction is too limited. In a real case situation for such a difficult site special working conditions would have to be acknowledged and 1.5m is considered feasible. Anything above this would be too dangerous. This limitation nevertheless results in the Contractor losing substantial amounts of working time during some months, so for example during September almost 50% of the working time is lost (as can be inferred from Table 8.1). This figure is even higher for some of the other months and reflects the tough conditions that the present case study would place on a Contractor.

By adding together all of these periods it is possible to obtain the percentage of the time each month when the contractor will be inactive and hence the materials placed can be computed by:

$$P_r = P_{r\_\max} \cdot \left(\frac{t_{total} - t_{inactive}}{t_{total}} \right) \tag{8.2}$$

where P_r is the actual placement rate on a given month, P_{r_max} is the maximum rate of placement as given on table 2, t_{total} is the total number of working time periods in a

month and $t_{inactive}$ is the number of periods that the Contractor is not able to work due to bad weather.

8.2.9. Delays due to Accidents

The trends in accident and death rates in the Japanese construction industry can be seen in Figs. 2.7 and 2.8. By looking at these figures appropriate values for the accident (R_{acc}=630) and death rate (R_{death}=12) per 100,000 workers per year were adopted. These values are for the construction industry as a whole, though Cruickshank and Cork (2005) found that generally the accident rates for coastal construction and general construction in the U.K. were similar, and hence the use of these values is believed to acceptable. From them the probability of an accident (P_{acc}) and death (P_{death}) occurring each day can be calculated by:

$$P_{acc} = R_{acc} x \left(\frac{Q}{Y} \right) \tag{8.3}$$

$$P_{death} = R_{death} x \left(\frac{Q}{Y} \right) \tag{8.4}$$

where Q is the number of workers active during a particular month calculated by using Table 8.2 and Y is the number of working days in one year.

The present simulation will assume that if an accident happens one week (5 working days) will be lost, whereas if one death occurs one entire month will be lost. These values are thought to be representative of the Japanese construction industry, although the reality is that there is a great variation according to the nature of each accident. By adding the results all time lost due during the month the total lost time due to accidents and deaths (t_{health}) can be obtained. Eq. 8.2 would thus become:

$$P_r = P_{r\_\max} \cdot \left(\frac{t_{total} - t_{inactive} - t_{health}}{t_{total}} \right) \tag{8.5}$$

8.2.10. Damage to each section

The simulation will consider sequentially the wave climate in each of the 6-hour periods that make up each month, and will compute possible damage to each component of each breakwater section for the periods when H_0'>1.5m. Fig. 8.5 shows the flow-path in the computation of the damage to each of the sections in the breakwater. First, the erosion to the seaside toe armour is considered. Then the sliding/tilting movement of the caisson is evaluated, and a check is made to see if the overturning limit is reached. If there is no toe armour or if it was all eroded then erosion of the foundation material is considered. Finally if this erosion is greater than 10% of the foundation material the caisson is considered to have failed due to scouring.

8.2.10.1. Damage to toe armour or foundation material.

In order to estimate the damage to either the toe armour or the foundation material two different methods are used depending on the depth ratio *d/h* in front of the breakwater, where *d* is the water depth at top of toe berm and *h* the water depth in front of the toe berm.

If *d/h* >0.5 then the method by Madrigal and Valdes (1995) is used, which estimates the damage to the berm using the following equation:

$$N_s = \frac{H}{\Delta D_{n50}} = \left(5.8 \frac{d}{h} - 0.6 \right) N_{od}^{0.19} \tag{8.6}$$

where H is the significant wave height in front of breakwater, $\Delta=(\rho_s/\rho)-1$, ρ_s is the mass density of stones, ρ is the density of water, D_{n50} the equivalent cube length of median stone and N_{od} the number of units displaced out of the armour layer within a strip of width of D_{n50}. For a standard toe size of about 3-5 stones wide and 2-3 stones high:

$$N_{od} = \begin{cases} 0.5 & \text{no damage (1-3\% units displaced)} \\ 2 & \text{acceptable damage(1-3\% units displaced)} \\ 5 & \text{severe damage (20-30\% units displaced)} \end{cases}$$

If d/h <0.5 then the method by Merkle (1989) is used where also

$$N_s = \frac{H_s}{\Delta D_{n50}} \tag{8.7}$$

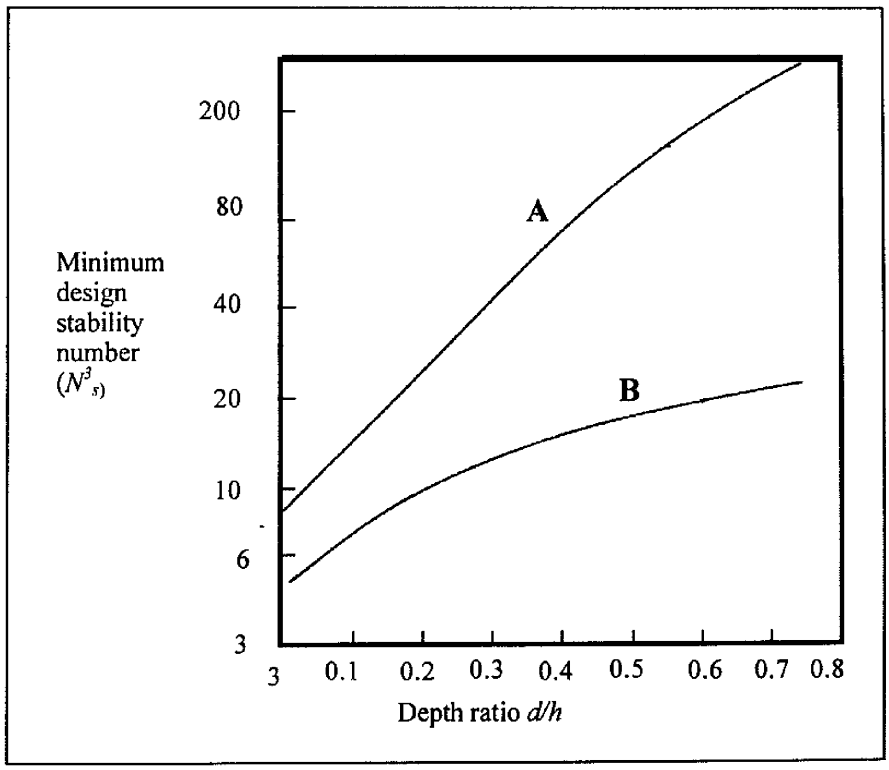

Fig. 8.7: Lower boundary of N_s-values

The curves shown in Fig. 8.7 are the lower boundaries of N_s values associated with acceptable toe berm stability. Curve A is used for the design of the toe armour and curve B is used for the design of the rubble foundation. There are several problems associated with the use of this formula in the present simulation:

1. This empirical method is valid for regular waves and irregular waves are used in the present simulation.
2. No formula is provided for the determination of these curves, and hence their incorporation into the computer simulation is difficult
3. The percentage of eroded area is not provided, so it is assumed that once failure occurs the entire berm is removed.

The validity of using this method in the present simulation this is questionable, but it is necessary to incorporate it in order to simulate damage at the deeper end of the breakwater. The toe foundation of the breakwater studied in this paper has been well designed so that once it is installed no damage will occur to it at the deeper end. In the rare occasions when a sufficiently large storm is able to erode the foundations at this end then it is safe to assume that the entire foundation has been removed. As only one of the caissons (the one situated at the deepest end) falls within this category the results are not believed to be greatly affected in any case.

8.2.10.2. Damage to the caisson breakwater

Damage to the caisson breakwater can be estimated using the method outlined in Chapter 5 of the current dissertation, which allows for the computation of sliding and tilting. This method takes into account the effect of the shoreside toe material in restricting the sliding of the caisson, so that during the construction phase -before it is placed- the caissons are particularly vulnerable to sliding. The present simulation does

not include the effect of other finishings (such as return walls on top of the caisson, finishing slabs, etc) in order to simplify the model. In reality all these finishing would increase the weight of the caisson and hence it's FS but in order to be conservative their exclusion was thought to be appropriate.

Shimosako and Takahashi (2000) proposed a tolerable limit for the sliding distance of 0.3m before a caisson is deemed to have failed and remedial action is needed. Goda and Takagi (2000) proposed a smaller tolerable sliding distance of 0.1m and in the present simulation this second more restrictive limit is used. A maximum angle of tilt of 5 degrees is proposed, though by using the foundation parameters proposed earlier the sliding limit will be reached before such a rotation can take place. If during the construction stage the caisson is displaced over these values (which is more likely to happen than after it is finished due to the absence of shoreside toe armour during part of the construction) then the section is considered to have failed and remedial action takes place. The sand is removed from the caisson and the caisson is re-floated the month after the damage takes place. The subsequent month the caisson is placed again and filled with sand once more. Goda and Takagi (2000) proposed the cost of replacing the caisson to be equal to the original cost of the caisson. This point of view will also be adopted in the current simulation.

After each wave a check is made to see whether the overturning limit is reached by using Eq. 2.26 in Chapter 2. If FS<1 then the caisson is considered to have failed by overturning and must be replaced.

In addition to these failure modes, the breakwater is also considered to fail if more than 10% of the foundation material is eroded from under it. The caisson sections are

particularly vulnerable to this immediately after the caisson has been placed but before the seaside toe armour is in place, and this scouring failure is considered to be critical during construction.

8.2.11. Computational Time

The present simulation was carried out using a Desktop Pentium IV at 2.26 GHz with 1,024MB of RAM. The computational time varied depending on the month of the year that the construction was stated (the computer was asked to ignore small H_0 in the damage computation, and hence it took longer to compute the months of July to October in general), with 3000 simulations taking between 6 and 8 hours on average to complete.

8.2.12. Calculation of Insurance Premium

The Risk associated with a certain project can be defined as:

$$Risk = \Pr obability \times Cost \tag{8.6}$$

In order to insure a certain item the premium must be at least equal to the risk involved in its construction, plus a certain mark-up to include the costs related to the administration and profits of the insurance company. In the present simulation this mark-up is assumed to be 30% of the risk associated with the project.

Due to the difficulties associated with the case study construction site there is a high probability that foundation materials will be eroded during the construction before the toe armour is placed. The estimation of the quantity of this eroded material would be difficult and costly in practice due to the nature of underwater surveying. As this

material is cheap (see Table 8.2) it appears improbable that it would be insured, and hence the risk associated with losing it would be taken entirely by the Contractor or the Client. The caisson itself is the most costly part of the construction and hence the present simulation only considers the insuring of this structure.

Regarding accident in Japan all insurance is covered by the government-run Worker's Accident Compensation system, and hence no additional cost is uncured by the Contractor due to accidents or deaths. The Contractor would normally pay a premium based on the number of workers employed, and hence it can be considered that this cost is included in the salary of the workers and taken into account in the monthly cost shown on Table 8.2.

8.3. Discussion of the Results

In order to analyse the effect of the wave climate on the construction sequence a total of 12 different simulations were carried out, with each one starting construction on a different month of the year. Fig. 8.8 shows the chance of the entire breakwater being completed in a certain number of months according to the date of commencement of construction. This figure shows, for example, how for constructions starting the month of May there is a high probability that the entire breakwater will be completed in 7 months, whereas if it is started in September or November there is less than a 5% chance that the breakwater will be completed in that time. Figs. 8.9 and 8.10 show the expected construction cost and the average number of caissons along the breakwater that can be expected to fail during the construction period –by failure is understood either the breakwater sliding over its allowable limit, overturning or excessive foundation material being eroded from under it- for each of the start dates.

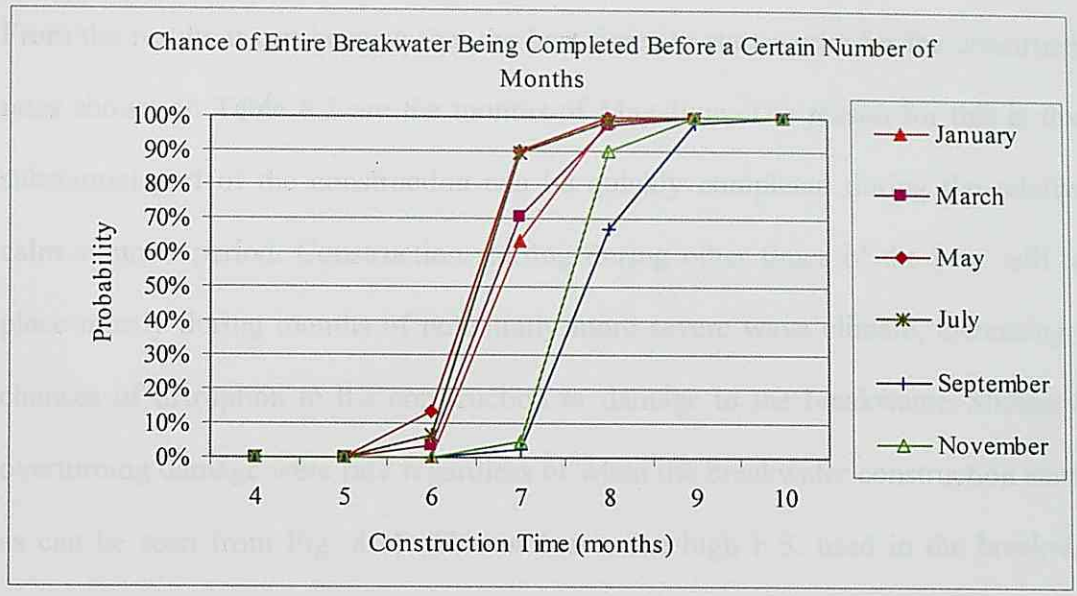

Fig. 8.8. Probability of breakwater completion after a certain number of months.

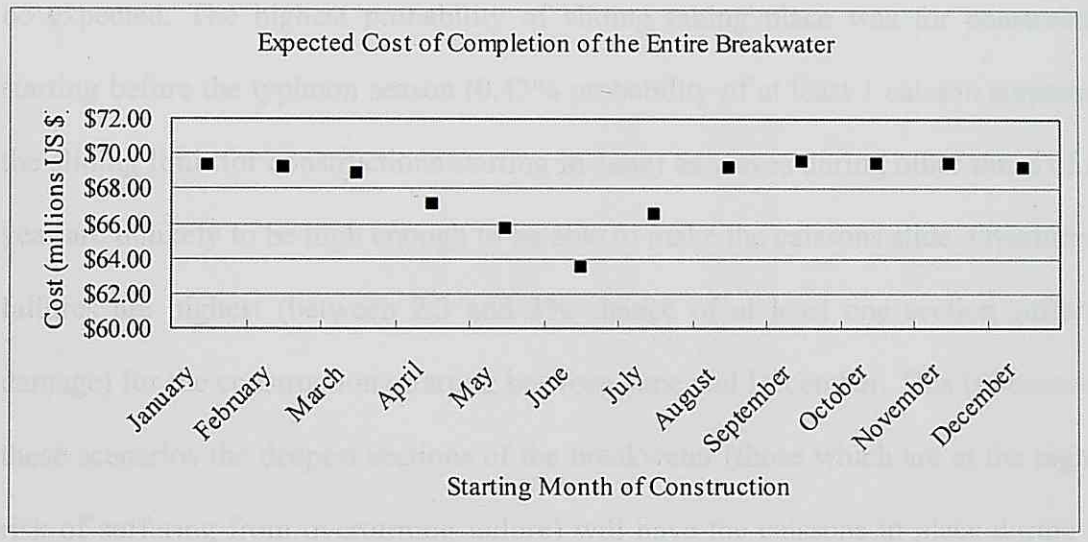

Fig.8.9. Expected completion cost

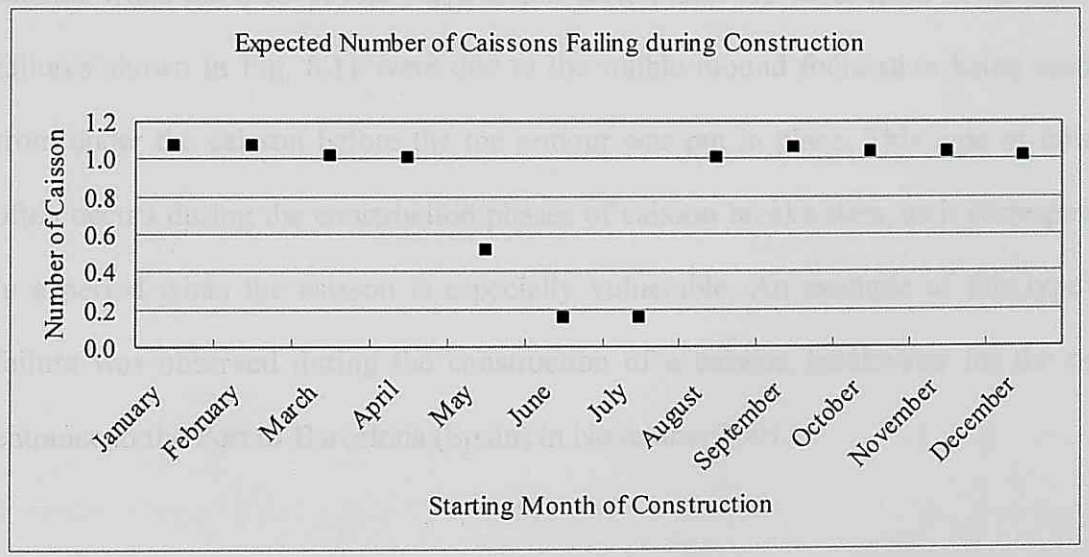

Fig. 8.10. Expected number of caissons failing during construction

From the results it can be seen that the best times to start works for the construction rates shown on Table 8.2 are the months of May-June. The reason for this is that a substantial part of the construction can be quickly completed during the relatively calm summer period. Construction starting during other times of the year will take place mostly during months of potentially more severe wave climate, increasing the chances of disruption to the construction or damage to the breakwater. Sliding and overturning damage were rare regardless of when the breakwater construction started, as can be seen from Fig. 8.11. This is due to the high F.S. used in the breakwater construction, resulting in a low probability of these failure modes occurring, as could be expected. The highest probability of sliding taking place was for construction starting before the typhoon season (0.43% probability of at least 1 caisson surpassing the sliding limit for constructions starting in June) as waves during other times of the year are unlikely to be high enough to be able to make the caissons slide. Overturning failures are highest (between 2.3 and 3% chance of at least one section suffering damage) for the constructions starting between June and December. This is because in these scenarios the deepest sections of the breakwater (those which are at the highest risk of suffering from overturning failure) will have the caissons in place during the months when the most severe wave action takes place. However most of the caisson failures shown in Fig. 8.11 were due to the rubble mound foundation being eroded from under the caisson before the toe armour was put in place. This type of failure often occurs during the construction phases of caisson breakwaters, as it corresponds to a period when the caisson is especially vulnerable. An example of this type of failure was observed during the construction of a caisson breakwater for the new entrance to the Port of Barcelona (Spain) in November 2001.

The expected number of failures shown in Fig. 8.11 is **an average of the number of caissons for the entire breakwater** that can be expected to fail during construction due to each failure mode. This does not mean that in each simulation 1.1 sections fail due to erosion when the construction starts the month of January. In some simulations a number of caisson sections will fail simultaneously due to a particularly large storm occurring, and the average obtained from the Monte Carlo Simulation is the number shown.

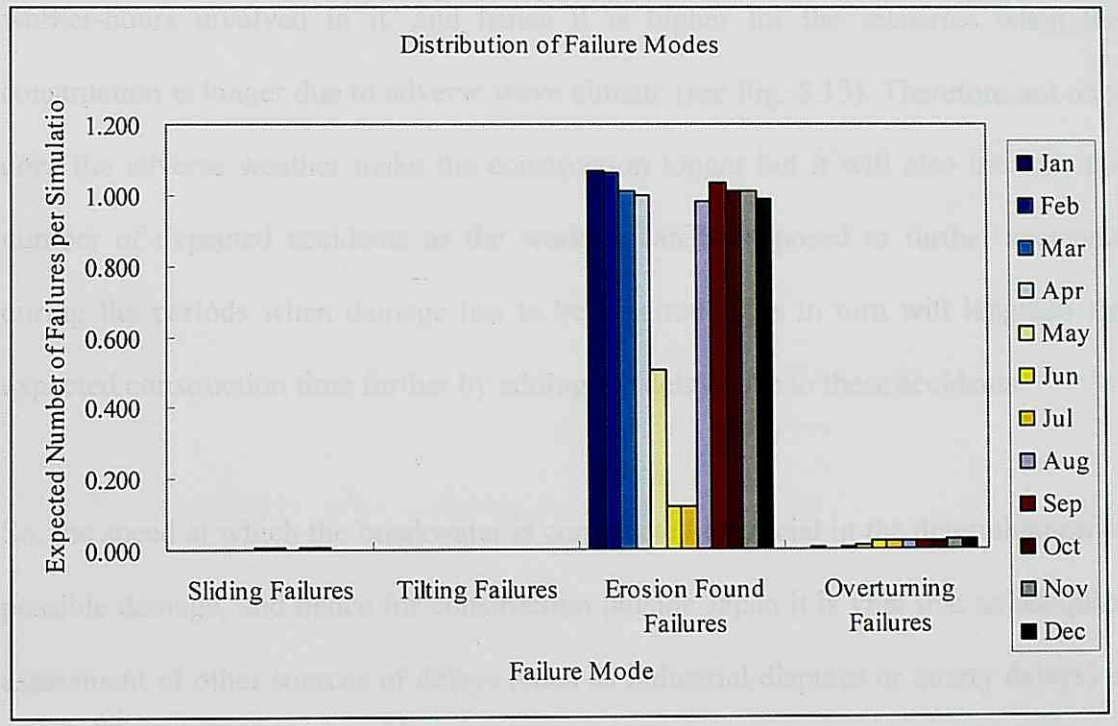

Fig. 8.11. Expected Occurrence of each failure mode

Figs. 8.8 to 8.10 show in a graphical way what is established Japanese Contractors construction practice i.e. the best time to start a breakwater construction is during the calm summer month, and typically a Japanese contractor would try to avoid the most risky part of the works occurring during the typhoon or winter seasons. A Japanese Contractor would usually thus start construction in the month of April coinciding with the beginning of the Japanese financial year, with large breakwaters being interrupted

during the typhoon season in order to avoid possible damage. This reflects in the estimated premium that would have to be paid, with $1.06m for June compared with $7.63m for construction starting in February as shown in Fig. 8.12. Hence when establishing the premium for the construction of a caisson breakwater extreme care must be placed in obtaining accurate statistics of the annual variation of the wave climate in the area.

The average number of accidents during construction is a function of the amount of worker-hours involved in it, and hence it is higher for the scenarios when the construction is longer due to adverse wave climate (see Fig. 8.13). Therefore not only does the adverse weather make the construction longer but it will also increase the number of expected accidents as the workers can be exposed to further accidents during the periods when damage has to be repaired. This in turn will lengthen the expected construction time further by adding the delays due to these accidents.

So, the speed at which the breakwater is constructed is crucial in the determination of possible damage, and hence for construction outside Japan it is vital that an adequate assessment of other sources of delays (such as industrial disputes or quarry delays) is made. However, in the present simulation these factors are not crucial due to the nature of the Japanese construction industry and hence the results obtained above could form the basis for the calculation of insurance premiums in Japan

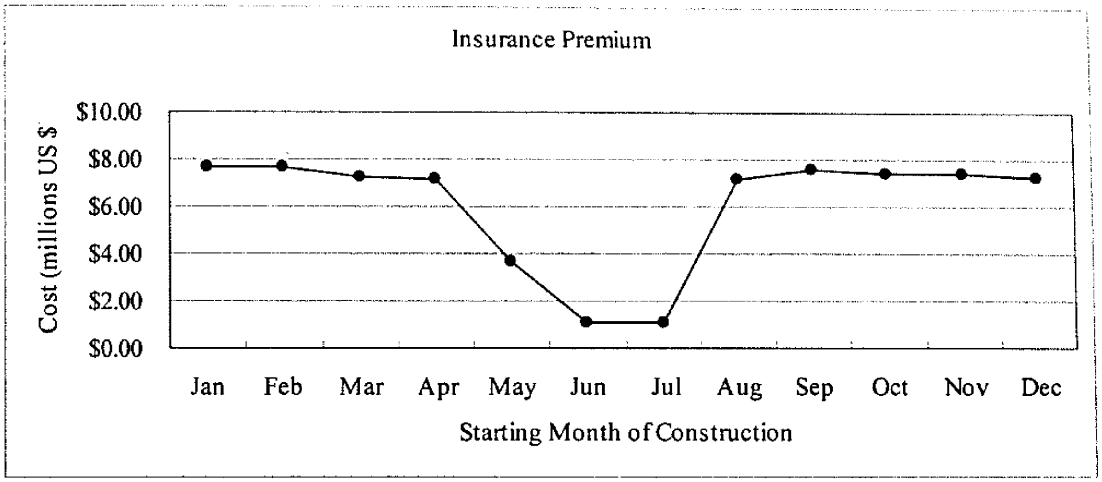

Fig. 8.12. Cost of the Insurance Premium

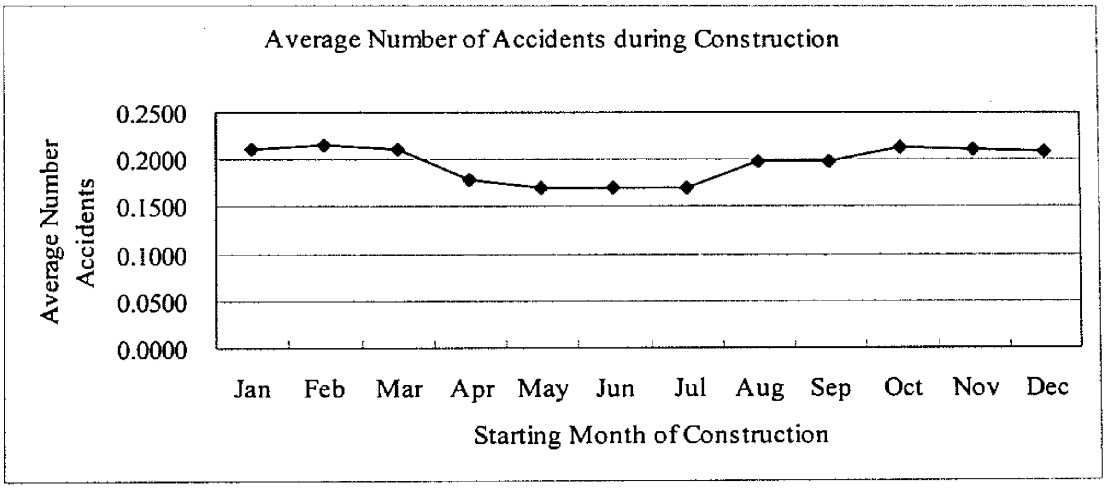

Fig. 8.13. Average Number of Accidents during Construction

One of the main limitations of the computational procedure described lies in the fact that all damage is calculated after all the materials have been placed for a given month. This is somewhat artificial, and it would have been more realistic to compute the placement of materials and damage on a daily basis. However the computational time would increase significantly and it was felt that the procedure used was a reasonably good approximation.

Due to the relatively low cost assigned to the contractor overheads the results do not show a great sensitivity towards a delay in the construction time. If the completion of the entire project (not just the breakwater but the entire port development) depended

on the completion of the breakwater then a much higher value would have to be included in this section to reflect delays in other areas.

Finally to be noted is how the results obtained are highly dependent on the wave climate in a given area. If the model were to be applied to a different area (such as the island of Hokkaido in the north of Japan or other areas of the world) the wave climate parameters would have to be changed.

A clear limitation of the present method is that it does not consider as a source of risk any factors other than the wave climate and accidents. As in many countries construction is often disrupted by many other factors this model can only be applied in its present form to places where these other factors can be safely ignored, such as Japan.

8.4. Conclusions

The proposed methodology is able to provide an indication of the expected time and cost to complete an entire caisson breakwater, which could serve as the basis for a management tool to help in the development of a construction plan for a caisson breakwater. By modifying the various parameters, types and number of machinery and workforce involved the engineers can gain an insight into the expected time it would take to build a certain breakwater and the degree of risk involved. Potential construction bottlenecks that could arrive from specification limitations and excessive risk to certain sections being damaged due to inclement weather can be easily identified. The results presented compare well with accepted Japanese construction practice and can serve as the basis for a more extensive construction management tool

for consultants and contractors. As the source or risk is limited to the wave climate and possible site accidents the application of the model is restricted to countries were other problems in construction (such as labour strikes) can be safely neglected (the present case concerns itself only with Japan). Moreover, by providing a clear idea of the risk involved in the construction process it could allow for an objective assessment of the cost to insure a breakwater during its construction to be made.

CHAPTER 9

CONCLUSIONS AND RECOMMENDATIONS FOR FURTHER STUDY

9.1. Conclusions

The present thesis has focused on the development of a risk assessment methodology for caisson breakwaters. The concept of reliability is a key element of this methodology, and the computation of the displacements that the caisson would be subjected to under different types of waves is of paramount importance for its accurate evaluation. A new methodology for the evaluation of the movement of the caisson was proposed, based on that of Shimosako and Takahashi (1998, 1999) but with the inclusion of tilting. This model uses simple soil mechanics theory to evaluate the vertical displacement at the back of the caisson, which depends heavily on the degree of consolidation of the rubble material. The model is heavily influenced by the choice of the gravel parameters, and hence care must be taken to employ accurate values if the model is to be applied to a real life breakwater.

Laboratory experiments were carried out to determine the distributions of loading throughout the rubble mound foundation due to a variety of wave load types, ranging from non-breaking to perfect impact breaking. The pressures exerted by a caisson breakwater on the top area of the foundation were shown to be similar to those

predicted using traditional Boussinesq Theory. Most of the deformation takes place in a narrow strip 1cm deep at the top of the foundation, and thus this value can be adopted as the active depth of foundations in the computation of the vertical displacement of the caisson. However, care must be exercised when using this value, and if sections or loads that greatly differ from those used in the present thesis are considered, it is recommended that the active depth is calculated using the equations provided.

In order to verify the new DBRD method proposed three separate approaches were used. First, laboratory experiments were carried out to obtain the probability distributions functions for sliding and tilting, which were adequately reproduced by the simulation. The failure mechanism of a caisson breakwater subjected to impact waves was shown to be the sliding/tilting mode.

Secondly, the model was used to try to replicate the damage that actually took place at Susami West Breakwater in 2004. Though one of the caissons suffered greater vertical movement that could be predicted by the model, all the other caissons appeared to fit into the probability distribution obtained from the simulation. All of the caissons' sliding distances fell within the obtained sliding distribution, and thus it appears that the model can be applied to calculate the damage that would take place on a prototype breakwater that was subjected to a $H_{1/3}$ higher than it was designed for.

Finally, solitary waves were employed in laboratory experiments to try to understand the failure mode of caisson breakwaters under different types of tsunami attack, which influenced the loads recorded at the back of the caisson. By using the methodology

shown in Chapter 5 it was possible to roughly estimate the vertical displacement that could be expected for a certain wave, though further research is needed at this stage.

Thus the model proposed is quite robust and can be applied to a variety of wave conditions, provided that the gravel parameters are accurate. However the model so far has not been verified in large scale laboratory tests, and it should be applied to more real failure cases before it can be used in real design.

The DBRD Method was then employed in a new methodology for the risk assessment of a breakwater during the construction phase. The proposed methodology is able to provide an indication of the expected time and cost to complete an entire caisson breakwater, comparing well with accepted Japanese construction practice. Thus it could serve as the basis for a management tool to help in the development of a construction plan for a caisson breakwater, allowing engineers to check the effects of different construction machinery on the works. As the source or risk is limited to the wave climate and construction accidents the application of the model is restricted to countries were other problems during construction (such as labour strikes) can be safely neglected (namely Japan). By providing a clear idea of the risk involved in the construction process it allows for an objective assessment of the cost to insure a breakwater during its construction to be made.

9.2. Recommendations for Further Study

One of the main areas of uncertainty in the present model lies in the determination of the gravel parameters, which were obtained using small-scale experiments. It is recommended that large scale experiments using unconstrained gravel should be

carried out to ascertain whether the parameters employed in the present simulation were accurate or not.

Due to the small scale employed in the present experiments it was not possible to accurately measure the pressure due to solitary waves on the vertical face of the caisson. Larger scale experiments should be carried out to determine the time history of this pressure in order to be able to compute the sliding distance of the caisson due to this type of wave attack. Also, it is necessary to clarify at what height within the vertical face the maximum pressure is exerted, which is thought to be dependent on the solitary wave type.

To further verify the present model more real life failures should be obtained, and the role of wave-dissipating concrete blocks should be ascertained, in order to see if the application of the model proposed to Susami breakwater was adequate or not.

Regarding the methodology for the construction phases, it would be necessary to include all other failure modes (slip failure, etc) in the computation in order to eliminate some of the simplifications of the system. Also, in order to apply the model to developing countries it is necessary to include non-weather related delays, such as the effects of labour disputes or other possible site problems.

REFERENCES

Balas, C.E. (1998). "A risk management model for coastal projects". PhD Thesis, Graduate School of Natural and Applied Sciences, Middle East Technical Univ., Ankara, Turkey.

Balas, C.E. and Ergin, A. (2002) *"Reliability-Based Risk Assessment in Coastal Projects: Case Study in Turkey"*, Journal of Waterway, Port, Coastal and Ocean Engineering, pp52-61, March-April.

Bullock, G. N., Crawford, A. R., Hewson, P. J., Walken, M.J.A. & Bird, P. A. D. (2001). *"The influence of air and scale on wave impact pressures"*, Coastal Engineering 42, 291-312.

Burcharth, H. F. (1991). *"Introduction of partial coefficient in the design of rubble mound breakwaters"*, Proc. Coastal Structures Breakwaters, Institute of Civil Engineers., London, pp. 543-565.

Burcharth, H. F. (1992). *"Reliability-based design of coastal structures: Structural integrity"*, Proc. Short Course, 23rd Int. Conf. Coastal Eng., Venice, ASCE, pp.511-545.

Burcharth, H.F. and Sorensen, J.D.(1998). *"Design of Vertical Wall Caisson Breakwaters Using Partial Safety Factors"*. Proc. Coastal engineering 1998 pp2138-2151.

Chongsuvivatwong et al (1998). "A Multi-Centre Cross Sectional Survey on Safety at Construction Sites in Thailand", 1994-1995. Journal of Occupational Health 1998; 40, pp319-324.

CERC (1984), *"Shore Protection Manual"*, Co. Eng. Res. Center, U.S. Corps of Eng., Vicksburg.

Coastal Engineering Manual (CEM). Published by US Army Corps of Engineers (USACE).

Cornell, C.A. (1970). *"A first order reliability theory of structural designs"*. Structural Reliability and Codified Design, SM Study No. 3, University of Waterloo, Ontario, Canada.

Craig, R. F. (2004). *"Craig's Soil Mechanics"*, Spon Press, London

Cruickshank, I. & Cork, S. (2005). *"Construction Health and Safety in Coastal and Maritime Engineering"*. HR Wallingford. Published by Thomas Telford, London.

De Groot, M.B.; Andersen, K.H.; Burcharth, H.F.; Ibsen, L.B.; Kortenhaus, A.; Lundgren, H.; Magda, W. et al. (1996). *"Foundation design of caisson breakwaters"*. Norwegian Geotechnical Institute, no. 198, 2 volumes, Oslo, Norway, 126 pp; 9 Appendices.

Esteban, M. and Shibayama, T. (2006). *"Laboratory Experiments on the Progression of Damage on Caisson Breakwaters."* Proc 30th Int. Conf. Coastal Eng., San Diego, ASCE

Esteban, M., and Shibayama, T. (2006). *"Laboratory Study on the Progression of Damage on Caisson Breakwaters Under Impact Waves."* Techno-Ocean/19th JASNAOE Ocean Engineering Symposium, Kobe.

Esteban, M., Takagi, H. and Shibayama, T. (2007). *"Proposed Methodology for Evaluation of the Cost to Insure a Breakwater During the Construction Phase"*. Proc. 4th International Conference on Asian And Pacific Coasts (APAC 2007), Nanjing. (abstract accepted, full paper under review)

Esteban, M., Takagi, H. and Shibayama, T. (2007). "Improvement in Calculation of Resistance Force on Caisson Sliding due to Tilting". Coastal Engineering Journal (in print)

Esteban, M., Takagi, H. and Shibayama, T. (2007). *"Evaluation of the Active Depth of Foundations Under a Caisson Breakwater Subjected to Impact Waves"*. Coastal Structures 2007 International Conference, Venice.

Esteban, M., Takagi, H. and Shibayama, T. (2007). "Improvement in Calculation of Resistance Force on Caisson Sliding due to Tilting"., Coastal Engineering Journal (in print)

Goda, Y. (1974). *"New wave pressure formulae for composite breakwater"*, Proc. 14th Int. Conf. Coastal Engineering, Copenhagen, ASCE, pp.1702-1720.

Goda, Y. (1985)."*Random Seas and Design of Maritime Structures*". University of Tokyo Press.

Goda, Y. (1999). *"Wave Actions and Damage on Maritime Structures"*. Lecture Note at DHL-JICA Seminar. Ankara, Turkey.

Goda, Y. and Takagi, H. (2000). *"A Reliability Design Method of Caisson Breakwaters with Optimal Wave Heights"*. Coastal Engineering Journal, Vol. 42, No.4, pp357-387.

Goda, Y. (2001). *"Extreme wave statistics for reliability-based design of caisson breakwater"*. Proc. Of Int. Workshop on Advanced Design of Maritime Structures in the 21st Century, PHRI & MLIT, Japan, pp.1-13.

Goda, Y. (2004). "Spread parameter of extreme wave height distribution for performance -based design of maritime structures", J. Waterway Port Coastal Ocean Eng., ASCE, 130, 1, pp. 29-38.

Hanzawa, M., Yamagata, N., Nishihara, T., Takahashi, S., Takayama, T. and Tomiyasu, R. (2003). *"Performance of composite breakwaters from the viewpoint of expected sliding distance of caisson"*, Coastal Structure 2003, ASCE.

Hayakawa, Y. (1990). "Mean seasonal changes of dissolved inorganic nutrients in the Ofunato estuary", Nippon Suisan Gakkaishi, 56, 11, 1717-1729.

Hillyer, T.M., Stakhiv, E.Z., and Sudar, R.A. (1997). "An evaluation of the economic performance of the U.S. Army Corps of Engineers shore protection program." J. Coastal Res.,13(1), pp8-22.

HSE (Health and Safety Executive). "*Key Facts Injuries in the Construction Industry 1961 to 1995/6*". UK HSE Reports –available online-.

Horikawa, K., Ozawa, Y. & Takahashi, K. (1972) *"Expected sliding distance of high mound composite breakwaters"*, Proc. Of Coastal Engineering, JSCE, Vol. 17, pp 177-184 (In Japanese).

Ikeno, M., Mori, N. and Tanaka, H.. (2001). "Experimental Study on Tsunami force and Impulsive Force by a Drifter under Breaking Bore like Tsunamis", Proceedings of Coastal Engineering, JSCE, Vol. 48.

Ikeno, M. and Tanaka, H. (2003). *"Experimental Study on Impulse Force of Drift Body and Tsunami Running up to Land"*, Proceedings of Coastal Engineering, JSCE, Vol. 50.

Ito, Y., Fujishima, M. & Kitatani, T. (1966). *"On the stability of breakwaters"*, Rept. Of Port and Harbour Research Institute, Vol. 5, No. 14: 1-134 (in Japanese).

Jayaratne, M.P.R., Jayatilake, N.B., and Shibayama, T. (2006). *"Restoration of damaged coastal dunes in Hambantota bay. A soft solution to tsunami and storm surge conditions"*. Proceedings of the "Tsunami, Storm Surge and other Coastal Disasters Symposium, Sri Lanka.

Japan Construction Health and Safety. Website:www.jicosh.gr.jp/english/statistics/

Kato, F., Inagaki, S. and Fukuhama, M. (2006). *"Wave Force on Coastal Dike due to Tsunami"*. Proc. 30th Int. Conf. on Coastal Eng., ASCE, pp 5150-5161.

Kim, YG. & Watanabe, T. (1993). "*International Comparison of Labor Accidents in the Construction Industry*". The fourth East Asia-Pacific conference on Structural Engineering & Construction, Seoul, Korea. Pp 22-3 to 22-8.

Kim, T.M., Takayama, T. (2003). "Computational Improvement for Expected Sliding Distance of a Caisson-Type Breakwater by Introduction of a Doubly-Truncated Normal Distribution", Coastal Engineering Journal, Vol.45, No.3 (2003) 387-419.

Kim, T-M. and Takayama, T. (2004). "*Effect of caisson tilting on the sliding distance of a caisson*". Annual Journal of Civil Engineering in the Ocean, JSCE, 20, pp. 89-94.

Kim, T.M., Takayama, T. & Miyawaki, Y. (2004) "Laboratory Experiments on the Sliding Distance and Tilting Angle of a Caisson Breakwater Subject to Wave Impact", Proc. 29th Int. Conf. on Coastal Eng., ASCE, pp 3762-3773.

Kim, T.M., Yasuda, T., Mase, H. & Takayama, T. (2005). "*Computational Analysis of Caisson Sliding Distance Due to Typhoon Tokage*", Asian and Pacific Coasts Conference, pp 565-576.

Kirkgöz, M.S. (1978). "*Breaking Waves: their action on slopes and impact on vertical seawalls*". Thesis presented to the University of Liverpool, U.K.

Kirkgöz, M.S. (1995). "*Breaking Wave Impact on Vertical and Sloping Coastal Structures*", Ocean Engng, Vol.22, No.1, pp 35-48, 1995.

Kunishima, M & Shoji, M (1996). "*The Principles of Construction Management*". Sankaido Publishing Co., Ltd, Tokyo.

Madrigal, B. G., and Valdés, J. M. (1995). "*Study of Rubble Mound Foundation Stability*" Proceedings of the Final Workshop, MAST II, MCS-Project.

Markle, D.G. (1989). "Stability of Toe Berm Armor Stone and Toe Buttressing Stone on Rubble-Mound Breakwaters and Jetties; Physical Model Investigation,"

Technical Report REMR-CO-12, U.S. Army Engineer Waterways Experiment Station, Vicksburg, MS.

Mase, H. (2001). "Multi-directional random wave transformation model based on energy balance equation". Coastal Engineering Journal., 43(4), pp. 317-337.

Minikin, R.R.(1950). *"Winds, Waves and Maritime Structures"*, Griffin, London, pp38-39.

Miyazawa, K. and Y. Hayakawa. (1994). "A Large-scale Structure and the Environmental Capacity for Aquaculture – Effects of an Artificial Structure (Breakwater at the Entrance of the Ofunato Estuary) on Aquaculture and Water Qualities in the Estuary" –, Bulletin on Coastal Oceanography, 32, 1, 29–38. (in Japanese)

Mizutami, J.M. Kobayashi, M. (1991). *"Strength Characteristics of Rubble by Large Scale Triaxial Compression Test"*. Technical Note of the Port and Harbour Research Institute, Ministry of Transport, Japan. No. 699 (In Japanese).

Mizutani, S. and Imamura, F.(2000). *"Hydraulic Experimental Study on Wave Force of a Bore Acting on a Structure"*, Proceedings of Coastal Engineering, JSCE, Vol. 47.

Mizutani, S. and Imamura, F. (2002) *"Design of Coastal Structure Including the Impact and Overflow of Tsunamis"*, Proceedings of Coastal Engineering, JSCE, Vol. 49.

Mockett, I.D. and Simm, J.D. (2002). "Risk levels in coastal and river engineering: a guidance framework for design." Thomas Telford Publishing.

Morris, M. and Simm, J. (2000). "Construction risk in river and estuary engineering. A guidance manual". Thomas Telford Publishing.

Nagai, T. (1999). "Long Term Statistics Report on Nationwide Ocean Wave Information Network for Ports and Harbours (NOWPHAS) 1970-1999". Japanese Ports and Airports Research Institute (P.A.R.I.). In Japanese.

Naksuksakul, S. (2006). *"Risk Based Safety Analysis for Coastal Area Against Tsunami and Storm Surge"*. Doctoral Dissertation, Yokohama National University.

Oumeraci, H. (1992). "Review and analysis of vertical breakwater failures –lessons learned", Internal Note, as quoted by Goda (1999).

Oumeraci, H.& Kortenhaus, A. (1994). *"Analysis of dynamic response of caisson breakwaters"*. Coastal Engineering, Special Issue on 'Vertical Breakwaters', Eds.: -Oumeraci, H. et al., Amsterdam, The Netherlands: Elsevier B.V., vol. 22, nos. 1/2, pp. 159-183.

Peregrine, H. & Kalliadasis, S. (1996) *"Filling flows, cliff erosion and cleaning flows"*, J. Fluid Mechanics 310, 365-374.

PROVERBS (1996-1999). Various authors. Commission of the European Union (EU): Probabilistic Design Tools for Vertical Breakwaters (PROVERBS) - concept paper 1996-1999; MAST contract MAS3-CT95-0041; Leichtweiss Institut für Wasserbau, Braunschweig, 1999.

Sasaki, J. (2006). *"Environmental Impact of Tsunami disaster prevention structures"*. Proceedings of the "Tsunami, Storm Surge and other Coastal Disasters Symposium, Sri Lanka.

Shibayama, T., Sasaki, J., Takagi, H., Achiari, H., *"Tsunami disaster survey after central Java Tsunami in 2006"*. Proceedings of the "Tsunami, Storm Surge and other Coastal Disasters Symposium, Sri Lanka.

Shimosako, K., and Takahashi, S. (1998). *"Reliability design method of composite breakwater using expected sliding distance"*. Report of the Port and Harbour Research Institute 37, 3, pp. 3-30 (in Japanese)

Shimosako, K., and Takahashi, S. (1999). "Application of deformation-based reliability design for coastal structures –Expected sliding distance method of composite breakwaters -". Coastal Structures '99, ed. I.J. Losada, Spain, Balkemare, pp. 363-371.

Shimosako, K. & Takahashi, S. (2000). "*Application of Expected Sliding Distance Method for Composite Breakwaters Design*", Proc. 27th Int. Conf. on Coastal Eng., ASCE, pp 1885-1898.

Shuto, N. (1974). *"Nonlinear long waves in a channel of variable section"*, Coastal Engineering in Japan, Vol. 17, pp. 1-12.

US Department of Labour (1990). "*Analysis of Construction Fatalities*" –The OSHA Data Base 1985-1989.

Takagi, H. and Shibayama, T. (2006). "*A new approach on performance-based design of caisson breakwater in deep water*", Annual Journal of Coastal Engineering, JSCE, Vol.53, pp.901-905 (in Japanese).

Takagi, H. (2007). "*Verification of the Level III Reliability Based Design for Caisson Breakwaters Based on a Comparison Between Computational Results and an Actual Failure Example*". Annual Journal of Civil Engineering in the Ocean, JSCE, Vol 23. (in Japanese, in printing).

Takagi, H., Esteban, M.and Shibayama, T. (2007). *"Proposed Methodology for the Risk Assessment of the Construction of Caisson Breakwaters in Developing Countries"*, International Conference on Coastal and Port Engineering in Developing Countries, COPEDEC VII. (abstract accepted)

Takahashi, S., Tanimoto, K. and Thimosako, K. (1994). *"A Proposal of Impulsive Pressure Coefficient for Design of Composite Breakwaters"*. Proc. Of the International Conference on Hydro-technical Engineering for Port and Harbour Construction. Pp 489-504.

Takahashi, S. Shimosako, K., Kimura, K. and Suzuki, K. (2000). *"Typical Failures of Composite Breakwaters in Japan"*. ICCE Coastal Engineering Conference, pp. 1899-1910.

Takayama, T. and Fujii, H. (1991). *"Probabilistic estimation of stability of slide for caisson type breakwater"*, Report of the Port and Harbour Research Institute **30**, 4, pp.35-64 (in Japanese).

Takayama, T. and Ikeda, N. (1993). *"Estimation of sliding failure probability of present breakwaters for probabilistic design"* Report of the Port and Harbour Research Institute **31**, 5, pp. 3-32.

Takayama, T., Suzuki, Y., Kawai, H. and Fujisaku, H. (1994). *"Approach to probabilistic design for a breakwater"*, Technical Note of Port and Harbour Research Institute **785** (in Japanese).

Takayama, T., Ikesue, S. and Shimosako, K. (2000). "*Effect of directional occurrence distribution of extreme waves on composite breakwater reliability in sliding failure*", Proc. 27 th Int. Conf. Coastal Eng., Sydney, ASCE, pp. 1738-1750.

Tanimoto, K., Tsuruya, K., and Nakano, S. (1984). *"Tsunami Force of Nihonkai-Chubu Earthquake in 1983 and Cause of Revetment Damage"*, Proceedings of the 31st Japanese Conference on Coastal Engineering, JSCE.

Tanimoto, K., K. Furakawa and H. Nakamura (1996). "*Hydraulic resistant force and sliding distance model at sliding of a vertical caisson*", Proc. Coastal Engineering, JSCE 43:846-850 (in Japanese).

Thao Nguyen Danh (2007). *"Wave Breaking Impact on Breakwaters"*. Doctoral Dissertation Submitted to Yokohama National University.

Toyama, S. (1985). "*Application of the reliability design method to the safety of caisson breakwaters against sliding*", Technical Note of Port and Harbour Research Institute 540, 49, (in Japanese).

Van der Meer, J.W. (1987).*"Stability of breakwater armour layers – design formulae"*, Coastal Engineering 11: 219-239.

Van der Meer, J.W. (1988). *"Deterministic and Probabilistic design of a breakwater armour layers."* J. Waterway Port Coastal Ocean Eng. ASCE, 114, 1, pp 66-80.

APPENDIX A

LABORATORY EXPERIMENTS TO DETERMINE GRAVEL PARAMETERS

A.1. Introduction

In order to be able to adequately evaluate the deformations in the rubble mound foundation of a caisson breakwater it is of paramount importance to determine the parameters that govern the bearing capacity and compaction of the gravel. In order to do so a series of experiments based on the Japanese Soil Mechanics Codes of Practice were carried out at the Soil Mechanics Laboratory of Yokohama National University.

A.2. Void Ratio

The void ratio of a gravel material can be found using a very simple method as outlined below.

A.2.1. Theoretical Background

The void ratio of a foundation material (e) is defined as the ratio of the volume of voids to the volume of solids. The void ratio in a sample of gravel can be given by the equation

$$e = \frac{\rho_S}{\rho_a} - 1 \qquad \text{(A.1.)}$$

$$\rho_S = \frac{W_S}{V_S} \qquad \rho_a = \frac{W_S}{V} \tag{A.2.}$$

where,

e = void ratio

ρ_S = density of gravel particles only

ρ_a = density of gravel as a whole

W_S = weight of gravel particles only

V_S = volume of gravel particles only –excluding air and water voids-

V = volume of gravel particles including air and water voids

A.2.2. Methodology

In order to determine V_S a $1dm^3$ typical sample of the gravel was placed in a graduated transparent recipient. Then, $1dm^3$ (i.e. 1 litre) of water was placed in a separate container and the water was poured into the recipient containing the gravel till the wave reached the top of the $1dm^3$ mark. By measuring the remaining volume of water the void ratio of the gravel could be determined.

A.2.3. Results

For the unconsolidated soil condition after the recipient containing the gravel was filled up 0.555 litres of water remained in the water recipient. Both ρ_S and ρ_a could be determined for the initial unconsolidated soil:

ρ_a =1.33kg/0.001m^3,

ρ_S = 1.33kg/0.000555 m^3

e=0.80.

The ρ_d of any consolidated soil can then be determined by taking into account the difference in weight between the initial unconsolidated condition and each subsequent condition, and hence the void ratios of other more consolidated gravel can be calculated.

A.3. Relationship between Young's Modulus and Void Ratio.

The following test was carried out according to the Japanese Standard JIS A1210:1999 in order to examine the consolidation that can be expected in a sample of gravel when a steadily increasing load is applied to it. From these experiments the Young's Modulus for gravel of various void ratios can be determined.

A.3.1. Definition of Young's Modulus

The Young's Modulus (E) is a measure of the stiffness of a given material, and it is defined as the ratio, for small strains, of the rate of change of stress (σ) with strain (ε). This can be experimentally determined from the slope of a stress-strain curve created during tensile tests conducted on a sample of a given material, so that

$$E = \frac{\sigma}{\varepsilon} \tag{A.3}$$

In soil mechanics two different types of Young's Modulus can be defined, depending of whether the strain produced in the material is recovered or not at the end of the experiment:

- The Plastic Young's Modulus E_p, which corresponds to the plastic part of the deformation, and refers to the part of the strain which is not recovered at the end of the experiment

- The Elastic Young's Modulus, which corresponds to the elastic deformations in the gravel, which will be recovered at the end of the experiment.

A.3.2. Methodology

1000 cm^3 of gravel was placed in a metal cylindrical container measuring 12.3cm tall and 10cm in diameter. The weight of the container was measured (3.99 kg) before placing the gravel and the combined weight of container and gravel was then measured for a variety of gravel samples, each with a different void ratio. A summary of the tests that were carried out can be seen in Table A.1 below.

Table A.1 Summary of Consolidation Tests

Test Number	Weight of mould	Weight of specimen plus mould (kg)	Weight of specimen only (kg)	Void Ratio (e)
1	3.99	5.43	1.44	0.66416
2	3.99	5.45	1.46	0.64137
3	3.99	5.47	1.48	0.61919
4	3.99	5.52	1.53	0.56627
5	3.99	5.53	1.54	0.5561
6	3.99	5.61	1.62	0.47926
7	3.99	5.63	1.64	0.46122
8	3.99	5.75	1.76	0.36159

A cylindrical metallic loading head measuring 10cm in height and 5cm diameter was then placed on top of the gravel. Care was taken to ensure that the top of the gravel was reasonably flat so that the loading head was not inclined. The loading head was connected to a driving load that pushed it into the ground at a constant pace of 1mm per minute. The driving load was controlled using a Digital Speed Meter constructed by Oriental Motors (Japan). The load applied was variable in order to achieve a

constant penetration rate, and the machine provided information to a nearby PC on the load applied at each moment. Also, a digital strain gage was placed in order to measure the consolidation in the gravel, and the data obtain was stored also on a PC. An Excel file showing both the displacement and the force that was applied could thus be obtained. Fig. A.1 shows a photograph of the experimental apparatus identifying each of the elements described above.

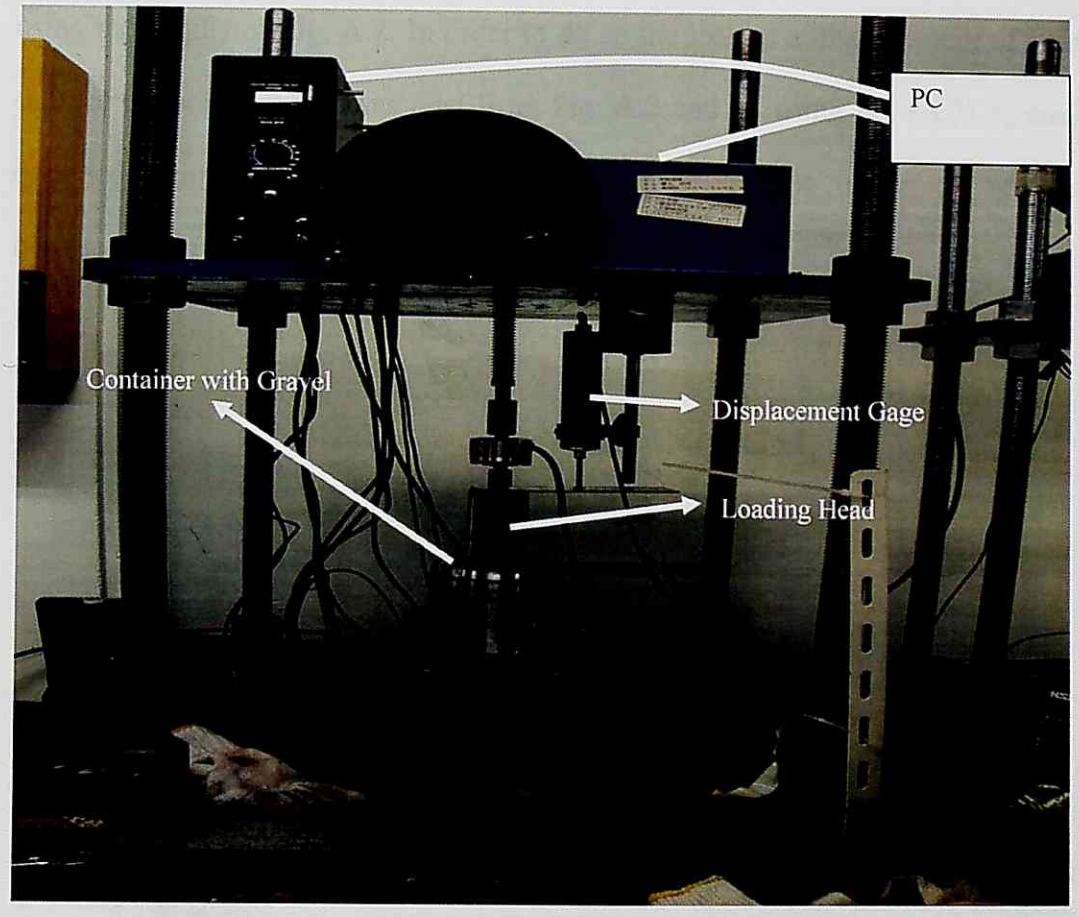

Fig. A.1. Consolidation Test Experimental Apparatus

A.3.3. Results and Analysis

The data obtained from the experiment was plotted in Fig. A.2. From this graph it can be seen how for gravels with an initially high void ratio (e) a great amount of consolidation will occur for limited applied loads, whereas those with a lower e will

require greater loads for the same displacement to take place. For all specimens the amount of load required to produce a set displacement is not linear, and regardless of the initial e a progressively larger force is needed for each further unit of displacement in the vertical direction to take place.

Generally the strains that are obtained in the gravel are not recovered at the end of the experiment, and hence it can be assumed that for the present experiment $E = E_p$. By using simple stress/strain theory it is possible to calculate the E_p for each soil sample using the results of Fig. A.2. In order to do so the load at a displacement of 1mm for each of the soil samples was read from Fig. A.2 and by using Eq. (A.3) E_p could be obtained. From the results of table A.2. it is possible to obtain the relationship between e and E_p as shown in Fig. A.3.

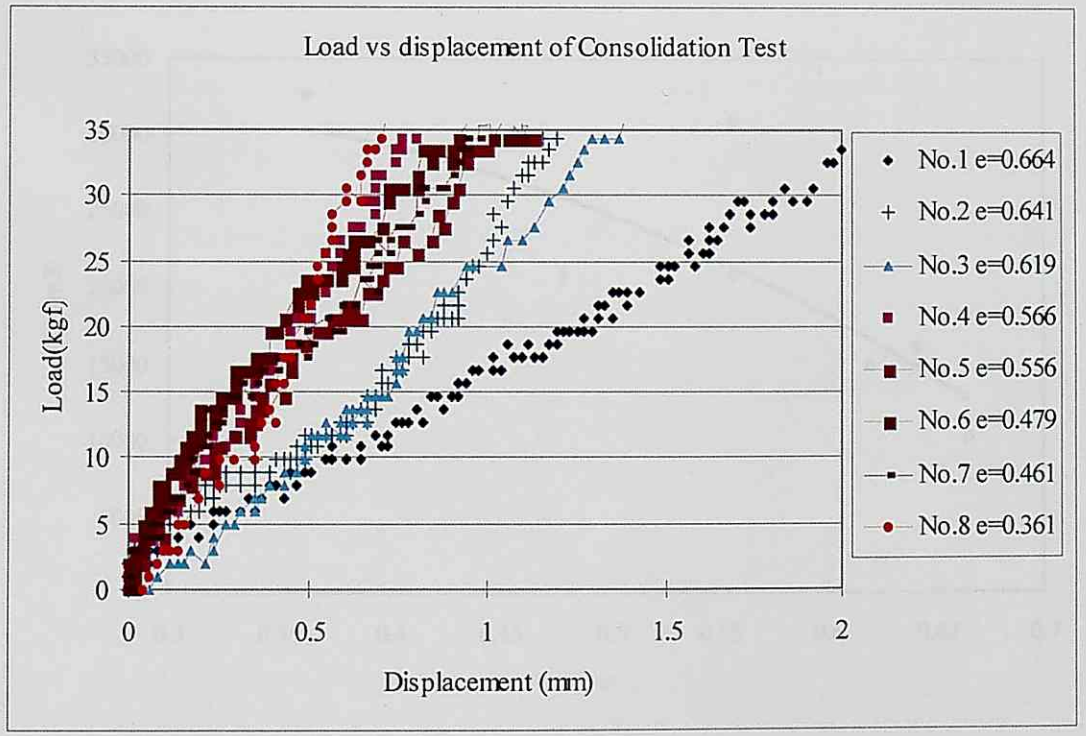

Fig. A.2. Load vs displacement in rubble.

Table A.2. Determination of E_p from Consolidation Experiments

Test Number	Force Applied (unit: kgf)	Force Applied (unit: N)	Stress σ (F/A) unit:N/m^2	Displacement (m)	Strain ε	Young's Modulus (E_p) Units:kN/m^2	Void ratio (e)
1	16.7178	163.9448	83517.46	0.001018	0.008278	10089.42	0.664164
2	26.5518	260.3829	132645.4	0.001018	0.008278	16024.38	0.641367
3	24.585	241.0953	122819.8	0.001018	0.008278	14837.39	0.619187
4	34.419	337.5334	171947.7	0.001018	0.008278	20772.34	0.566271
5	51.1368	501.4781	255465.2	0.001018	0.008278	30861.77	0.556102
6	34.419	337.5334	171947.7	0.001018	0.008278	20772.34	0.479257
7	38.3526	376.1086	191598.9	0.001018	0.008278	23146.33	0.461217
8	54.087	530.4096	270203.6	0.001018	0.008278	32642.25	0.361589

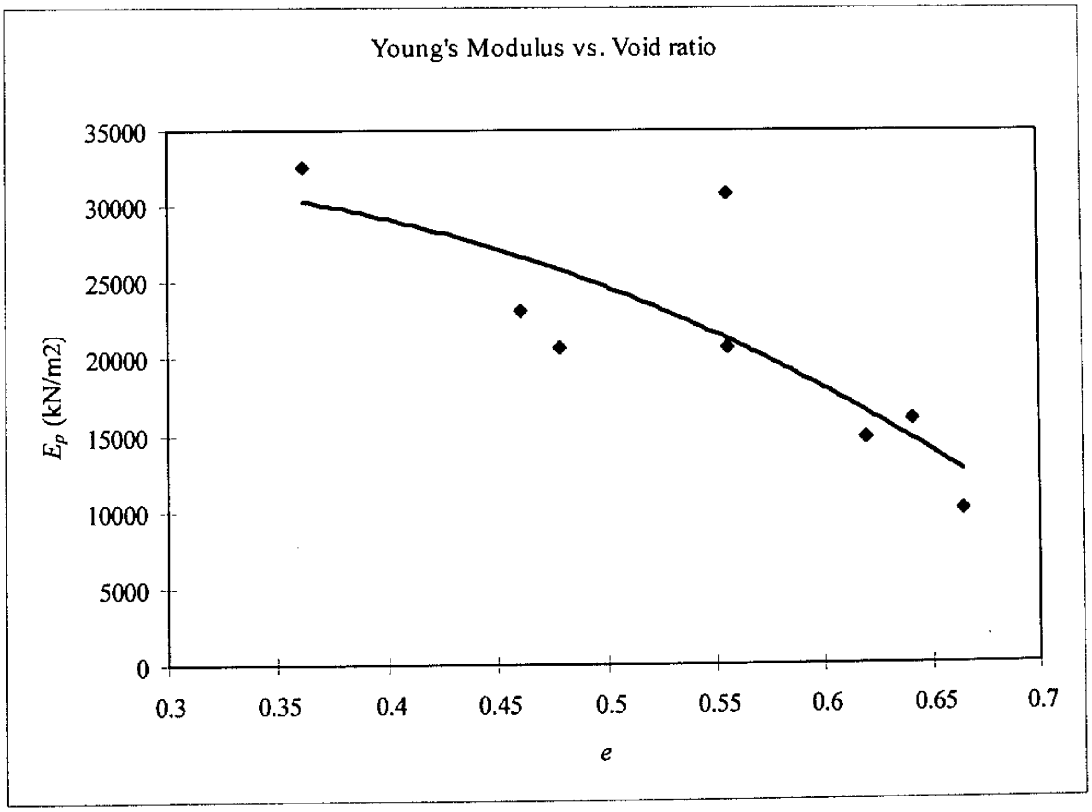

Fig. A.3 Relationship between E_p and e

A.3.4. Discussion

In the present experiments it has been assumed that $E = E_p$, which is not strictly true as there will always be a small percentage of the displacement which will be recovered at the end of the test. However, in the case of gravel materials this recovery is very small and its effect can be neglected for the purposes of the present research. The results show how there is a clear relationship between the e and E_p, with lower void ratio gravels having higher Young's Modulus.

However, there are several limitations in applying the results of the present experiments. First and foremost is the issue of the boundary conditions as during the experiments the gravel was confined into a small mound which constrained its movement. This would result in the gravel exhibiting a much greater strength than unconstrained gravel, such as that which forms the foundation of caisson breakwaters.

Secondly, it is not clear how homogeneous was the compaction achieved throughout the gravel profile. This could be responsible for some of the fluctuations observed in Fig. A.2, where there is often not much difference between the gravels with lower void ratios. Indeed, often the curves cross each other, indicating how there are other parameters influencing the strength in the soil. The type of movement of particles over one another as they attempt to compact is probably another cause of these fluctuations.

Also, the present experiments applied loads at a very slow rate, 1mm per minute, which is much slower than the rapid cycles of loading and unloading due to waves. Hence it is possible that the nature of the stress-strain curves is different, and that in

the case of loading by wind waves a significant percentage of the vertical displacement is recovered at the end of each load cycle. Therefore it is possible that in the case of wind waves the assumption than $E=E_p$ incurs more significant errors than in the present experiment.

Nevertheless the results presented provide a good indication of the type of gravel parameters that can be expected in the foundation of a caisson breakwater and how these parameters would be influenced by the degree of consolidation in the gravel.

A.3. Relationship between Compaction Energy and Void Ratio

The following test was carried out to the Japanese Standard JIS A 1210:1999 "Test Method for Soil Compaction using a Rammer"

A.3.1. Methodology

After drying the gravel in an oven for one hour to ensure that it was completely dry, it was placed in a metal cylindrical mould 12.3 cm tall and 10 cm in diameter. A removable top was then attached to the top of the mould as shown on Fig. A.4. The gravel was placed inside the mound in three different layers, with each layer consolidated using a drop rammer. After the third layer had been placed, the removable top was withdrawn and the excess gravel on top of the mould was removed. At this point the sample was weighted and it's void ratio determined.

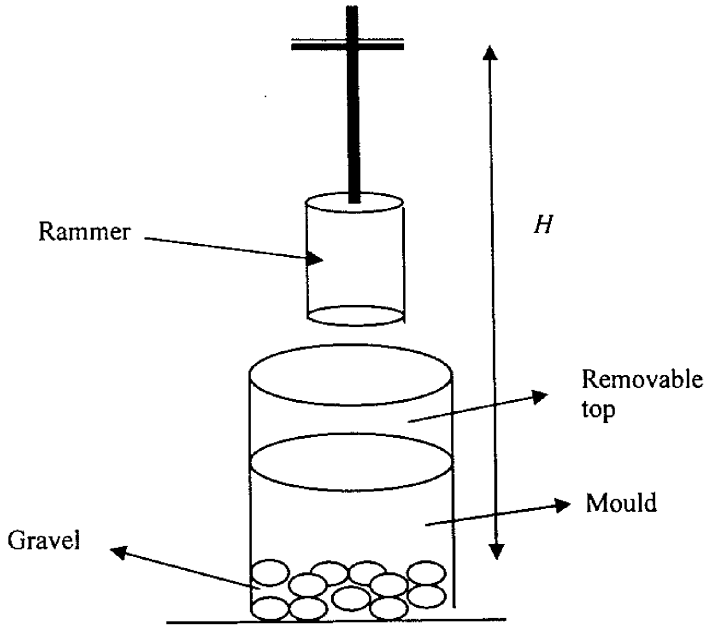

Fig. A.4. Schematic Representation of Rammer Test

The number of times the rammer was dropped was varied in order to change the compaction energy going into the sample material, given by the formula:

$$E_C = \frac{W_R \cdot H_{ram} \cdot N_B \cdot N_L}{U_{mou}} (kJ / m^3)$$

where:

E_C = Compaction Energy (kJ/m^3)

W_R = Rammer Weight (kN)

H_{ram} = Height of strike of the Rammer

N_L= Number of layers placed

U_{mou} = Mould volume

In the present experiment W_R = 2.5 kg, H = 30cm, U_{mou} = 1000 cm^3.

A.3.2. Results and Analysis

The results of the Rammer Test are summarized in Table A.3. From these results a relationship between E_c and e can be obtained, as shown in Fig. A.5.

The results show that there is a very clear relationship between the amount of compaction energy that goes into the gravel and the void ratio achieved due to this compaction. The relationship however is not linear, with the void ratio decreasing rapidly at first with very little energy applied to it. Once e<0.5 the rate of compaction decreases markedly, with very large amounts of energy having to be applied to achieve further compaction once e<0.45.

Table A.3. Results of Rammer Test

Test Number	No of strikes	Weight of mould (kg)	Weight of gravel plus mould (kg)	Weight of gravel W_S (kg)	Void Ratio (e)	Compaction energy E_C (kJ/m^3)
1	0	3.99	5.38	1.39	0.72403	0
2	5	3.99	5.54	1.55	0.54606	110250
3	10	3.99	5.55	1.56	0.53615	220500
4	15	3.99	5.61	1.62	0.47926	330750
5	20	3.99	5.65	1.66	0.44361	441000
6	25	3.99	5.65	1.66	0.44361	551250
7	30	3.99	5.68	1.69	0.41799	661500
8	1	3.99	5.53	1.54	0.5561	22050
9	2	3.99	5.59	1.6	0.49775	44100
10	3	3.99	5.57	1.58	0.51671	66150
11	4	3.99	5.56	1.57	0.52637	88200
12	8	3.99	5.59	1.6	0.49775	176400
13	13	3.99	5.63	1.64	0.46122	286650
14	0	3.99	5.44	1.45	0.65269	0
15	0	3.99	5.42	1.43	0.6758	0

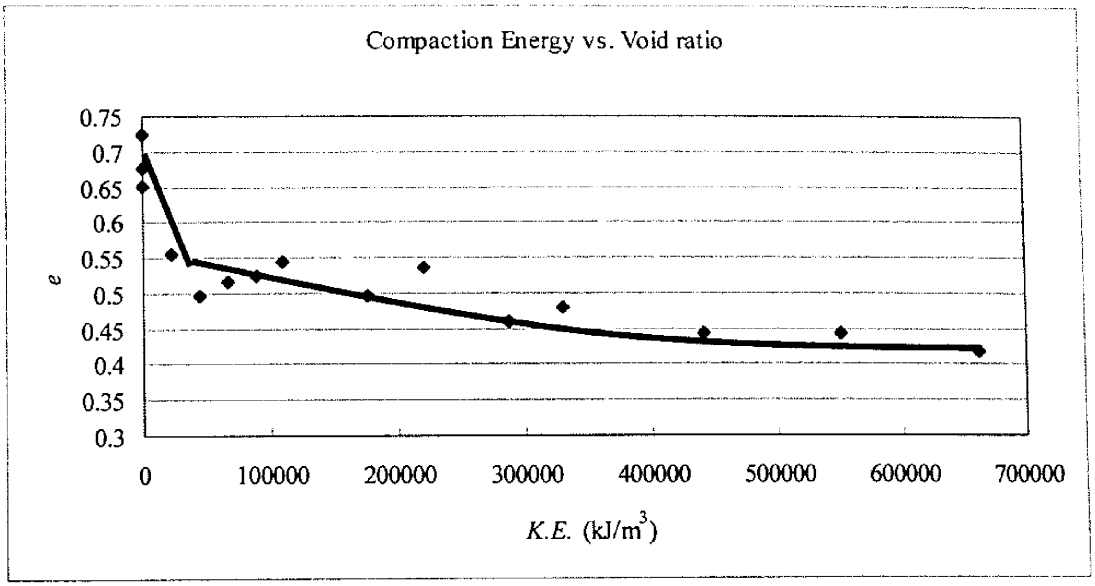

Fig. A.5. Relationship between Compaction Energy and Void Ratio

A.3.3. Discussion

The relationship between the amount of energy going into a sample of gravel and the reduction in the void ratio caused by compaction was shown by the experiment. To be noted is how although the rate of compaction slows down markedly after $e<0.45$, it never reaches 0. Although in theory there would be a limit to the density that can be achieved in granular material, in practice with each rammer strike some of the gravel particles break, creating smaller granular material capable of achieving higher densities. Thus it appears that around $e<0.45$ most of the compaction that occurs is because of this breakage of gravel elements into smaller particles, explaining the slow rate of compaction. This has to be kept in mind when using the relationships obtained from this experiment into real caisson foundations, as the breakage of gravel elements into smaller ones will be governed by the type or rock the particles are made of (as different types of rocks have different strengths).

However, in the case of prototype caissons failure occurs before the void ratio reaches such small values, and hence it is not crucial to consider this area of Fig. A.5. An

effect which is more likely to influence the applicability of the results obtained is that of boundary effects. In the experiment that was carried out the mould wall constrains the gravel, and is appears that by doing so it allows it to compaction much quicker than in an unconstrained soil. Although this effect cannot be underestimated the results nevertheless provide an adequate indication of what kind of compaction could be expected, and are probably adequate for the higher void ratio gravels. As the void ratio decreases the results probably deviate more from the unconstrained results, though these are less critical to the simulations the present thesis deals with.

APPENDIX B

SOLITARY WAVE TYPES

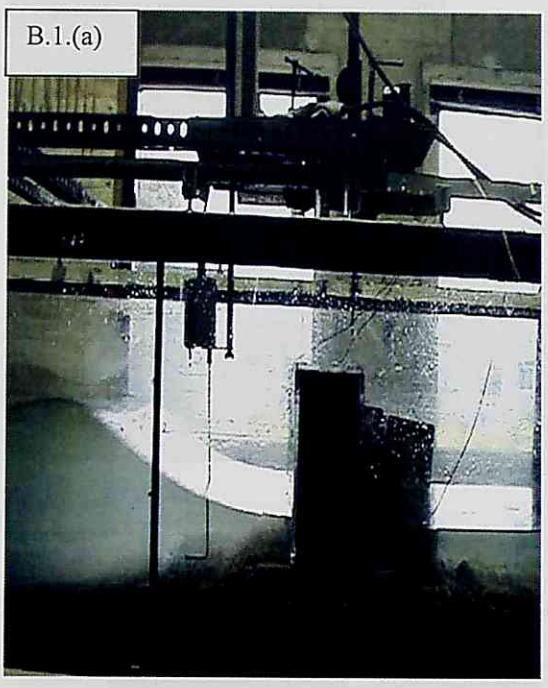

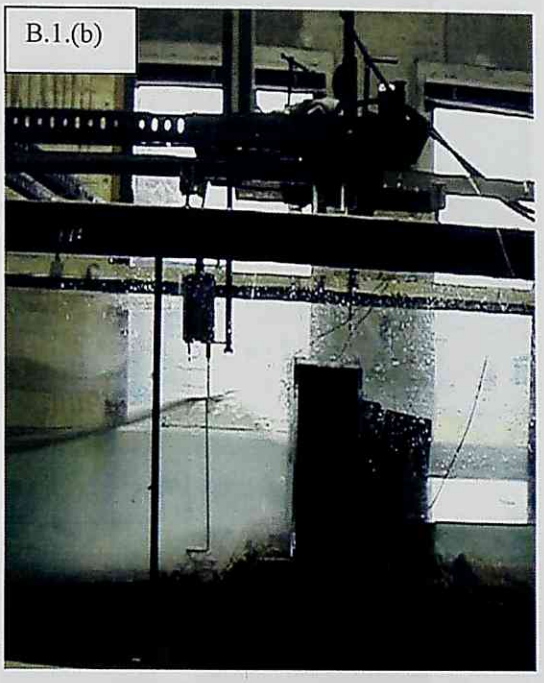

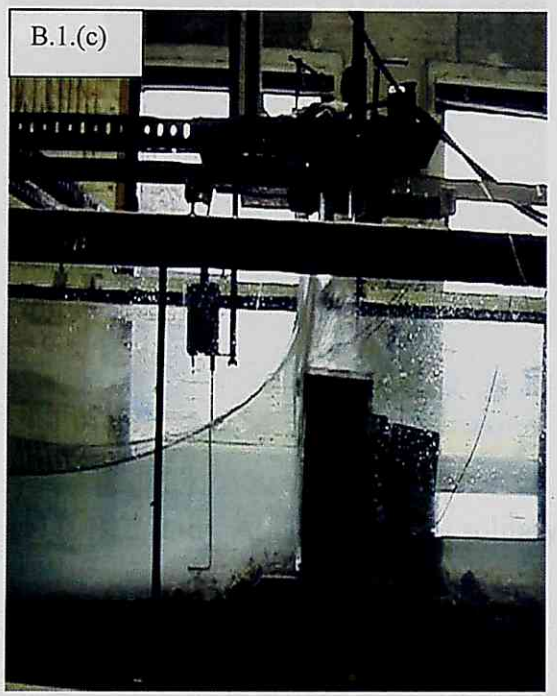

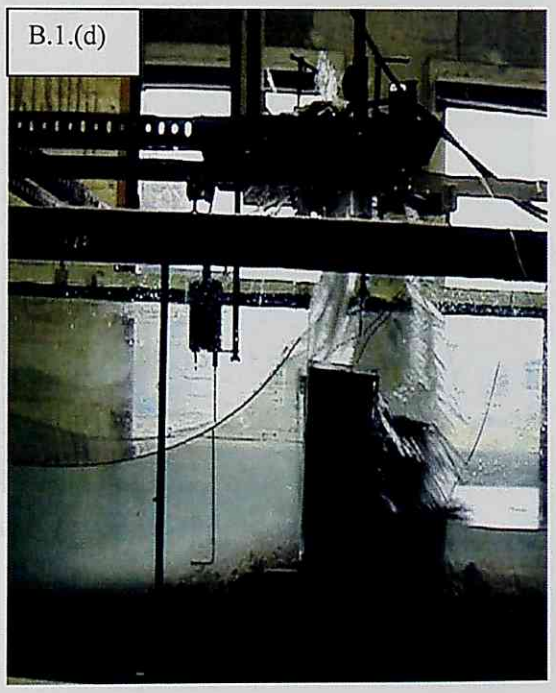

Figs B.1. (a-d). Non-breaking solitary wave type

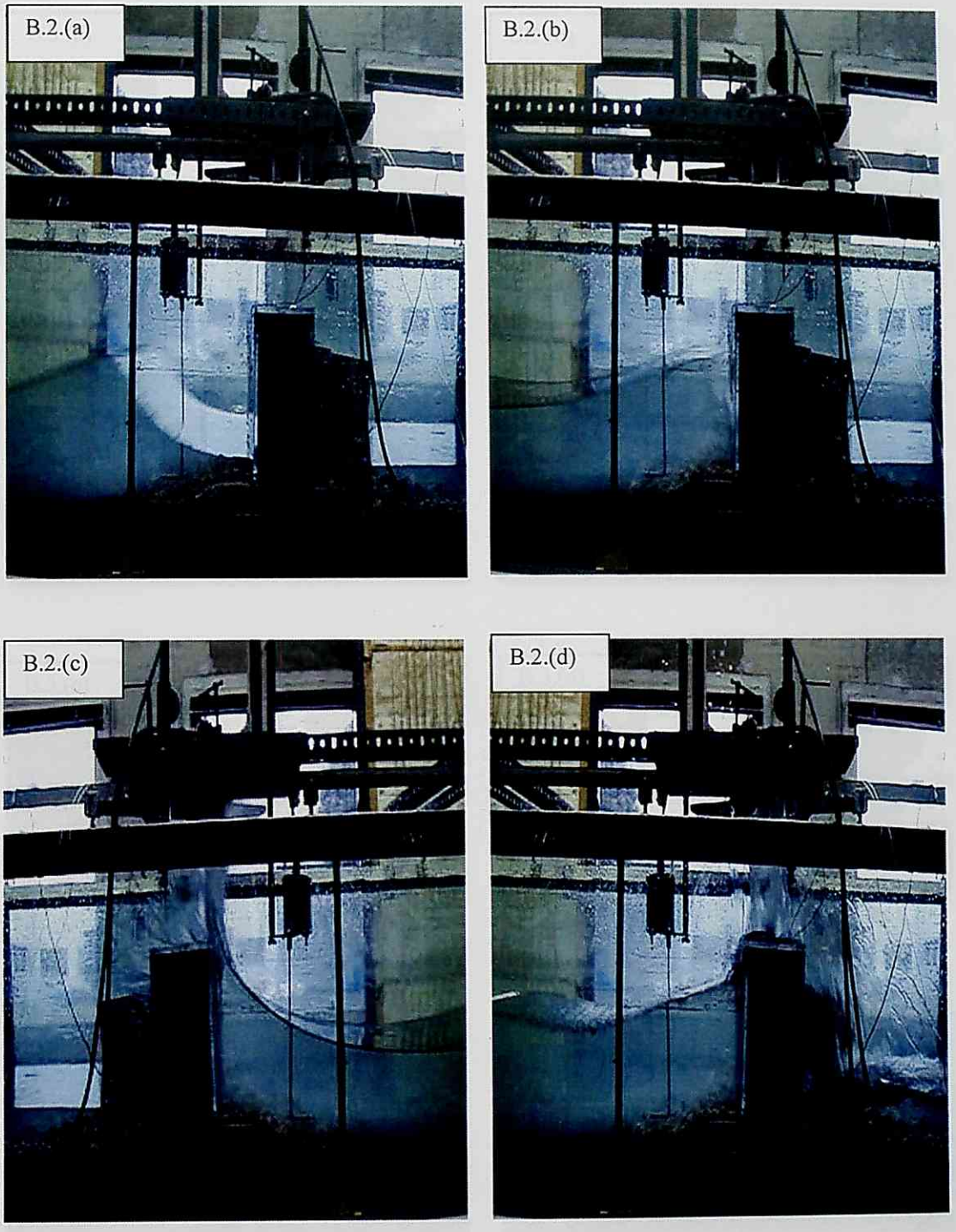

Figs B.2. (a-d). Almost breaking solitary wave type

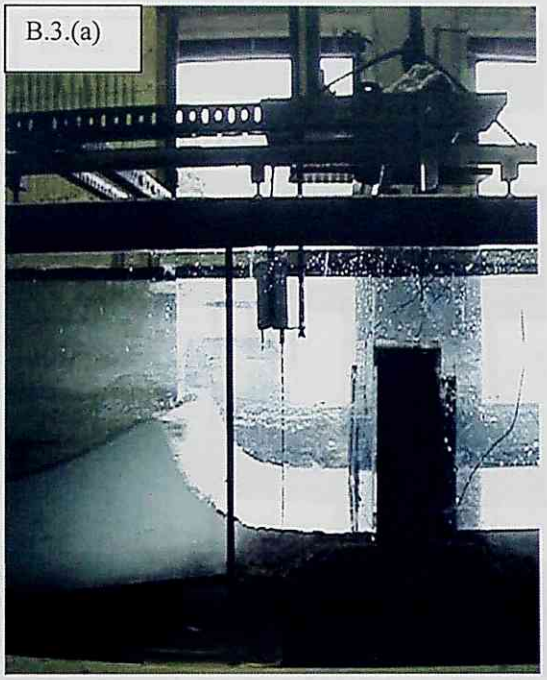

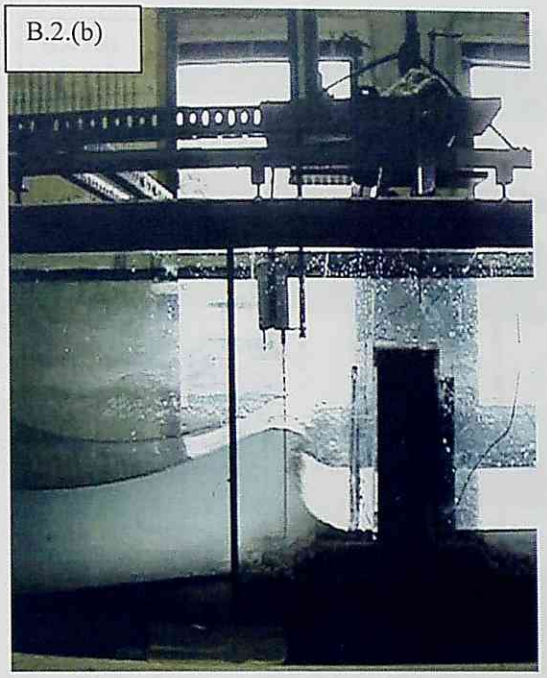

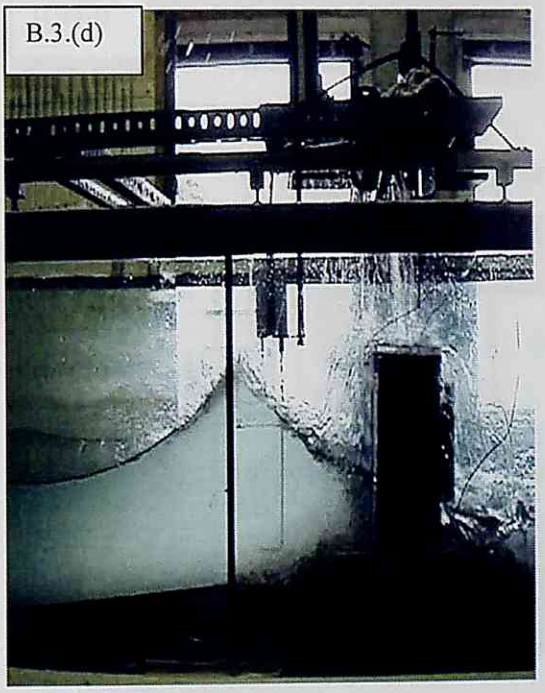

Figs B.3. (a-d). Breaking solitary wave type

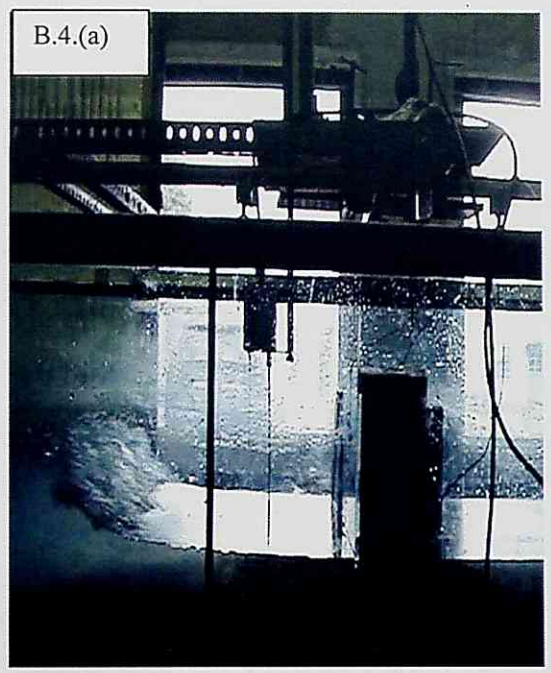

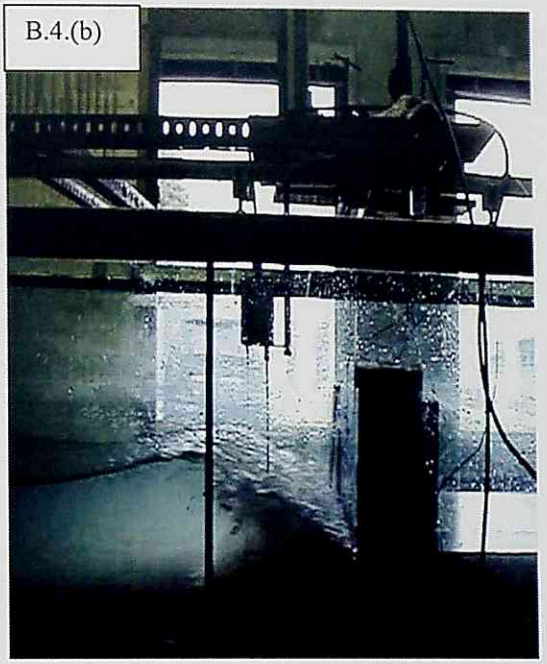

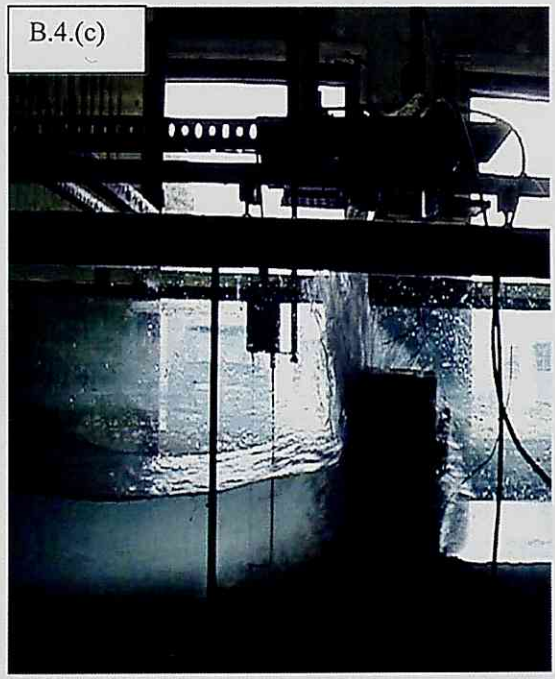

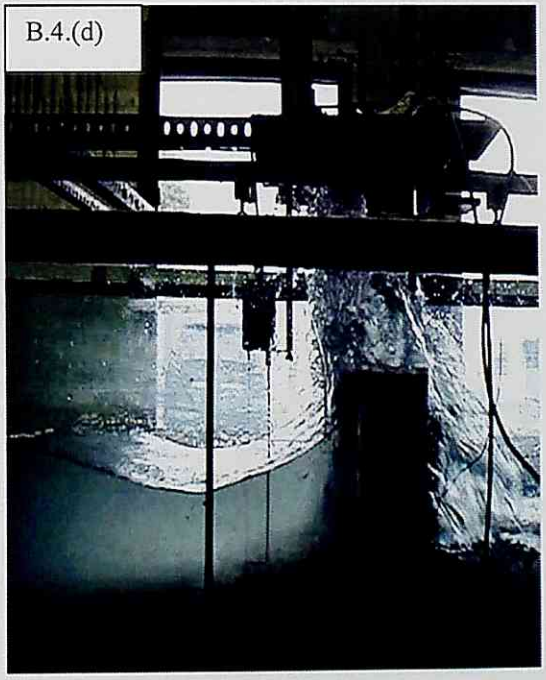

Figs B.4.. (a-d). Bore solitary wave type